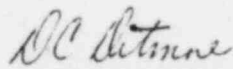


Licensing Topical Report

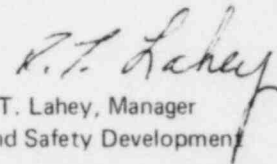
THE GENERAL ELECTRIC MARK III
PRESSURE SUPPRESSION CONTAINMENT SYSTEM
ANALYTICAL MODEL

W. J. Bilanin

Approved:



D. C. Ditmore, Manager
NSSS Performance & Safety Analysis



R. T. Lahey, Manager
Core and Safety Development

DISCLAIMER OF RESPONSIBILITY

This report was prepared as an account of research and development work performed by General Electric Company. It is being made available by General Electric Company without consideration in the interest of promoting the spread of technical knowledge. Neither General Electric Company nor the individual author:

- A. Makes any warranty or representation, expressed or implied, with respect to the accuracy, completeness, or usefulness of the information contained in this report, or that the use of any information disclosed in this report may not infringe privately owned rights; or*
- B. Assumes any responsibility for liability or damage which may result from the use of any information disclosed in this report.*

TABLE OF CONTENTS

	Page
ABSTRACT	1-1
1. INTRODUCTION	1-1
2. VESSEL BLOWDOWN MODEL	2-1
2.1 Blowdown Flow Rates	2-1
2.2 Vessel Depressurization Model	2-3
2.3 Assumptions.....	2-5
3. MARK III DRYWELL ANALYTICAL MODEL	3-1
3.1 Derivation of Equations	3-1
3.2 Assumptions.....	3-5
4. HORIZONTAL VENT CLEARING MODEL	4-1
4.1 Model Derivation and Key Assumptions.....	4-1
4.2 Assumptions.....	4-22
4.3 Experimental Verification	4-23
5. VENT FLOW MODEL	5-1
5.1 Introduction.....	5-1
5.2 Assumptions.....	5-1
5.3 Derivation of Equations.....	5-2
5.4 Previous Comparisons with Experimental Data	5-12
5.5 Nomenclature	5-13
6. VENT BACK PRESSURE MODEL	6-1
6.1 Introduction.....	6-1
6.2 Assumptions.....	6-1
6.3 Derivation of Equations.....	6-2
6.4 Experimental Verification	6-6
7. SUPPRESSION POOL AND CONTAINMENT FREE SPACE ANALYTICAL MODEL	7-1
7.1 Derivation of Equations.....	7-1
7.2 Assumptions.....	7-3
8. NUMERICAL METHODS	8-1
8.1 Introduction.....	8-1
8.2 Integration Method	8-1
8.3 Time Step Determination	8-1
9. ACKNOWLEDGMENTS	R-1
10. REFERENCES	R-1
 APPENDICES 	
A. COMPARISON OF PREDICTED AND EXPERIMENTAL VALUES	A-1
B. PIPE INVENTORY BLOWDOWN	B-1

LIST OF ILLUSTRATIONS

Figure	Title	Page
1-1	Mark III Reactor Building	1-2
1-2	Typical Mark III Containment Concept. Short Term Drywell Responso to a Steam Line Break	1-2
2-1	Critical Mass Flux Saturated Vapor Blowdown	2-2
2-2	Blowdown Area Associated with a Main Steam Line Rupture	2-8
4-1	Three-Vent Control Volumes	4-2
4-2	Control Volume 4	4-13
4-3	First Vent Uncovered	4-15
4-4	Second Vent Uncovered	4-18
4-5	Third Vent Uncovered	4-22
4-6	Large-Size Steam Blowdown Tests — 1, 2, 3 Vents	4-24
6-1	Typical Mark III Containment System Vent Back Pressure	6-6
6-2	70% BWR/6 Break Area/Vessel Volume; 1 Vent, 12-ft Submergence	6-7
6-3	100% BWR/6 Break Area/Vessel Volume; 1 Vent, 8-ft Submergence	6-7
6-4	100% BWR/6 Break Area/Vessel Volume; 1 Vent, 12-ft Submergence	6-8
6-5	200% BWR/6 Break Area/Vessel Volume; 1 Vent, 12-ft Submergence	6-8
6-6	70% BWR/6 Break Area/Vessel Volume; 2 Vents, 12-ft Submergence	6-9
6-7	100% BWR/6 Break Area/Vessel Volume; 2 Vents, 8-ft Submergence	6-9
6-8	100% BWR/6 Break Area/Vessel Volume; 2 Vents, 10-ft Submergence	6-10
6-9	200% BWR/6 Break Area/Vessel Volume; 2 Vents, 12-ft Submergence	6-10
A-1	Steam Blowdown, 70% BWR/6 Break Area/Vessel Volume; 1 Vent, 12-ft Submergence (Without Vent Back Pressure)	A-2
A-2	Steam Blowdown, 100% BWR/6 Break Area/Vessel Volume; 1 Vent, 8-ft Submergence (Without Vent Back Pressure)	A-3
A-3	Steam Blowdown, 100% BWR/6 Break Area/Vessel Volume; 1 Vent, 12-ft Submergence (Without Vent Back Pressure)	A-3
A-4	Steam Blowdown, 200% BWR/6 Break Area/Vessel Volume; 1 Vent, 12-ft Submergence (Without Vent Back Pressure)	A-4

LIST OF ILLUSTRATIONS (Continued)

Figure	Title	Page
A-5	Steam Blowdown, 70% BWR/6 Break Area/Vessel Volume; 2 Vents, 12-ft Submergence (Without Vent Back Pressure)	A-4
A-6	Steam Blowdown, 100% BWR/6 Break Area/Vessel Volume; 2 Vents, 8-ft Submergence (Without Vent Back Pressure)	A-5
A-7	Steam Blowdown, 100% BWR/6 Break Area/Vessel Volume; 2 Vents, 10-ft Submergence (Without Vent Back Pressure)	A-5
A-8	Steam Blowdown, 200% BWR/6 Break Area/Vessel Volume; 2 Vents, 12-ft Submergence (Without Vent Back Pressure)	A-6
A-9	Steam Blowdown, 100% BWR/6 Break Area/Vessel Volume; 3 Vents, 7-ft Submergence (Without Vent Back Pressure)	A-7
A-10	Steam Blowdown, 100% BWR/6 Break Area/Vessel Volume; 3 Vents, 11-ft Submergence (Without Vent Back Pressure)	A-8
A-11	Steam Blowdown, 200% BWR/6 Break Area/Vessel Volume; 3 Vents, 11-ft Submergence (Without Vent Back Pressure)	A-8
A-12	Steam Blowdown, 70% BWR/6 Break Area/Vessel Volume; 1 Vent, 12-ft Submergence (With Vent Back Pressure)	A-9
A-13	Steam Blowdown, 100% BWR/6 Break Area/Vessel Volume; 1 Vent, 8-ft Submergence (With Vent Back Pressure)	A-9
A-14	Steam Blowdown, 100% BWR/6 Break Area/Vessel Volume; 1 Vent, 12-ft Submergence (With Vent Back Pressure)	A-10
A-15	Steam Blowdown, 200% BWR/6 Break Area/Vessel Volume; 1 Vent, 12-ft Submergence (With Vent Back Pressure)	A-10
B-1	Discharge Properties for Ideal	B-4
B-2	Water Initial Discharge Rate	B-5
B-3	Comparison with Edwards Experiment	B-11
B-4	Typical BWR Recirculation Line Break	B-12
B-5	Typical BWR Steam Line Break	B-13

ABSTRACT

The analytical models used to simulate the short-term transient response of a Mark III pressure suppression containment to a postulated loss-of-coolant accident are presented. The governing equations are defined together with derivations of the simultaneous differential equations that simulate the transient conditions in the containment. The numerical techniques used to integrate these equations are discussed. All modeling and boundary condition assumptions are described and discussed. Model results are compared with experimental data from the General Electric Company's large-scale Mark III test facility; the comparisons indicate that the model is conservative. This conservatism is reflected in the design parameters that are being specified for those containment systems using the Mark III concept.

1. INTRODUCTION

In 1972 the General Electric Company introduced a new product line consisting of an improved and uprated sixth generation boiling water reactor nuclear steam supply system with a reference design third generation pressure suppression containment system. This combination was given the name BWR/6-Mark III.

The Mark III containment reference design is shown in Figure 1-1. The reactor primary system is surrounded by a cylindrical concrete drywell structure which is in turn surrounded by the primary containment. At the base of the drywell there is a series of horizontal holes in three rows that connect the drywell and containment; these holes (vents) are submerged in an annular pool of water that is retained by a weir wall inside the drywell. Any steam released in the drywell as a result of a loss-of-coolant accident will be forced to flow through the horizontal vent system and into the suppression pool where it will be condensed. This containment concept represents a direct development from the earlier Mark I (torus—light bulb) and Mark II (over-under) concepts and retains many of their major features such as a drywell, vent system, and a large suppression pool of water.

At the time Mark III was introduced, its performance characteristics had been established on the basis of scaled testing; preliminary design parameters for the full-scale system were evaluated with existing Mark I and Mark II analytical models that had been modified for Mark III evaluations and which had been checked against the available scaled test data.

Immediately following introduction of the new product line, the General Electric Company started an intensive experimental and analytical effort to confirm the Mark III design. The experimental work involves a large-scale facility capable of testing a variety of horizontal vent configurations over a wide range of accident conditions. Details of the test facility and the testing program are discussed in Reference 1.

The purpose of this topical report is to document the analytical methods now being used by the General Electric Company to simulate the short-term transient response of a Mark III system to a loss-of-coolant accident.

These models are similar to those being used at the time Mark III was introduced but they incorporate some significant refinements that have resulted from the analytical and experimental work conducted over the last 2 years.

A typical short-term Mark III containment system steam line break loss-of-coolant accident response is shown in Figure 1-2. Immediately following postulated pipe rupture, the drywell pressure will start to increase at approximately 20 psi/second; this rising pressure will accelerate the water initially standing in the weir annulus and horizontal vents and at approximately 1, 1.2, and 1.5 seconds the first, second, and third rows of vents will be cleared. The Mark III venting area is of sufficient size to terminate the drywell pressure increase when the second row of vents clears; when all the vents are cleared the drywell pressure will start to decrease rapidly. Because the maximum drywell pressure occurs during the vent clearing process, it is important that the simulation of this transient be based on sound modeling, adequate experiments, and conservative assumptions. One of the objectives of this report is to demonstrate that this has been accomplished.

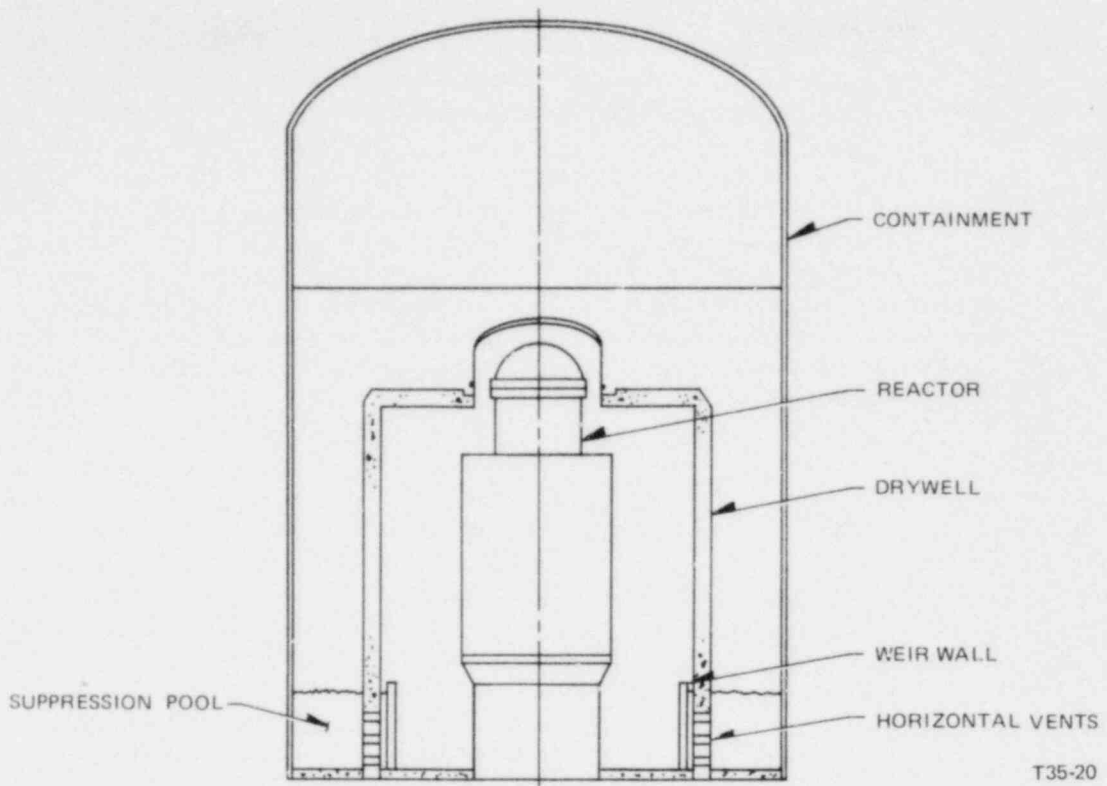


Figure 1-1. Mark III Reactor Building

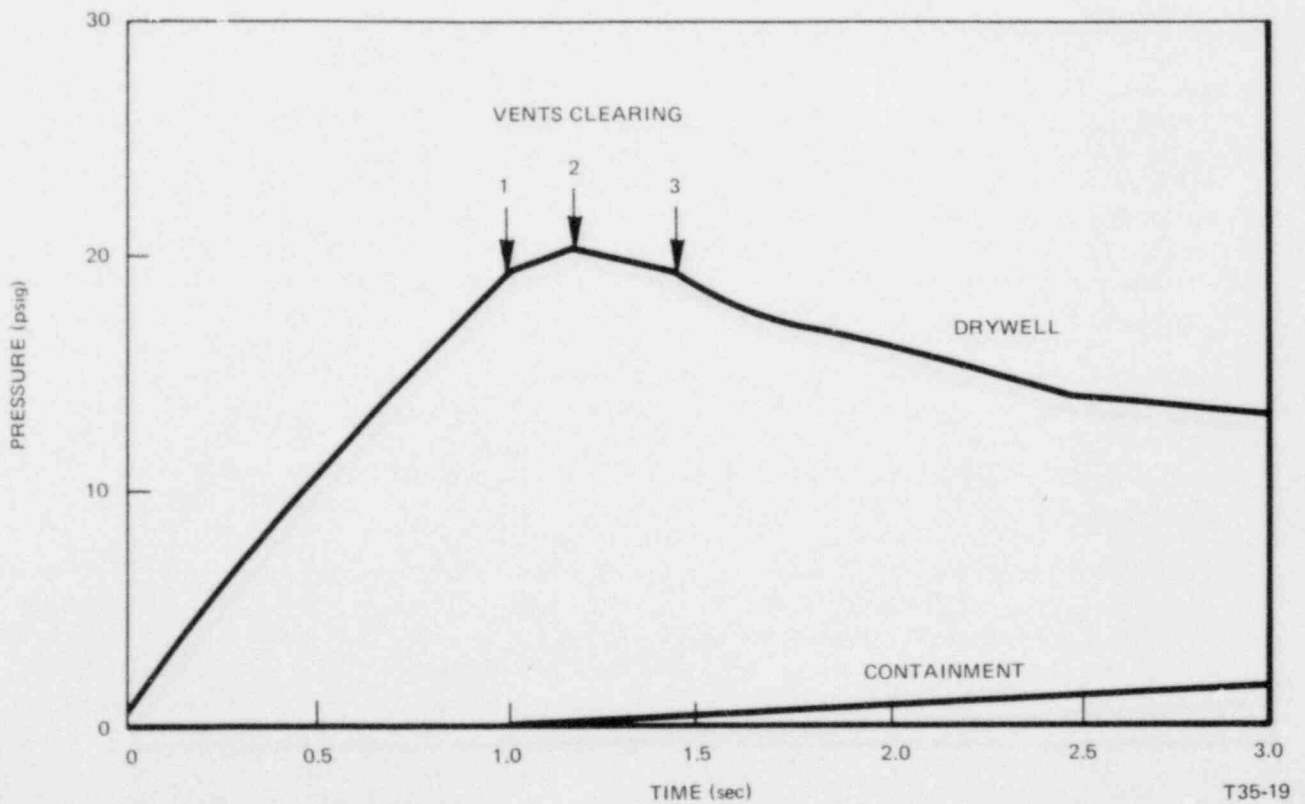


Figure 1-2. Typical Mark III Containment Concept. Short Term Drywell Response to a Steam Line Break

During the early phases of the loss-of-coolant accident, the air initially in the drywell will be purged to the containment. Because this air will be injected under the suppression pool surface, it is important that any phenomena associated with the dynamic interaction of the air and water will be described and accounted for. The air bubble model described in Section 6 does this.

The long-term decay-heat-induced containment heatup response is not shown but is discussed for the sake of completeness.

Following the drywell air purge there will be a period of quasi-steady-state steam flow through the vents which will continue until the reactor is depressurized. At that time all the energy initially contained within the reactor primary coolant pressure boundary will be dumped to the suppression pool; the suppression pool temperature will increase approximately 40°F as a result of this dump. Following blowdown, all of the drywell air will be in the containment and the containment pressure will be in the order of 5 psig. It should be noted that the maximum containment pressure does not occur during the short-term blowdown phase of the accident but occurs during the long term (4 to 6 hours) decay-heat-induced containment heatup transient that follows blowdown. This is fundamentally different from earlier pressure suppression designs which experience peak primary containment pressures during reactor blowdown; since the long-term transient is slow and can be evaluated with simple models this change must be considered an advantage for Mark III. It should be noted that the Mark III drywell is not a part of the primary fission product barrier, but is used to channel blowdown flow from the reactor vessel through the vent system and into the suppression pool during a loss-of-coolant accident.

It can be seen that any over-all analytical model that is developed to simulate the transient described would naturally consist of a series of submodels. These submodels would include individual models for the reactor, drywell, vent clearing, vent flow, the suppression pool during both the air-injection phase and during the subsequent heatup phase, and the containment free space.

With the exception of the vent clearing and suppression pool bubble models, the techniques being used for Mark III analysis are essentially the same as those that have been approved by the AEC staff for analysis of the Mark I and II pressure suppression containments. However, for the sake of completeness and because there have been some minor refinements to the earlier models, this report includes a complete derivation of all the models together with a description and discussion of the many assumptions that must be made.

The new vent clearing and pool bubble models have been verified by comparing their predictions against test data from the large-scale facility. These comparisons, which show both models to be conservative, are included. Experimental verification of the other models has been presented in Reference 2 and is not repeated in this document.

When simulating the response of a full-scale containment to a loss-of-coolant accident, there are two sources of conservatism in the peak temperatures and pressures that an analytical model would predict. First, there are the conservatisms in the model itself. For example, even when provided with all the observed boundary conditions from the test facility, the vent clearing model still predicts a slower vent clearing transient than the observed transient. Second, there are the deliberate conservatisms involved in the various boundary condition assumptions that must be made; an example of this type of conservatism is the assumption that during an accident there is no heat transfer to the drywell walls. In practice, for either a full-scale containment or a test facility, there will be heat transfer to the walls and this heat transfer will tend to reduce the maximum temperatures and pressures.

To demonstrate the overall conservatism in the peak pressures specified for Mark III, the over-all analytical model was applied to a selection of the large-scale test facility runs. The model was run with all the conservative assumptions used for Mark III analyses and the results show an average predicted drywell pressure of 27% higher than the observed pressures. These comparisons are presented in Appendix A.

2. VESSEL BLOWDOWN MODEL

The analytical model used to simulate the response of the reactor vessel to a loss-of-coolant accident is presented in this section.

Because the break mass flow rate is of central importance to the whole containment model, it is discussed in some detail. It is demonstrated that conservatism exists between the mass flow rates used in the analysis and those which would actually occur.

To determine the design basis blowdown flow rate for the Mark III containment system drywell design pressure, guillotine severance of the main steam line and recirculation line were each analyzed. Though the analyses resulted in the main steam line break being the design basis accident (DBA) for the drywell design pressure, the methods for calculating the blowdown flow rates for both cases are discussed.

2.1 BLOWDOWN FLOW RATES

Following a postulated loss-of-coolant accident (LOCA), the rate at which reactor coolant will be injected into the drywell is determined by a combination of (1) the critical choked flow rate through the available critical flow area and (2) the transient blowdown flow rate associated with the decompression of the broken line (referred to as the pipe inventory effect). The rate at which reactor coolant will leave the vessel through the available critical flow area is evaluated with the Moody flow model.³ It is generally agreed that this model, which assumes annular, isentropic flow, thermodynamic phase equilibrium, and maximized slip ratio, is conservative when applied in a BWR accident analysis. All the evidence suggests that actual flow rates through large breaks would be less than those predicted by the model. The conservatisms associated with the Moody model prediction of reactor vessel liquid blow-down flow rates is discussed in References 2 and 4.

Since the design basis accident for the BWR/6-Mark III combination is the main steam line break, results of the first phase of the Mark III Confirmatory Test Program have been examined with a view toward evaluating the performance of the Moody critical flow model for saturated steam blowdowns. For the Pressure Suppression Test Facility (PSTF) tests, three different break flow areas were used. The area to vessel volume ratio represent 70, 100, and 200 percent of the steam line area to vessel volume ratio for a typical BWR/6. This spectrum of break flow areas will permit the performance of the Moody model for saturated steam blowdowns to be evaluated for vessel depressurization rates bounding those expected to occur in the Mark III containment system during a design basis accident steam line rupture. The PSTF blowdown flow rates were obtained from an isentropic flow calculation using measured venturi inlet and throat conditions. These flow rates were time integrated and compared to the total vessel mass loss during the blowdown. The integrated flow rate agreed well with the total vessel mass loss confirming the applicability of the isentropic venturi calculation for obtaining PSTF blowdown flow rates.

Figure 2-1 is a comparison of the PSTF steam blowdown mass fluxes to flow rates predicted with the Moody model as a function of vessel stagnation pressure

It can be seen that the Moody model is conservative but comes close to predicting the experimentally observed steam blowdown flow rates, this is not surprising because for a single-phase gas flow, the model essentially reduces to the classical isentropic ideal gas treatment of critical flow.

The transient blowdown flow rate associated with the decompression of a broken line was obtained by a detailed solution of the fluid flow equations for a high-pressure pipe ruptured at one end. The results were as follows: for a high-pressure pipe initially containing steam, the flow rate through the broken end of the line corresponds to approximately 0.7 of the flow rate predicted by the Moody critical flow model at initial pipe pressure and using the entire pipe area. For liquid-filled pipes, the decompression flow rate corresponds to approximately 0.5 times the Moody critical flow, again assuming initial pipe pressure and the entire pipe area. These flow rates will exist until the fluid originally in the pipe is depleted. Following depletion, the flow will correspond to the Moody predicted flow rate corresponding to the available minimum flow area upstream. For a detailed discussion of assumptions and the method used for calculating high-pressure pipe decompression flow rates, refer to Appendix B for pipes initially containing liquid and steam.

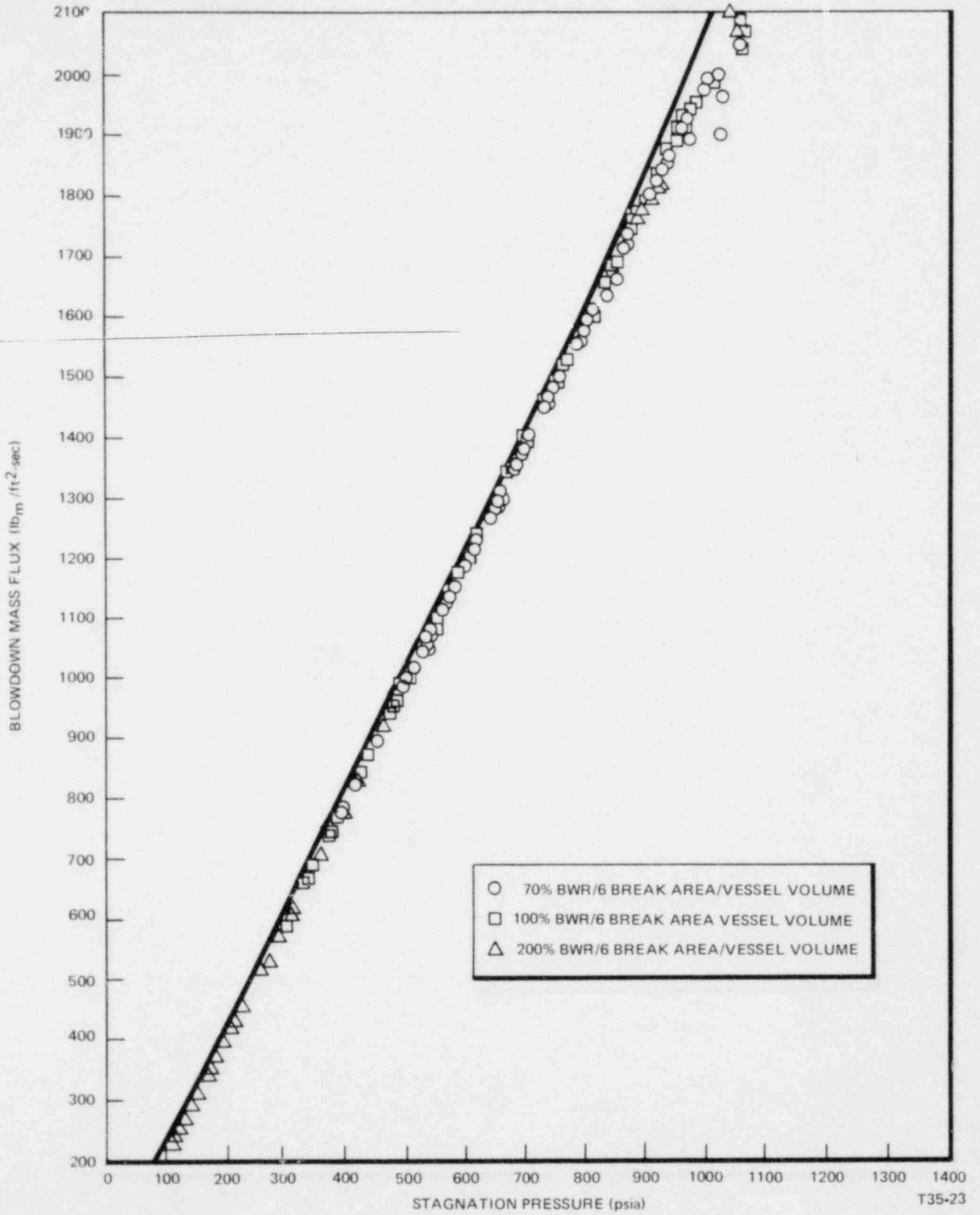
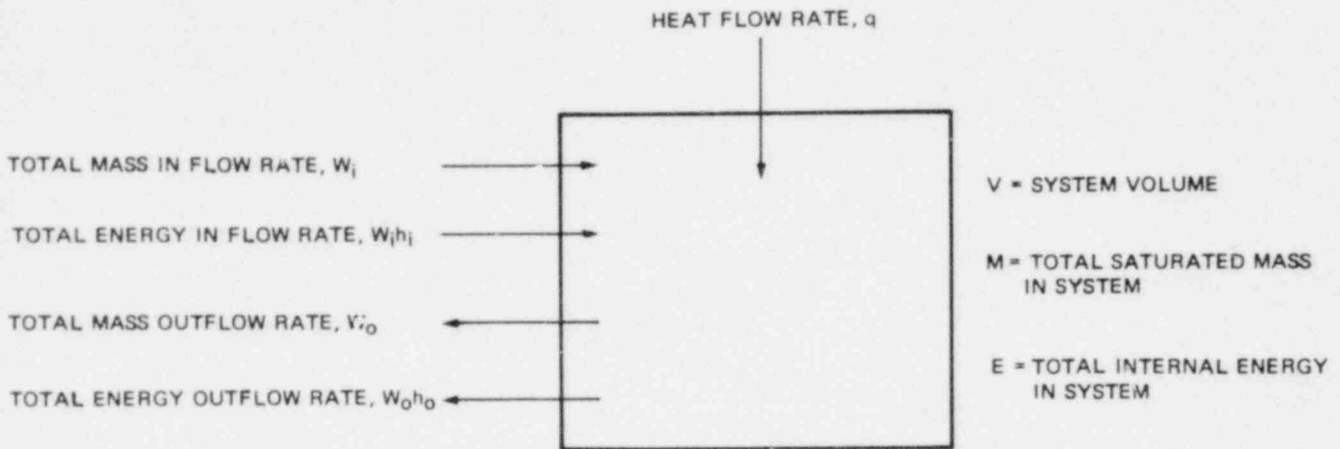


Figure 2-1. Critical Mass Flux Saturated Vapor Blowdown

The above discussion has been limited to describing the blowdown rates used in the containment analytical model; it presupposes that the thermodynamic conditions in the reactor vessel at any time are known. To use the Moody model, the stagnation pressure and enthalpy of the fluid assumed to be passing through the break must be known. The remainder of this section describes the model and assumptions used to calculate the transient thermodynamic conditions in the reactor vessel following a loss-of-coolant accident and thus the blowdown flow rates.

2.2 VESSEL DEPRESSURIZATION MODEL

Consider the system shown below:



The equations of mass, energy, and state will be written and the equation for the depressurization rate derived. For this analysis, it is assumed that the reactor vessel can be simulated by a single pressure representation.

From conservation of mass, we have

$$w_o - w_i + \frac{dM}{dt} = 0 \tag{2-1}$$

Conservation of energy yields

$$w_o h_o - w_i h_i - q + \frac{dE}{dt} = 0 \tag{2-2}$$

Assuming the system to be a saturated one, the equation of state can be written:

$$e = e_f + x \cdot e_{fg} \tag{2-3}$$

(Thermodynamic properties are in usual notation)

Expanding this and remembering that

$$x = \frac{1}{v_{fg}} \left(\frac{V}{M} - v_f \right)$$

we have

$$e = \frac{E}{M} = e_f + \frac{e_{fg}}{v_{fg}} \left(\frac{V}{M} - v_f \right) \tag{2-4}$$

Differentiating (2-4) with respect to time:

$$\frac{M \frac{dE}{dt} - E \frac{dM}{dt}}{M^2} = \frac{de_f}{dP} \cdot \frac{dP}{dt} + \frac{e_{fg}}{v_{fg}} \left(\frac{-V}{M^2} \frac{dM}{dt} - \frac{dv_f}{dP} \cdot \frac{dP}{dt} \right) + \left(\frac{V}{M} - v_f \right) \left[\frac{d}{dP} \left(\frac{e_{fg}}{v_{fg}} \right) \frac{dP}{dt} \right] \tag{2-5}$$

Let the symbol (x)' express:

$$\frac{d(x)}{dP}$$

$$\frac{M \frac{dE}{dt} - E \frac{dM}{dt}}{M^2} = \left[(e_f)' - \frac{e_{fg}}{v_{fg}} (v_f)' + \left(\frac{V}{M} - v_f \right) \left(\frac{e_{fg}}{v_{fg}} \right)' \right] \frac{dP}{dt} - \frac{e_{fg}}{v_{fg}} \frac{V}{M^2} \frac{dM}{dt} \tag{2-6}$$

Rearrange terms:

$$\frac{dP}{dt} \left[(e_f)' - \left(\frac{e_{fg}}{v_{fg}} \cdot v_f \right)' + \frac{V}{M} \left(\frac{e_{fg}}{v_{fg}} \right)' \right] = \frac{M \frac{dE}{dt} - E \frac{dM}{dt} + \frac{e_{fg}}{v_{fg}} V \frac{dM}{dt}}{M^2} \tag{2-7}$$

Substituting Equations (2-1) and (2-2):

$$\frac{dP}{dt} \left[(e_f)' - \left(\frac{e_{fg}}{v_{fg}} \cdot v_f \right)' + \frac{V}{M} \left(\frac{e_{fg}}{v_{fg}} \right)' \right] = \frac{(q + w_i h_i - w_o h_o) - \left(\frac{E}{M} - \frac{e_{fg}}{v_{fg}} \frac{V}{M} \right) (w_i - w_o)}{M} \tag{2-8}$$

Solving for dP/dt:

$$\frac{dP}{dt} = \frac{q + w_i h_i - w_o h_o - \left(e_f - \frac{e_{fg}}{v_{fg}} v_f \right) (w_i - w_o)}{M \left[(e_f)' - \left(\frac{e_{fg}}{v_{fg}} v_f \right)' + \frac{V}{M} \left(\frac{e_{fg}}{v_{fg}} \right)' \right]} \tag{2-9}$$

Placing this equation in functional form, we have the following relationship for obtaining decompression rate:

$$\frac{dP}{dt} = \frac{q + w_i h_i - w_o h_o - [f(P)] (w_i - w_o)}{M \left[F \left(P \frac{V}{M} \right) \right]} \tag{2-10}$$

Where

$$f(P) = \rho_f - e_{fg} \cdot \frac{v_f}{v_{fg}} \quad (2-11)$$

and

$$F \left(P \frac{V}{M} \right) = e_f' - \left(e_{fg} \cdot \frac{v_f}{v_{fg}} \right)' + \frac{V}{M} \left(\frac{e_{fg}}{v_{fg}} \right)' \quad (2-12)$$

At any time during the depressurization transient, all the terms in Equation (2-10) are known from the current vessel pressure and inventory, the specified energy and mass additions to the system and the break flow rate, w_Q . The current depressurization rate can thus be evaluated and, together with the mass and energy rates, can be integrated using the finite time interval techniques described in Section 8.

2.3 ASSUMPTIONS

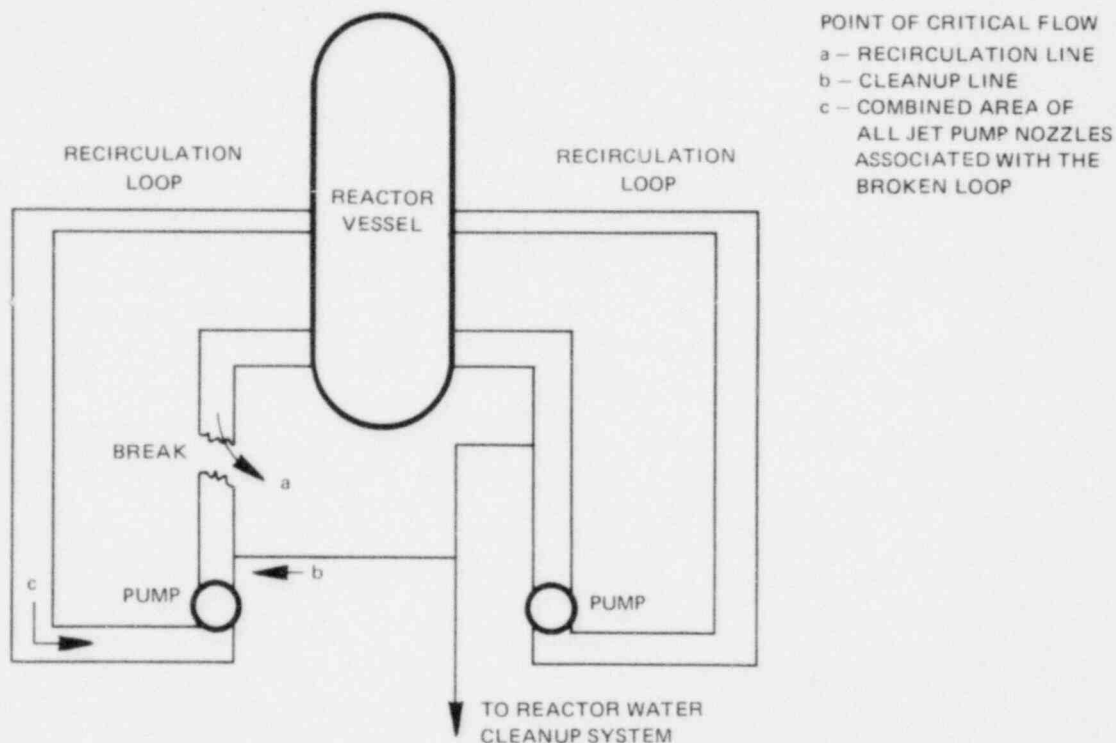
When evaluating the boundary conditions for Equation (2-10), appropriate assumptions are made to maximize the vessel pressure and thus the vessel blowdown flow rate. In some cases, the assumptions used for evaluating the boundary conditions are independent of the type of primary system line break being considered, whereas for other cases, the assumptions are dependent on break type. The following assumptions are independent of break type; the assumptions apply for both a steam line and recirculation line breaks.

1. The reactor is assumed to be at the maximum possible steady-state power level at the time the accident occurs. This maximizes the reactor pressure during the blowdown which in turn maximizes the blowdown flow rate.
2. The reactor core is assumed to go subcritical at the time of accident initiation due to void formation. Scram also occurs in less than 1 second from receipt of the high drywell pressure and low water level signals, but the difference in shutdown time between zero and 1 second is negligible. The transient release of the fuel relaxation energy is accounted for.
3. The feedwater flow was assumed to stop instantaneously at time zero. This assumption is used because the relatively cold feedwater flow, if considered to continue, would tend to depressurize the reactor vessel, thereby reducing the discharge rate of steam and water into the drywell.
4. Vessel blowdown flow rates are calculated using Moody's critical flow model.³
5. Immediately following a postulated pipe rupture, the fluid inventory in the broken pipe itself will start depressurizing and flow out the break. The transient manner in which this fluid enters the drywell is evaluated with the models discussed in Appendix B.

When analyzing a recirculation line break the following break-dependent assumptions are used.

1. As discussed above, the flow through the break is based on the Moody blowdown flow rate. The conservatism of this procedure has been demonstrated; however, it should be emphasized that this conservatism is further compounded by the method in which the model is applied. Specifically, during the first part of a recirculation line break transient (up to 20 seconds), a "liquid only" outflow is assumed because this maximizes the energy release to the containment. "Liquid only" outflow means that all vapor formed in the vessel due to bulk flashing rises to the surface rather than being entrained in the exiting flow through the recirculation line. Some entrainment of the vapor would occur and would significantly reduce the reactor vessel discharge flow rates.

- The break flow quality is assumed to change to a homogeneous mixture of the vessel inventory at the time in the transient when the "collapsed" liquid level would reach the elevation of the main recirculation line. This is conservative because a realistic evaluation of the transient shows that the region outside the core shroud would become exhausted of liquid well before the theoretical "collapsed" level would reach the recirculation line elevation.
- The quasi-steady critical flow break area through which the reactor coolant can escape to the drywell is the sum of the areas of the recirculation line, cleanup line and broken loop jet pump nozzles. The following sketch shows the sources of the total break area used for the containment system response to recirculation line break accident.



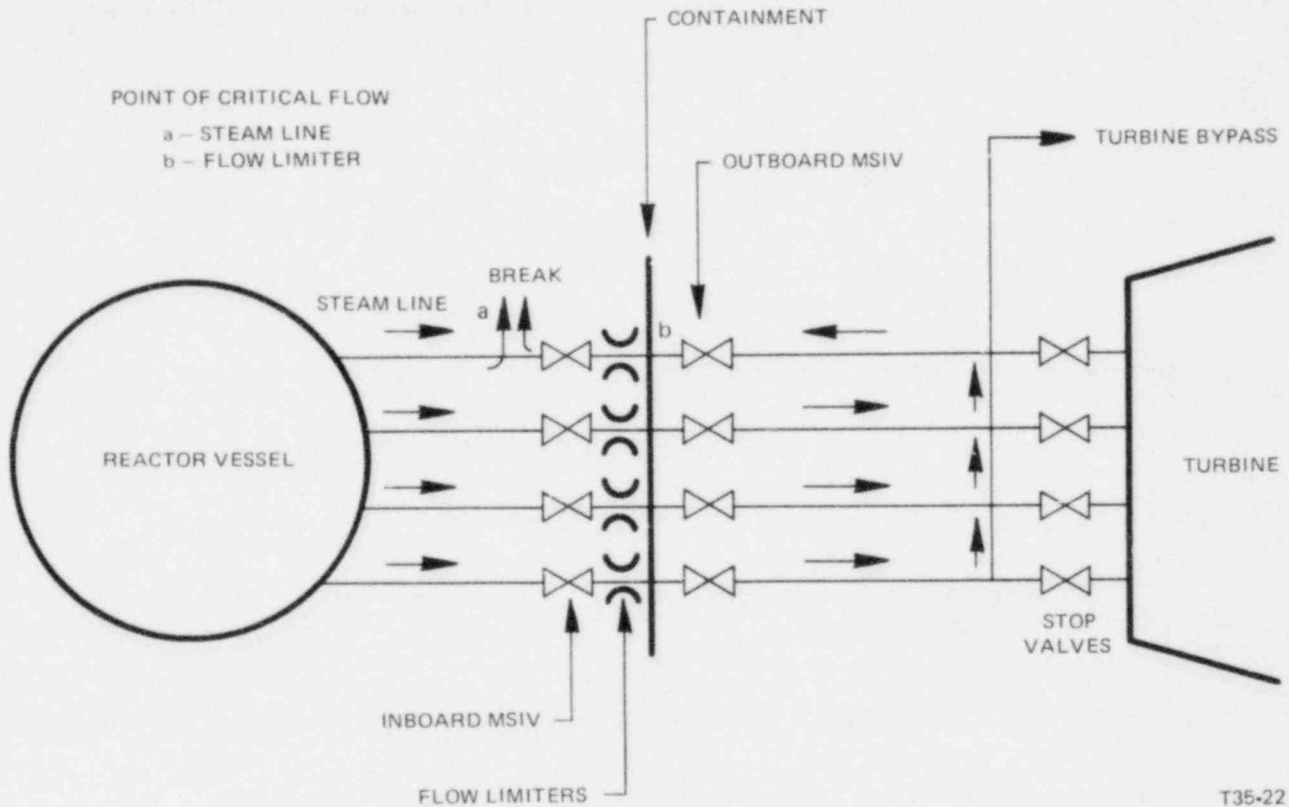
- The main steam line isolation valves are assumed to start closing at 0.5 second after the accident, and the valves are assumed to be fully closed in 3 seconds following closure initiation. With fast closure of these valves, the reactor vessel is maintained at a high pressure, which maximizes the discharge of high-energy steam and water into the drywell.

When analyzing a **steam line break** the following break-dependent assumptions are used.

- Immediately following the postulated rupture of a main steam line, the total steam flow leaving the reactor accelerates to approximately twice rated steam flow. The resulting mismatch between the steam leaving the vessel and the steam being generated in the core would cause a depressurization of the reactor vessel at approximately 50 psi/second. This depressurization will result in the formation of bubbles within the reactor vessel water inventory which in turn would result in a rapid increase in the water level. At some time after the break, the level will reach the elevation of the steam nozzles and the reactor blowdown would change from steam to a two-phase mixture of liquid and steam. When calculating the two-phase blowdown flow rate, it is assumed that the quality of the two-phase flow corresponds to the over-all average vessel quality. This is conservative because it results in fluid qualities which are considerably lower than those that would actually occur and peak drywell pressure increases with decreasing break flow quality. The time at which the two-phase break flow would start (the so called level rise time) was evaluated using the detailed reactor primary system thermal-hydraulic model described in Reference 5.

A parametric study of level rise time as a function of reactor power level and break size was performed. The parametric studies showed the level rise time could be anywhere from 1.5 to 4 seconds depending upon reactor size, reactor power level, etc. For containment pressure calculations, a level rise time of 1.0 second is usually used for BWR/6-Mark III containment systems. The use of this lower bound number is conservative because the calculated drywell pressure increases as the level rise time decreases.

- The critical flow break area through which reactor coolant can escape to the drywell is the sum of the pipe line flow area and the flow limiter flow area. The following sketch shows the sources of the total break area used for containment system response to a main steam line break design basis accident.



T35-22

The main steam line isolation valves (MSIV) initiation signals are generated approximately 0.5 second after the break occurs. After 4.2 seconds the isolation valves in the broken line will have closed sufficiently so that the valve flow area will be equal to the flow restrictor area. At that time, the point of critical flow will move from the flow restrictor to the valve flow area. Subsequent closure of the valves in the broken line will terminate flow from this side of the break. This will occur 5.5 seconds after the postulated failure of the main steam line. Figure 2-2 shows the effective blowdown area transient.

For a recirculation line break an MSIV closure time of 3 seconds was used to maximize reactor vessel pressure. For the steam line break a longer MSIV closure time is used to maximize the duration of flow limiter discharge.

- Turbine stop valves close 0.2 second after the accident due to high reactor water level. Since any steam flow to the turbine tends to reduce the reactor pressure and thus reduces the break flow rate, fast closure of the turbine stop valves is a conservative assumption.

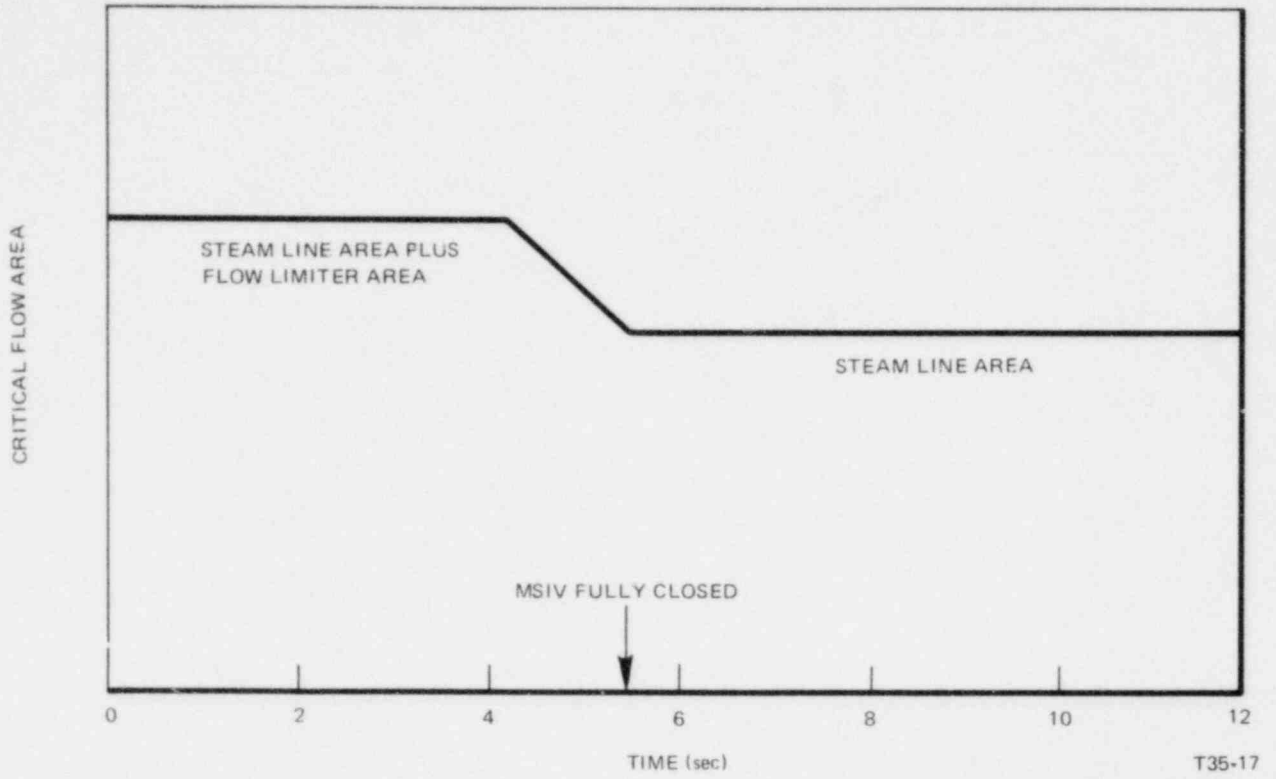


Figure 2-2. Blowdown Area Associated with a Main Steam Line Rupture

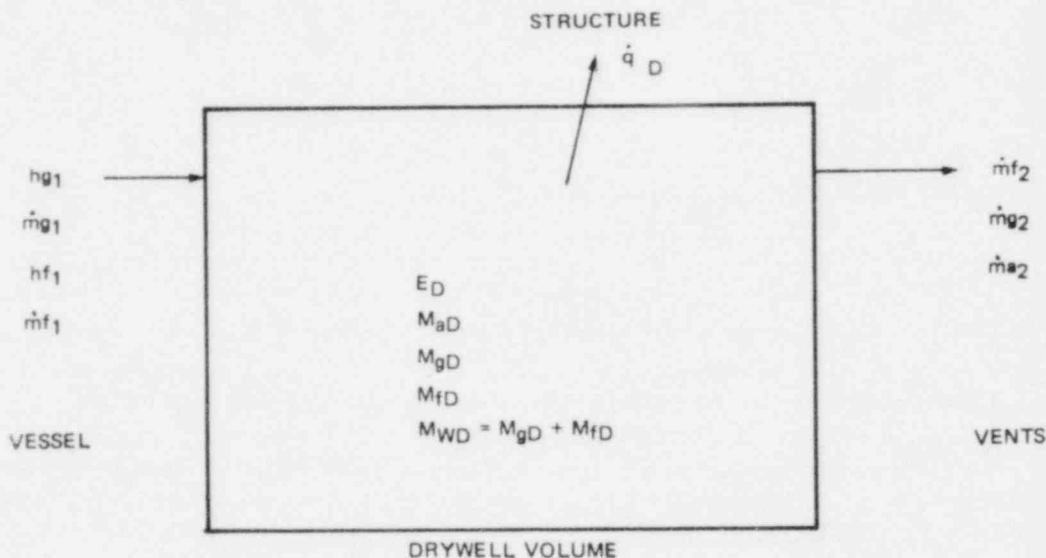
3. MARK III DRYWELL ANALYTICAL MODEL

3.1 DERIVATION OF EQUATIONS

Following the postulated break in the primary system, the fluid entering the Mark III drywell will result in a rapid increase in the drywell pressure. This pressure will cause the water initially in the vent system to be expelled. Once this has been accomplished, flow of air, vapor, and liquid will pass through the vents into the suppression pool. The equations and assumptions used to simulate the drywell conditions during the loss-of-coolant accident are presented in this section.

The over-all approach to the simulation of the Mark III drywell transient is to assume the drywell to be a single-pressure system whose total energy and mass of air, vapor, and water are known at all times from an integration of the various flows across the system boundary. The equations presented are solved with the finite time step techniques outlined in Section 8.

Consider the system shown in the following sketch:



Where

- E_D = Total internal energy of air and water in the drywell, Btu
- M_{aD} = Mass of air in drywell, lb
- M_{gD} = Mass of water vapor in drywell, lb
- M_{fD} = Mass of liquid water in drywell, lb
- \dot{m}_{g1} = Flow rate of steam entering the drywell from the primary system, lb/sec
- h_{g1} = Enthalpy of steam entering the drywell from the primary system, Btu/lb.
- \dot{m}_{f1} = Flow rate of liquid water entering the drywell from the primary system, lb/sec
- h_{f1} = Enthalpy of liquid water entering the drywell from the primary system, Btu/lb
- \dot{q}_D = Heat transfer rate to the drywell structure, Btu/sec
- \dot{m}_{f2} = Flow rate of liquid water leaving the drywell through the vents, lb/sec
- \dot{m}_{g2} = Flow rate of steam leaving the drywell through the vents, lb/sec
- \dot{m}_{a2} = Flow rate of air leaving the drywell through the vents, lb/sec

The rate of change of total energy in the fluids in the drywell equals the algebraic sum of the energy of the fluids entering and leaving the drywell and the energy transferred to the drywell structure. The flow leaving the drywell is assumed to be at the drywell temperature, T_D .

$$\frac{dE_D}{dt} = \dot{E}_D = h_{g1} \dot{m}_{g1} + h_{f1} \dot{m}_{f1} - h_g(T_D) \dot{m}_{g2} - h_f(T_D) \dot{m}_{f2} - C_{va}(T_D + 460) \dot{m}_{a2} - \dot{q}_D \quad (3-1)$$

A mass balance on the water gives

$$\frac{dM_{wD}}{dt} = \dot{M}_{wD} = \dot{m}_{g1} + \dot{m}_{f1} - \dot{m}_{g2} - \dot{m}_{f2} \quad (3-2)$$

and on the air gives:

$$\frac{dM_{aD}}{dt} = \dot{M}_{aD} = - \dot{m}_{a2} \quad (3-3)$$

where

- \dot{E}_D = Rate of change of total drywell energy
- \dot{M}_{wD} = Rate of change of drywell water inventory
- \dot{M}_{aD} = Rate of change of drywell air inventory

At any time during the transient these derivatives can be evaluated and thus the values of E_D , M_{wD} and M_{aD} , at the end of the time step being considered, can be calculated. These values are then used to calculate the new drywell temperature and pressure; this process depends upon the thermodynamic conditions in the drywell.

During the time at which the peak drywell pressure occurs, the thermodynamic condition in the drywell can be either a homogeneous mixture of air, saturated vapor and water, or a homogeneous mixture of air and superheated vapor. The type of break together with the assumptions made concerning the energy exchange between the two phases existing in the drywell determines which of the two homogeneous mixtures will exist at any particular time in the transient. As the numerical integration proceeds, there is a continuous check of the drywell atmosphere.

With known end-of-time-step values of E_D , M_{wD} , and M_{aD} , the corresponding drywell temperature and pressure cannot be evaluated until the thermodynamic condition of the drywell constituents is known (i.e., whether the water phase is saturated or superheated). To determine this, a temperature extrapolation is performed based on the calculated energy derivative and assuming that energy is approximately proportional to temperature. Using the extrapolated drywell temperature the quality of the water phase in the drywell is calculated to determine whether conditions are superheated.

$$X = \frac{v - v_f}{v_g - v_f} \quad (3-3a)$$

where

$$v = \frac{v}{M_w} \quad (3-3b)$$

and v_g and v_f are saturated properties at T . If $X \leq 1.0$, then saturated conditions exist; if $X > 1.0$, the drywell is filled with superheated steam, which is assumed to be in thermodynamic equilibrium with air.

Having made this determination, the exact drywell temperature and pressure may now be calculated; the following is a detailed description of this procedure for saturated and superheated conditions, respectively.

3.1.1 Saturated Conditions in Drywell ($X \leq 1.0$)

Assuming that the steam and liquid water in the drywell follow the saturation line and that thermodynamic equilibrium exists between the steam, liquid, and air, i.e., all three phases are at the same temperature, the total energy in the air and water in the drywell is:

$$E_D = \left[e_f + \frac{e_{fg}}{v_{fg}} \left(\frac{V_D}{M_{wD}} - v_f \right) \right] M_{wD} + C_{va} (T_D + 460) M_{aD} \quad (3-4)$$

Where:

- e_f = Saturated liquid internal energy, Btu/lb
- e_{fg} = Latent internal energy of vaporization, Btu/lb
- v_{fg} = Saturated vapor specific volume, minus saturated liquid specific volume, ft^3/lb
- V_D = Volume of drywell, ft^3
- M_{wD} = Total mass of water, both liquid and steam, in drywell, lb
- v_f = Specific volume of saturated liquid, ft^3/lb
- C_{va} = Specific heat of air (assumed constant), Btu/lb- $^{\circ}\text{F}$
- T_D = Temperature of steam, liquid and air in drywell, $^{\circ}\text{F}$.

Solving Equation (3-4) for the fluid temperature gives:

$$T_D = -460 + \frac{E_D}{C_{va} M_{aD}} - \frac{M_{wD}}{C_{va} M_{aD}} \left[e_f + \frac{e_{fg}}{v_{fg}} \left(\frac{V_D}{M_{wD}} - v_f \right) \right] \quad (3-5)$$

At any instant, the total energy, E_D , and masses, M_{wD} , and M_{aD} are known but the saturation properties are functions of the unknown temperature T_D . This relationship yields a transcendental expression which cannot be solved algebraically, but requires an iterative solution, i.e., keep guessing T_D until Equation (3-5) is satisfied.

With known temperatures, the steam quality in the drywell can be determined from the saturation properties.

$$X_D = \frac{V_D/M_{wD} - v_f(T_D)}{v_{fg}(T_D)} \quad (3-6)$$

Where:

- X_D = Steam quality in the drywell.
- $v_f(T_D)$ = Specific volume of fluid evaluated at a saturation temperature T_D , ft^3/lb

The mass of liquid water in the drywell is by definition of steam quality:

$$M_{fD} = (1 - X_D) M_{wD} \quad (3-7)$$

The volume occupied by the liquid water in the drywell is

$$V_{fD} = M_{fD} \cdot v_f(T_D) \quad (3-8)$$

Where:

$$V_{fD} = \text{Volume of liquid water in drywell, ft}^3$$

The volume available for the gases is the total drywell volume minus the liquid volume.

$$V_{aD} = V_D - V_{fD} \quad (3-9)$$

Where:

$$V_{aD} = \text{Volume occupied by the gases in the drywell, ft}^3$$

The partial pressure of the air in the drywell can then be found using the state equation for air:

$$P_{aD} = \frac{M_{aD} \cdot R_a \cdot (T_D + 460)}{144 V_{aD}} \quad (3-10)$$

Where:

$$P_{aD} = \text{Partial pressure of air in drywell, psi}$$

$$R_a = \text{Gas constant for air}$$

The water partial pressure is found from the saturation line at the drywell temperature:

$$P_w = P_{sat} \quad (3-11)$$

Where:

$$P_w = \text{Partial pressure of water vapor in drywell, psi}$$

The total pressure in the drywell is the sum of the air and water partial pressures:

$$P_D = P_{aD} + P_w \quad (3-12)$$

Where:

$$P_D = \text{Total pressure in drywell, psia}$$

The saturated conditions in the drywell at the end of the time step are thus fully defined and the process can be repeated for the next time step.

3.1.2 Superheated Conditions in Drywell ($X > 1.0$)

If for the extrapolated drywell temperature T , the quality in the drywell is calculated to be greater than 1.0, then the drywell contains a mixture of air and superheated vapor. Under these conditions, the total energy in the air and vapor is given by:

$$E_D = M_{wD} e_v + C_{va} (T_D + 460) M_{aD} \quad (3-13)$$

Where:

e_v = superheated vapor internal energy, Btu/lb

Solving Equation (3-13) for the vapor temperature gives:

$$T_D = -460 + \frac{E_D}{C_{va} M_{aD}} - \frac{M_{wD} e_v}{C_{va} M_{aD}} \quad (3-14)$$

At the end of any time step, the total energy, E_D , and masses, M_{wD} and M_{aD} , are known but the superheated vapor enthalpy is a function of the unknown temperature T_D . This relationship yields a transcendental expression which requires an iterative solution. Having iteratively solved for T_D enables the partial pressure of air and vapor in the drywell to be found.

Using the state equation for air:

$$P_{aD} = \frac{M_{aD} \cdot P_a \cdot (T_D + 460)}{144 \cdot V_{aD}} \quad (3-15)$$

The superheated vapor partial pressure, P_v , is found from the superheated properties at the drywell temperature.

$$P_v = P_{sup} \quad (3-16)$$

Where:

P_v = Partial pressure of superheated vapor in drywell, psi

The total pressure in the drywell is the sum of air and vapor partial pressures.

$$P_D = P_{aD} + P_v \quad (3-17)$$

The superheated conditions in the drywell at the end of the time step are thus fully defined and the process can be repeated for the next time step.

In summary, for either a homogeneous mixture of air and saturated liquid and vapor, or a homogeneous mixture of air and superheated vapor the transient drywell pressure and temperature can be calculated.

3.2 ASSUMPTIONS

The following assumptions are employed when using the above equations to simulate the response of a Mark III drywell to a postulated loss-of-coolant accident.

1. When simulating the drywell response to a recirculation line break accident, it is assumed that the drywell atmosphere consists of a saturated mixture of air, water, and steam in thermodynamic equilibrium.
2. Immediately following a steam line break, the blowdown flow will be saturated reactor steam. As discussed in Section 2, the rapid reactor vessel depressurization associated with steam blowdown will cause the reactor water level to rise and the level is assumed to reach the elevation of the main steam line nozzles 1 second after the break. This will result in the blowdown flow changing from steam to a two-phase mixture of reactor steam and water. Prior to the two-phase flow at 1 second, the decompressing reactor steam is assumed to become superheated and the drywell temperature and pressure are evaluated by the iteration procedure discussed in Subsection 3.1. Immediately following the two-phase flow, the decompressing reactor steam and liquid will remain in the saturated state and at typical drywell pressures the liquid will decompress to approximately 40%

steam by weight. At the time this two-phase blowdown starts, the drywell is full of superheated steam and noncondensable gases at calculated temperatures approaching 330°F; if instantaneous and complete mixing between these gases and the two-phase blowdown flow is assumed, then there will be a drywell pressure decrease of up to 2 psi when two-phase flow begins. This decrease results from the assumptions of complete mixing and thermodynamic equilibrium which in effect causes the decompressed reactor liquid (which is at approximately 225°F) to evaporatively cool the high-temperature steam and air.

Because it results in lower peak calculated drywell pressures, the assumption of instantaneous homogenous mixing is modified for a period immediately following the start of two-phase flow. When calculating the drywell pressure it is assumed that the decompressed reactor liquid does not contribute to the drywell thermodynamic transient. This involves deleting the h_f, \dot{m}_f term in Equation (3-1). However, in order to maintain conservation of mass and energy, the blowdown liquid is continuously monitored and is used when calculating the drywell density for the vent flow model. This monitored mass also allows for a subsequent return to the assumption of homogenous mixing in the drywell following the peak calculated drywell pressure. Thus following the start of two-phase flow, only saturated steam will be mixing with the high-temperature mixture of superheated steam and air in the drywell. This procedure eliminates the discontinuity in the calculated drywell pressure transient and provides yet another conservatism in peak calculated drywell pressure.

3. The composition of the fluid entering the vent system is a homogeneous mixture of the fluid in the drywell. Similarly, the assumption of homogeneous flow results in a high flow rate of liquid droplets into the vents. This is conservative since it results in high pressure losses in the vents.
4. No heat is lost from the contained gases. In actual practice there would be some condensation of the drywell steam on the surfaces of the drywell and vent system but since this would reduce the peak drywell pressure, it is ignored in the calculations.

4. HORIZONTAL VENT CLEARING MODEL

The analytical model used to simulate the vent clearing response of the vent system to a loss-of-coolant accident is presented in this section.

4.1 MODEL DERIVATION AND KEY ASSUMPTIONS

The integral form of the continuity and momentum equations applied to a series of control volumes establishes the basis of the following derivation of the horizontal vent clearing model.

The Mark III containment horizontal vents are modeled as shown in Figure 4-1. P_D is the drywell pressure and control volumes 1, 2, and 3 represent the annulus of water between the weir and the drywell wall. The three rows of horizontal vents are represented by control volumes 4, 5, and 6. P_S is the pressure above the suppression pool and the vent submergence depths are specified by H_1 , H_2 , and H_3 .

The laws which are applied to the control volumes of Figure 4-1 are:

Conservation of Mass
Equation of Continuity
Momentum Theorem

The form of these equations⁶ is as follows:

1. Conservation of Mass as applied to individual control volumes.

$$\frac{\partial (M_{cv})}{\partial t} = \int dW_{in} - \int dW_{out} \quad (1)$$

2. Equation of Continuity as applied to control volume junctions.

$$\int \rho V_n dA_{in} = \int \rho V_n dA_{out} \quad (2)$$

3. Momentum Theorem as applied to individual control volumes.

$$\frac{\partial (M V_x)_{cv}}{\partial t} + \int V_x dW_{out} - \int V_x dW_{in} = \sum F_x gc \quad (3)$$

The major assumptions made regarding the application of these formula are:

1. Flow is one-dimensional
2. Flow is non-steady
3. Flow is incompressible
4. Friction is negligible

Although friction is assumed to be negligible, irreversible losses are included for the turning losses the fluid experiences when flowing from the annulus into a horizontal vent. The assumption of one-dimensional and incompressible flow allows the integral form of the governing equations to be reduced to the following forms:

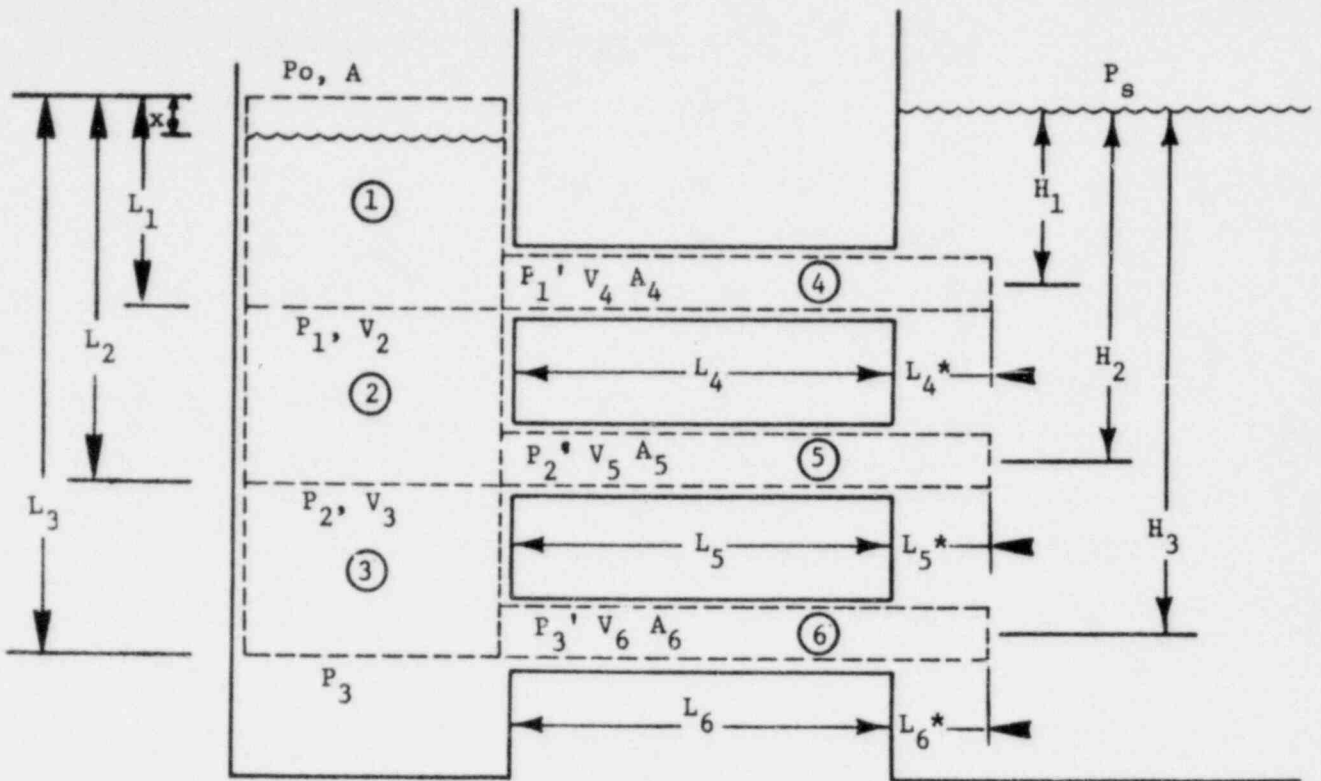


Figure 4-1. Three-Vent Control Volumes

1. Conservation of Mass as applied to individual control volumes.

$$\frac{d(M_{cv})}{dt} = W_{in} - W_{out} \quad (4)$$

2. Equation of Continuity as applied to control volume junctions.

$$\rho V_n A_{in} = \rho V_n A_{out} \quad (5)$$

3. Momentum Theorem as applied to individual control volumes.

$$\frac{d(M V_x)_{cv}}{dt} + V_x W_{out} - V_x W_{in} = \sum F_x \quad (6)$$

The vent clearing transient is broken up into several parts, depending on which control volumes have cleared.

PART 1, control volume 1 uncleared.

Examine control volume 1.

1. Conservation of Mass:

$$W_{in} = 0 \quad (7)$$

$$W_{out} = \rho V_2 A + \rho V_4 A_4 \quad (8)$$

Thus from Equation (4):

$$\frac{dm}{dt} = -\rho V_2 A - \rho V_4 A_4 \quad (9)$$

2. Equation of Continuity applied between control volumes 1, 2, and 4:

$$\rho V_n A_{in} = \rho \frac{dx}{dt} A \quad (10)$$

$$\rho V_n A_{out} = \rho V_2 A + \rho V_4 A_4 \quad (11)$$

Thus from Equation (5):

$$\rho \frac{dx}{dt} A = \rho V_2 A + \rho V_4 A_4 \quad (12)$$

and dividing thru by ρA gives:

$$\frac{dx}{dt} = V_2 + V_4 \frac{A_4}{A} \quad (13)$$

3. Momentum Theorem:

$$V_x W_{in} = 0 \quad (14)$$

Note that the momentum flux is the product of the mass flux (regardless of its direction) times the velocity in the direction the momentum theorem is being applied; thus we have:

$$V_x W_{out} = V_2 \rho V_2 A + V_2 \rho V_4 A_4 \quad (15)$$

Thus from Equation (6)

$$\frac{d(M V_x)}{dt} + \rho V_2^2 A + \rho V_2 V_4 A_4 - 0 = g_c \sum F_x \quad (16)$$

Or, expanding the first term:

$$M \frac{d V_x}{dt} + V_x \frac{dm}{dt} + \rho V_2^2 A + \rho V_2 V_4 A_4 = g_c \sum F_x \quad (17)$$

The mass in the control volume is

$$M = \rho A (L_1 - x) \quad (18)$$

And also:

$$V_x = \frac{dx}{dt} \quad (19)$$

Then putting Equations (9), (18), and (19) into Equation (17):

$$\begin{aligned} \rho A (L_1 - x) \frac{d^2 x}{dt^2} + \frac{dx}{dt} (-\rho V_2 A - \rho V_4 A_4) + \rho V_2^2 A \\ + \rho V_2 V_4 A_4 = g_c \sum F_x \end{aligned} \quad (20)$$

The forces acting on the control volume in the x direction are the net pressure difference and the body weight:

$$\sum F_x = P_D A - P_1 A + \rho A (L_1 - x) \frac{g}{g_c} \quad (21)$$

Then putting Equations (13) and (21) into Equation (20) we have:

$$\begin{aligned} \rho A (L_1 - x) \frac{d^2 x}{dt^2} + \frac{dx}{dt} \left(-\frac{dx}{dt} \right) + \rho V_2^2 A + \rho V_2 V_4 A_4 \\ = g_c A (P_D - P_1) + \rho A (L_1 - x) g \end{aligned} \quad (22)$$

Dividing Equation (22) by ρA and rearranging results in:

$$\frac{d^2 x}{dt^2} = \frac{\frac{g_c}{\rho} (P_D - P_1) + (L_1 - x) g + \left(\frac{dx}{dt} \right)^2 - V_2^2 - V_2 V_4 \frac{A_4}{A}}{(L_1 - x)} \quad (23)$$

Squaring Equation (13) we see

$$\left(\frac{dx}{dt} \right)^2 = V_2^2 + 2 V_2 V_4 \frac{A_4}{A} + \left(V_4 \frac{A_4}{A} \right)^2 \quad (24)$$

Substituting Equation (24) into (23) and simplifying results in:

$$\boxed{\frac{d^2 x}{dt^2} = \frac{\frac{g_c}{\rho} (P_D - P_1) + (L_1 - x) g + V_4 \frac{A_4}{A} \frac{dx}{dt}}{L_1 - x}} \quad (25)$$

Thus the acceleration of the upper surface is known if P_1 is known. It will be solved for in terms of other known quantities in what follows below.

Note that by taking d/dt of Equation (13):

$$\boxed{\frac{d^2 x}{dt^2} = \frac{d V_2}{dt} + \frac{A_4}{A} \frac{d V_4}{dt}} \quad (26)$$

Examine control volume 2.

1. Conservation of Mass:

$$W_{in} = \rho V_2 A$$

$$W_{out} = \rho V_3 A + \rho V_5 A_5 \quad (27)$$

Thus from Equation (4):

$$\frac{dm}{dt} = \rho V_2 A - \rho V_3 A - \rho V_5 A_5 \quad (28)$$

2. Equation of Continuity applied between control volumes 2, 3, and 5:

$$\rho V_n A_{in} = \rho V_2 A \quad (29)$$

$$\rho V_n \dot{m}_{out} = \rho V_3 A + \rho V_5 A_5 \quad (30)$$

Thus from Equation (5):

$$\rho V_2 A = \rho V_3 A + \rho V_5 A_5 \quad (31)$$

Putting Equation (31) into Equation (28) we find:

$$\frac{dm}{dt} = 0 \quad (32)$$

And dividing (31) by $A \rho$ gives:

$$V_2 = V_3 + V_5 \frac{A_5}{A} \quad (33)$$

3. Momentum Theorem:

$$V_x W_{in} = V_2 \rho V_2 A \quad (34)$$

$$V_x W_{out} = V_3 \rho V_3 A + V_5 \rho V_5 A_5 \quad (35)$$

Thus from Equation (6):

$$\frac{d(M V_x)}{dt} + \rho V_3^2 A + \rho V_3 V_5 A_5 - \rho V_2^2 A = g_c \sum F_x \quad (36)$$

And expanding the first term:

$$M \frac{dV_x}{dt} + V_x \frac{dm}{dt} + \rho V_3^2 A + \rho V_3 V_5 A_5 - \rho V_2^2 A = g_c \sum F_x \quad (37)$$

The mass in the control volume is:

$$M = \rho A (L_2 - L_1) \quad (38)$$

And also:

$$V_x = V_2 \quad (39)$$

Then putting Equations (32), (38), and (39) into Equation (37):

$$\rho A (L_2 - L_1) \frac{dV_2}{dt} + \rho V_3^2 A + \rho V_3 V_5 A_5 - \rho V_2^2 A = g_c \sum F_x \quad (40)$$

The forces acting on control volume 2 are similar to those acting on 1:

$$\sum F_x = P_1 A - P_2 A + \rho A (L_2 - L_1) \frac{g}{g_c} \quad (41)$$

Then putting Equation (41) into (40) we have:

$$\rho A (L_2 - L_1) \frac{dV_2}{dt} + \rho V_3^2 A + \rho V_3 V_5 A_5 - \rho V_2^2 A = g_c A (P_1 - P_2) + \rho A (L_2 - L_1) g \tag{42}$$

Dividing Equation (42) by ρA and rearranging results in:

$$\frac{dV_2}{dt} = \frac{\frac{g_c}{\rho} (P_1 - P_2) + (L_2 - L_1) g + V_2^2 - V_3^2 - V_3 V_5 \frac{A_5}{A}}{L_2 - L_1} \tag{43}$$

Squaring Equation (33) we see:

$$V_2^2 = V_3^2 + 2 V_3 V_5 \frac{A_5}{A} + \left(V_5 \frac{A_5}{A} \right)^2 \tag{44}$$

Substituting Equation (44) into (43) and simplifying we find:

$$\frac{dV_2}{dt} = \frac{\frac{g_c}{\rho} (P_1 - P_2) + (L_2 - L_1) g + V_2 V_5 \frac{A_5}{A}}{L_2 - L_1} \tag{45}$$

Finally we take d/dt of Equation (33) to obtain:

$$\frac{dV_2}{dt} = \frac{dV_3}{dt} + \frac{A_5}{A} \frac{dV_5}{dt} \tag{46}$$

Examine control volume 3.

1. Conservation of Mass

$$W_{in} = \rho V_3 A \tag{47}$$

$$W_{out} = \rho V_6 A_6 \tag{48}$$

Thus from Equation (4):

$$\frac{dm}{dt} = \rho V_3 A - \rho V_6 A_6 \tag{49}$$

2. Equation of Continuity applied between control volumes 3 and 6

$$\rho V_n A_{in} = \rho V_3 A \tag{50}$$

$$\rho V_n A_{out} = \rho V_6 A_6$$

Thus from Equation (5):

$$\rho V_3 A = \rho V_6 A_6 \quad (51)$$

Putting Equation (51) into Equation (49) we find:

$$\frac{dm}{dt} = 0 \quad (52)$$

Dividing Equation (51) by $A \rho$ gives:

$$V_3 = V_6 \frac{A_6}{A} \quad (53)$$

3. Momentum Theorem:

$$V_x W_{in} = V_3 \rho V_3 A \quad (54)$$

$$V_x W_{out} = 0 \quad (55)$$

(Note that V_x out the bottom = 0)

Thus from Equation (6):

$$\frac{d(M V_x)}{dt} + 0 - \rho V_3^2 A = g_c \sum F_x \quad (56)$$

Expand the first term:

$$M \frac{d V_x}{dt} + V_x \frac{dm}{dt} - \rho V_3^2 A = g_c \sum F_x \quad (57)$$

The mass in the control volume is:

$$M = \rho A (L_3 - L_2) \quad (58)$$

And also:

$$V_x = V_3 \quad (59)$$

Then putting Equations (52), (58), and (59) into Equation (57) we have:

$$\rho A (L_3 - L_2) \frac{d V_3}{dt} - \rho V_3^2 A = g_c \sum F_x \quad (60)$$

The forces acting on control volume 3 in the x direction are similar to those acting on 1 and 2:

$$\sum F_x = P_2 A - P_3 A + \rho A (L_3 - L_2) \frac{g}{g_c} \quad (61)$$

Then putting Equation (61) into (60) we have:

$$\rho A (L_3 - L_2) \frac{d V_3}{dt} - \rho V_3^2 A = g_c A (P_2 - P_3) + \rho A (L_3 - L_2) g \quad (62)$$

Dividing Equation (62) by ρA and rearranging:

$$\frac{dV_3}{dt} \frac{g_c}{\rho} \frac{(P_2 - P_3) + (L_3 - L_2)g + V_3^2}{L_3 - L_2} \quad (63)$$

And by taking d/dt of Equation (53) we have:

$$\frac{dV_3}{dt} = \frac{A_6}{A} \frac{dV_6}{dt} \quad (64)$$

Examine control volume 4.

1. Conservation of Mass

$$W_{in} = \rho V_4 A_4 \quad (65)$$

$$W_{out} = \rho V_4 A_4 \quad (66)$$

Thus from Equation (4):

$$\frac{dm}{dt} = \rho V_4 A_4 - \rho V_4 A_4 = 0 \quad (67)$$

2. Momentum Theorem

$$V_x W_{in} = V_4 \rho V_4 A_4 \quad (68)$$

$$V_x W_{out} = V_4 \rho V_4 A_4 \quad (69)$$

Thus from Equation (6):

$$\frac{d(M V_x)}{dt} + \rho V_4^2 A_4 - \rho V_4^2 A_4 = g_c \sum F_x \quad (70)$$

Expanding the first term:

$$M \frac{dV_x}{dt} + V_x \frac{dm}{dt} = g_c \sum F_x \quad (71)$$

The mass in the control volume is:

$$M = \rho A_4 (L_4 + L_4^*) \quad (72)$$

And:

$$V_x = V_4 \quad (73)$$

Then putting Equations (67), (72), and (73) into Equation (71) we have:

$$\rho A_4 (L_4 + L_4^*) \frac{dV_4}{dt} = g_c \sum F_x \quad (74)$$

The only forces acting in the direction of the momentum theorem are the two pressure forces:

$$\sum F_x = P_1' A_4 - \left(P_s + H_1 \rho \frac{g}{g_c} \right) A_4 \quad (75)$$

From a total pressure balance we see that:

$$P_1 + \frac{\rho V_2^2}{2 g_c} - K_1 \frac{\rho V_4^2}{2 g_c} = P_1' + \frac{\rho V_4^2}{2 g_c} \quad (76)$$

Solving Equation (76) for P_1' :

$$P_1' = P_1 + \frac{\rho V_2^2}{2 g_c} - \frac{(1 + K_1) \rho V_4^2}{2 g_c} \quad (77)$$

Substituting Equation (77) into Equation (75) we have:

$$\sum F_x = A_4 \left[P_1 + \frac{\rho V_2^2}{2 g_c} - \frac{(1 + K_1) \rho V_4^2}{2 g_c} - P_s - H_1 \rho \frac{g}{g_c} \right] \quad (78)$$

Putting Equation (78) into Equation (74):

$$\rho A_4 (L_4 + L_4^*) \frac{dV_4}{dt} = g_c A_4 \left[P_1 + \frac{\rho V_2^2}{2 g_c} - \frac{(1 + K_1) \rho V_4^2}{2 g_c} - P_s - H_1 \rho \frac{g}{g_c} \right] \quad (79)$$

Dividing thru by ρA_4 and rearranging:

$$\boxed{\frac{dV_4}{dt} = \frac{g_c}{\rho} \frac{(P_1 - P_s) + \frac{V_2^2}{2} - \frac{(1 + K_1) V_4^2}{2} - H_1 g}{L_4 + L_4^*}} \quad (80)$$

Examine control volume 5.

Control volume 5 is similar to control volume 4 and thus we write by inspection:

$$\boxed{\frac{dV_5}{dt} = \frac{g_c}{\rho} \frac{(P_2 - P_s) + \frac{V_3^2}{2} - \frac{(1 + K_2) V_5^2}{2} - H_2 g}{L_5 + L_5^*}} \quad (81)$$

Examine control volume 6.

Control volume 6 is similar to 4 and 5 except that:

$$P_3' = P_3 - \frac{(1 + K_3) \rho V_6^2}{2 g_c} \tag{82}$$

And thus we write:

$$\frac{d V_6}{dt} = \frac{\frac{g_c}{\rho} (P_3 - P_5) - \frac{(1 + K_3) V_6^2}{2} - H_3 g}{L_6 + L_6^*} \tag{83}$$

With the series of equations in boxes we have a system of nine equations and nine unknowns. We now proceed to solve for unknowns P_1 , P_2 , and P_3 . Some of the tedious algebraic manipulations will not be shown.

Putting Equations (63) and (83) into Equation (64) and solving for P_3 :

$$P_3 = \frac{A (L_6 + L_6^*) \left[\frac{g_c}{\rho} P_2 + (L_3 - L_2) g + V_3^2 \right] + A_6 (L_3 - L_2)}{\frac{g_c}{\rho} \left[A (L_6 + L_6^*) + A_6 (L_3 - L_2) \right]} \tag{84}$$

$$\left[\frac{g_c}{\rho} P_5 + \frac{(1 + K_3)}{2} V_6^2 + H_3 g \right]$$

Put Equations (45), (63), and (81) into (46) and solve for P_2 .

First, let the following identities be defined:

$$B = A (L_6 + L_6^*) \tag{85}$$

$$C = A_6 (L_3 - L_2) \tag{86}$$

$$D = \frac{A_4 (L_2 - L_1)}{A (L_4 + L_4^*)} \tag{87}$$

$$E = \frac{A_5 (L_2 - L_1)}{A (L_5 + L_5^*)} \tag{88}$$

$$L_{21} = \frac{L_2 - L_1}{L_1 - x} \tag{89}$$

$$L_{23} = \frac{L_2 - L_1}{L_3 - L_2} \tag{90}$$

Then we find:

$$\begin{aligned}
 P_2 = & \frac{P_1 + \frac{\rho}{g_c} \frac{A_5}{A} V_5 V_2 - L_{23} \frac{\rho}{g_c} V_3^2 + \frac{L_{23} \cdot B}{B+C} \left[(L_3 - L_2) \frac{\rho g}{g_c} + \frac{\rho}{g_c} V_3^2 \right]}{\left[1 + L_{23} + E - \frac{L_{23} B}{(B+C)} \right]} \\
 & + \frac{L_{23} \cdot C}{B+C} \left[P_5 + \frac{(1+K_3) \rho V_6^2}{2 g_c} + \frac{H_3 \rho g}{g_c} \right] - E \left[\frac{\rho}{2 g_c} V_3^2 - \frac{(1+K_2)}{2 g_c} \rho V_5^2 \right. \\
 & \left. - \frac{H_2 \rho g}{g_c} - P_5 \right]
 \end{aligned} \tag{91}$$

Put Equations (45), (63), (81), (84), and (91) into Equation (46) and solve for P_1 :

$$\begin{aligned}
 P_1 = & \frac{\left[L_{21} P_D \left(1 + L_{23} - L_{23} \frac{B}{B+C} + E \right) + P_5 \left(D + L_{23} D - L_{23} D \frac{B}{B+C} \right. \right. \\
 & \left. \left[L_{21} + D + L_{23} + L_{21} L_{23} + L_{23} D - L_{23} \frac{B}{B+C} - L_{21} L_{23} \frac{B}{B+C} \right. \right. \\
 & \left. \left. + L_{23} \frac{C}{B+C} + DE + E \right) + \frac{H_1 \rho g}{g_c} \left(D + L_{23} D - L_{23} D \frac{B}{B+C} + DE \right) \right. \\
 & \left. \left. - L_{23} D \frac{B}{B+C} + L_{21} E + DE + E \right] \right. \\
 & \left. + E \frac{H_2 \rho g}{g_c} + L_{23} \frac{C}{(B+C)} \frac{H_3 \rho g}{g_c} + \frac{B}{(B+C)} \frac{(L_2 - L_1) \rho g}{g_c} \right. \\
 & \left. + \frac{\rho}{g_c} \frac{A_4 V_4}{A} \frac{dx}{dt} \left(L_{21} + L_{21} L_{23} - L_{21} L_{23} \frac{B}{B+C} + L_{21} E \right) \right. \\
 & \left. - \frac{\rho V_2^2}{2 g_c} \left(D + L_{23} D - L_{23} D \frac{B}{B+C} + DE \right) + \frac{\rho V_3^2}{g_c} \left(L_{23} \frac{B}{B+C} \right. \right. \\
 & \left. \left. - L_{23} - \frac{E}{2} \right) + \frac{(1+K_1) \rho V_4^2}{2 g_c} \left(D + L_{23} D - L_{23} D \frac{B}{B+C} + ED \right) \right. \\
 & \left. + E \frac{(1+K_2) \rho V_5^2}{2 g_c} + L_{23} \frac{C}{(B+C)} \frac{(1+K_3) \rho V_6^2}{2 g_c} \right. \\
 & \left. + \frac{\rho A_5}{g_c A} V_5 V_2 \left(L_{23} \frac{B}{B+C} - L_{23} - E \right) \right]
 \end{aligned} \tag{92}$$

Calculation of the transient from $t = 0$ to $t = T_1$.

Initial conditions:

$$t = 0, x = 0$$

$$\frac{dx}{dt} = V_2 = V_3 = V_4 = V_5 = V_6 = 0$$

Final conditions:

$$t = T_1 \text{ (defined when } x = L_1)$$

$$V_2 = V_{21}, V_3 = V_{31}, V_4 = V_{41}, V_5 = V_{51}, V_6 = V_{61}$$

Procedure:

- 1) Solve Equation (92) for P_1
- 2) From Equation (26) get d^2x/dt^2 ; then

$$\frac{dx}{dt} = \int_0^t \frac{d^2x}{dt^2} dt \text{ and } x = \int_0^t \frac{dx}{dt} dt$$

- 3) Solve Equation (91) for P_2
- 4) From Equation (45) get dV_2/dt ; and $V_2 = \int_0^t \frac{dV_2}{dt} dt$
- 5) Solve Equation (84) for P_3
- 6) From Equation (63) get dV_3/dt ; and $V_3 = \int_0^t \frac{dV_3}{dt} dt$
- 7) From Equation (80) get dV_4/dt ; and $V_4 = \int_0^t \frac{dV_4}{dt} dt$
- 8) From Equation (81) get dV_5/dt ; and $V_5 = \int_0^t \frac{dV_5}{dt} dt$
- 9) From Equation (83) get dV_6/dt ; and $V_6 = \int_0^t \frac{dV_6}{dt} dt$

PART 2, Clearing a horizontal vent.

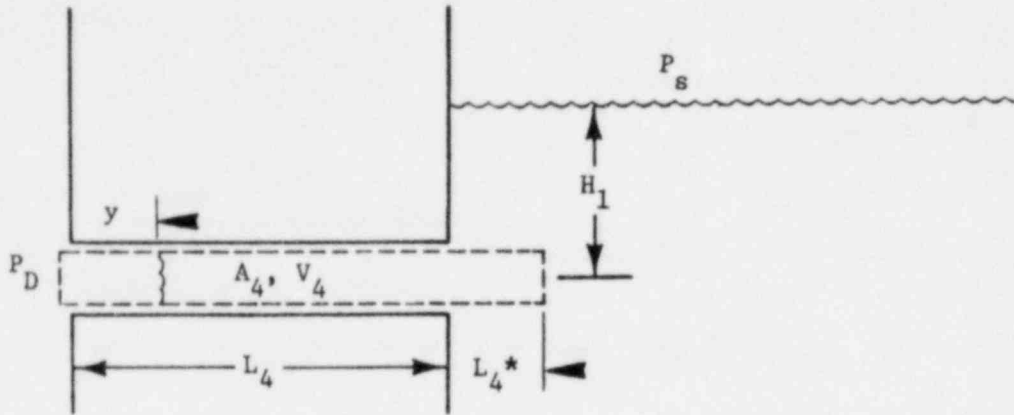


Figure 4-2. Control Volume 4

Examine control volume 4:

1. Conservation of Mass:

$$W_{in} = 0 \tag{93}$$

$$W_{out} = \rho V_4 A_4 \tag{94}$$

Thus from Equation (4):

$$\frac{dm}{dt} = -\rho V_4 A_4 \tag{95}$$

2. Equation of Continuity:

$$\rho V_n A_{in} = \rho \frac{dy}{dt} A_4 \tag{96}$$

$$\rho V_n A_{out} = \rho V_4 A_4 \tag{97}$$

Thus from Equation (5):

$$\rho \frac{dy}{dt} A_4 = \rho V_4 A_4 \tag{98}$$

and dividing thru by ρA_4 gives:

$$\frac{dy}{dt} = V_4 \tag{99}$$

3. Momentum Theorem:

$$V_y W_{in} = 0 \tag{100}$$

$$V_y W_{out} = V_4 \rho V_4 A_4 \tag{101}$$

Thus from Equation (6):

$$\frac{d(M V_y)}{dt} + \rho V_4^2 A_4 - 0 = g_c \sum F_y \quad (102)$$

Or, expanding the first term:

$$M \frac{dV_y}{dt} + V_y \frac{dm}{dt} + \rho V_4^2 A_4 = g_c \sum F_y \quad (103)$$

The mass in the control volume is:

$$M = \rho A_4 (L_4 - y + L_4^*) \quad (104)$$

And also note:

$$V_y = \frac{dy}{dt} \quad (105)$$

Then putting Equations (95), (99), (104), and (105) into Equation (103):

$$\rho A_4 (L_4 - y + L_4^*) \frac{d^2 y}{dt^2} = g_c \sum F_y \quad (106)$$

The forces acting on the control volume in the y direction are simply the two pressures at the ends:

$$\sum F_y = A_4 P_D - A_4 \left(P_s + \frac{H_1 \rho g}{g_c} \right) \quad (107)$$

Then putting Equation (107) into (106) we have:

$$\rho A_4 (L_4 - y + L_4^*) \frac{d^2 y}{dt^2} = g_c A_4 P_D - g_c A_4 \left(P_s + \frac{H_1 \rho g}{g_c} \right) \quad (108)$$

Dividing Equation (107) by ρA_4 and rearranging gives:

$$\boxed{\frac{d^2 y}{dt^2} = \frac{g_c (P_D - P_s) - H_1 g}{L_4 - y + L_4^*}} \quad (109)$$

Calculation of transient from $t = T_1$ to $t = T_1 + T_1^*$.

T_1^* is defined as the time to clear the top horizontal vent. The vent is defined as being clear when $y = L_4$.

Solve Equation (109) for d^2y/dt^2 ; then:

$$\frac{dy}{dt} = V_{41} + \int_{T_1}^t \frac{d^2 y}{dt^2} dt \quad (110)$$

$$y = (t - T_1) V_{41} + \int_{T_1}^t \frac{dy}{dt} dt \quad (111)$$

PART 3, after $x = L_1$, but before $y = L_4$ and before $x = L_2$.

The situation is illustrated in Figure 4-3. Control volume 2 is now similar to control volume 1 in Part 1; thus we examine Equation (25) and from similarity we can write:

$$\frac{d^2 x}{dt^2} = \frac{\frac{g_c}{\rho} (P_D - P_2) + (L_2 - x) g + V_5 \frac{A_5}{A} \frac{dx}{dt}}{L_2 - x} \quad (112)$$

The Equations for dV_3/dt (63), dV_5/dt (81), and dV_6/dt (83) are unchanged from Part 1. As before, we solve for the unknown pressures P_2 and P_3 . Note that dV_2/dt now equals d^2x/dt^2 , and putting Equations (112), (63), and (81) into Equation (45) and solving for P_3 we find:

$$P_3 = P_2 + \frac{\rho V_3^2}{g_c} + \frac{A_5 (L_3 - L_2)}{A (L_5 + L_5^*)} \left[P_2 - P_5 + \frac{\rho V_3^2}{2 g_c} - \frac{(1 + K_2) \rho V_5^2}{2 g_c} - \frac{H_2 \rho g}{g_c} \right] - \frac{(L_3 - L_2)}{(L_2 - x)} \left[P_D - P_2 + \frac{A_5 \rho V_5}{A g_c} \frac{dx}{dt} \right] \quad (113)$$

Set Equation (113) equal to Equation (84) and solve for P_2 . First define the following terms:

$$F = \frac{A_5 (L_3 - L_2)}{A (L_5 + L_5^*)} \quad (114)$$

$$L_{32} = \frac{L_3 - L_2}{L_2 - x} \quad (115)$$

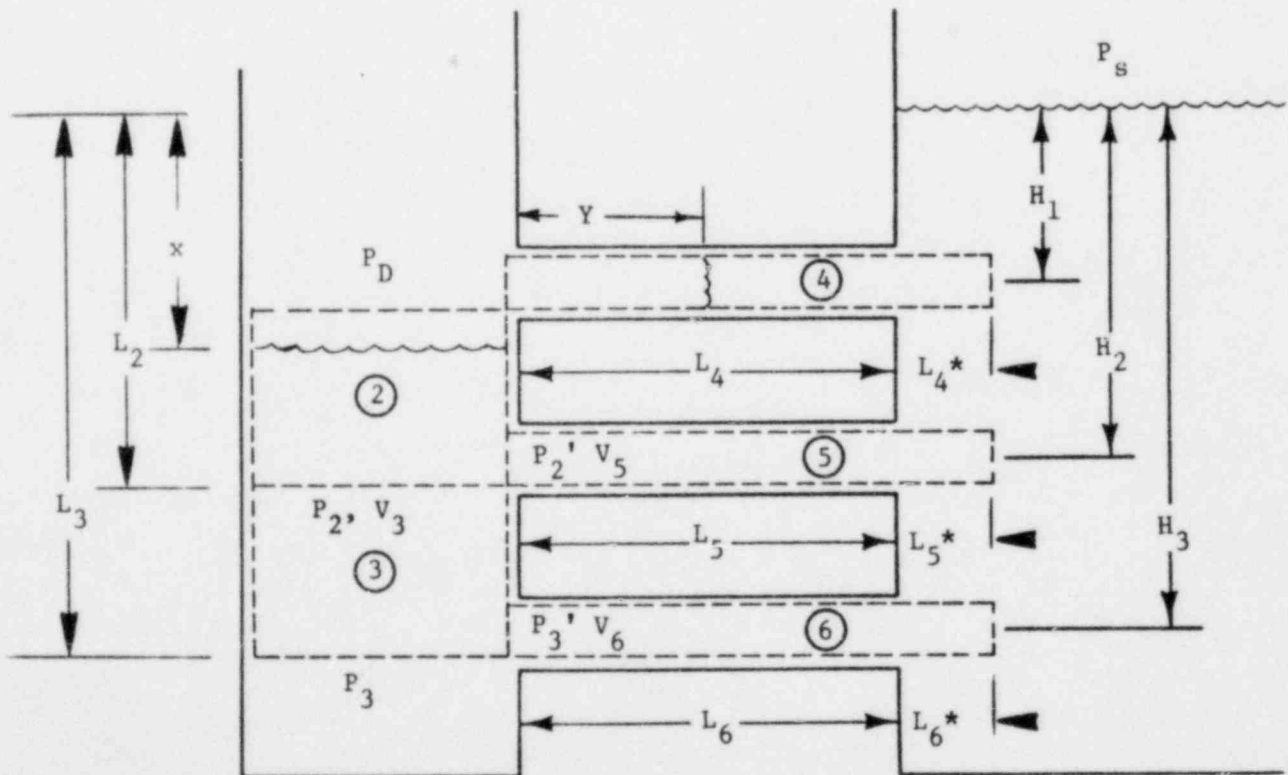


Figure 4-3. First Vent Uncovered

Then we find:

$$\begin{aligned}
 P_2 = & \frac{P_5 \left(F + \frac{C}{B+C} \right) + L_{32} P_D + \frac{\rho g}{g_c} \left[FH_2 + \frac{C}{B+C} H_3 + \frac{B(L_3 - L_2)}{B+C} \right]}{\left(1 + F + L_{32} - \frac{B}{B+C} \right)} \\
 & + \frac{\frac{\rho}{g_c} V_3^2 \left(\frac{B}{B+C} - 1 - \frac{F}{2} \right) + \frac{F(1+K_2)\rho V_5^2}{2g_c} + \frac{C}{(B+C)} \frac{(1+K_3)\rho V_6^2}{2g_c}}{\underline{\hspace{10em}}} \\
 & + \underline{L_{32} \frac{A_5}{A} \frac{\rho}{g_c} V_5 \frac{dx}{dt}}
 \end{aligned} \tag{116}$$

Calculation of transient time $t = T_1$ to $t = T_1 + T_1^*$ or $t = T_2$ (whichever comes first). T_2 is defined as time when $x = L_2$.

Initial conditions; $t = T_1$ and:

$$\begin{aligned}
 V_3 &= V_{31}, \quad \frac{dy}{dt} = V_{41}, \quad V_5 = V_{51} \\
 x &= L_1, \quad \frac{dx}{dt} = V_{21}, \quad V_6 = V_{61}
 \end{aligned}$$

Procedure:

1) Solve Equation (116) to get P_2

2) Get d^2x/dt^2 from Equation (112) and:

$$\frac{dx}{dt} = V_{21} + \int_{T_1}^t \frac{d^2x}{dt^2} dt; \quad x = L_1 + (t - T_1) V_{21} + \int_{T_1}^t \frac{dx}{dt} dt$$

3) Solve Equation (113) to get P_3

4) From Equation (63) get dV_3/dt and; $V_3 = V_{31} + \int_{T_1}^t \frac{dV_3}{dt} dt$

5) From Equation (109) get d^2y/dt^2 and;

$$\frac{dy}{dt} = V_{41} + \int_{T_1}^t \frac{d^2y}{dt^2} dt; \quad y = (t - T_1) V_{41} + \int_{T_1}^t \frac{dy}{dt} dt$$

6) From Equation (81) get dV_5/dt and; $V_5 = V_{51} + \int_{T_1}^t \frac{dV_5}{dt} dt$

7) From Equation (83) get dV_6/dt and; $V_6 = V_{61} + \int_{T_1}^t \frac{dV_6}{dt} dt$

Part 3a, case when $T_2 > T_1 + T_1^*$ (viz.: $y = L_4$ before $x = L_2$).

Equation of motion is similar to Equation (112) except that P_D is replaced by P'_D ; P'_D is less than P_D due to weir annulus entrance losses resulting from steam flow through the top vent. P'_D is calculated in terms of parameters continuously known.

$$P'_D = P_D - \frac{K \rho \dot{m}^2}{2g AW 144}$$

Where:

- k = Weir annulus entrance loss coefficient
- ρ = Drywell density
- \dot{m} = Mass flowrate through the top vent as calculated in Section 5
- AW = Weir annulus entrance area.

The equation expressing pressures P_3 and P_2 are similar to Equations (113) and (116), respectively, except that H_2 and H_3 are replaced by H_2' and H_3' . H_2' and H_3' are now equivalent heads corresponding to the hydrostatic head H_2 and H_3 plus a dynamic pressure ($P_{D_{yn.-1}}$). The dynamic pressure $P_{D_{yn.-1}}$ is a result of the suppression pool water being accelerated to accommodate the drywell air being injected into the suppression pool through one vent ($y = L_4$).

$$H_2' = H_2 + P_{D_{yn.-1}} \frac{144}{\rho}$$

$$H_3' = H_3 + P_{D_{yn.-1}} \frac{144}{\rho}$$

$P_{D_{yn.-1}}$ is a boundary condition evaluated by an analytical vent back pressure model discussed in Section 6. All other equations are the same except P'_D , H_2' , and H_3' replace P_D , H_2 , and H_3 , respectively. Continue transient as specified in Part 3 until $x = L_2$ (define $t = T_2$ when $x = L_2$).

At $t = T_2$, define:

$$V_3 = V_{32}$$

$$V_5 = V_{52}$$

$$V_6 = V_{62}$$

PART 4, case when $T_2 < T_1 + T_1^*$

(or, $x = L_2$ before $y = L_4$). The configuration is as shown in Figure 4-4.

Examine control volume 3.

1. Conservation of Mass:

$$W_{in} = 0 \tag{117}$$

$$W_{out} = \rho V_6 A_6 \tag{118}$$

Thus from Equation (4):

$$\frac{dm}{dt} = -\rho V_6 A_6 \tag{119}$$

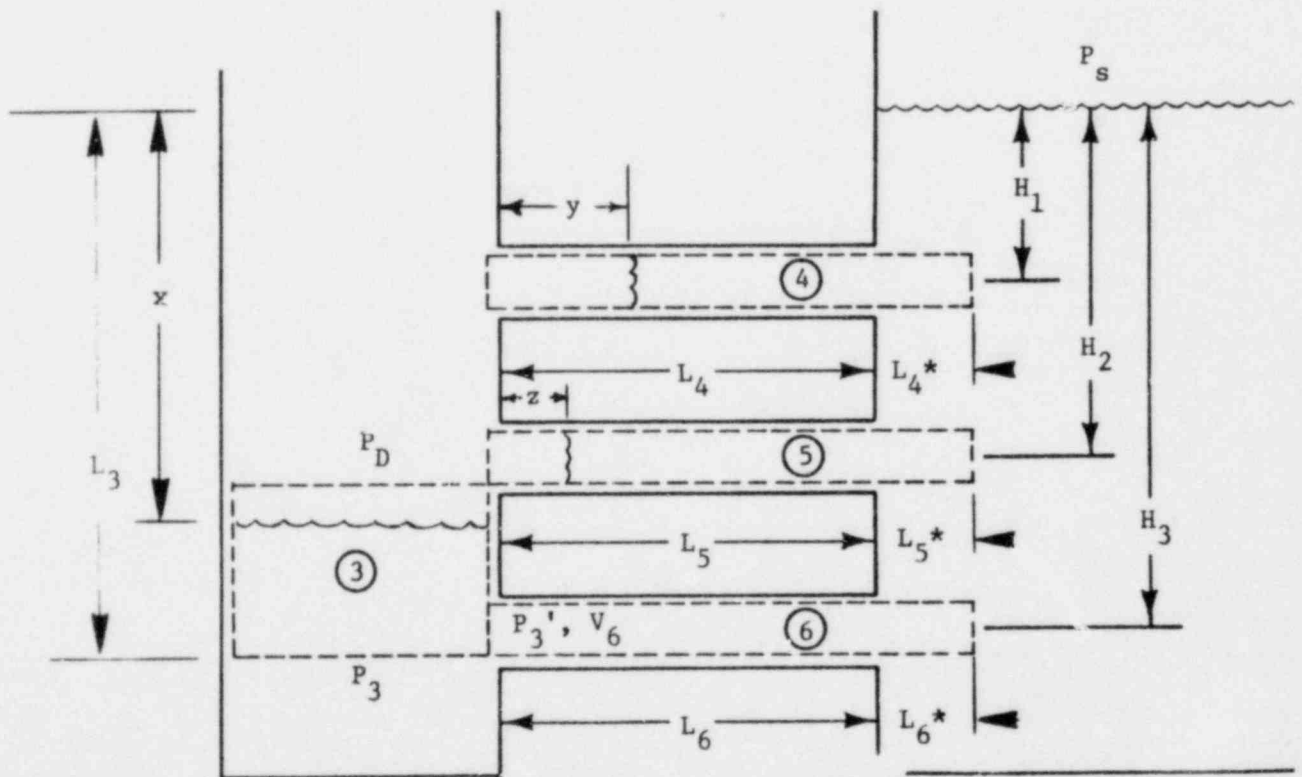


Figure 4-4. Second Vent Uncovered

2. Equation of Continuity applied between control volumes 3 and 6:

$$\rho V_n A_{in} = \rho \frac{dx}{dt} A \quad (120)$$

$$\rho V_n A_{out} = \rho V_6 A_6 \quad (121)$$

Thus from Equation (5):

$$\rho \frac{dx}{dt} A = \rho V_6 A_6 \quad (122)$$

dividing thru by ρA :

$$\frac{dx}{dt} = \frac{A_6}{A} V_6 \quad (123)$$

3. Momentum Theorem:

$$V_x W_{in} = 0 \quad (124)$$

$$V_x W_{out} = 0 \quad (125)$$

Thus from Equation (6):

$$\frac{d(M V_x)}{dt} = g_c \sum F_x \quad (126)$$

And expanding the first term:

$$M \frac{dV_x}{dt} + V_x \frac{dm}{dt} = g_c \sum F_x \quad (127)$$

The mass in the control volume:

$$M = \rho A (L_3 - x) \quad (128)$$

And we see:

$$V_x = \frac{dx}{dt} \quad (129)$$

Then putting Equations (119), (123), (128), and (129) into Equation (127) results in:

$$\rho A (L_3 - x) \frac{d^2x}{dt^2} + \frac{dx}{dt} \left(-\rho A \frac{dx}{dt} \right) = g_c \sum F_x \quad (130)$$

The forces acting on the control volume in the x direction are the pressure forces and the body weight:

$$\sum F_x = P_D A - P_3 A + \rho A (L_3 - x) \frac{g}{g_c} \quad (131)$$

Then putting Equation (131) into (130) we have:

$$\rho A (L_3 - x) \frac{d^2x}{dt^2} - \rho A \left(\frac{dx}{dt} \right)^2 = g_c A (P_D - P_3) + \rho A (L_3 - x) \quad (132)$$

Dividing Equation (132) by $A \rho$ and rearranging:

$$\frac{d^2x}{dt^2} = \frac{g_c (P_D - P_3) + (L_3 - x) g + \left(\frac{dx}{dt} \right)^2}{L_3 - x} \quad (133)$$

The equation for d^2y/dt^2 is still Equation (109) and from similarity we write:

$$\frac{d^2z}{dt^2} = \frac{g_c (P_D - P_3) - H_2 g}{L_5 - z + L_5^*} \quad (134)$$

The equation for dV_6/dt is still Equation (83). Noting that V_3 now equals dx/dt , we put Equation (83) and Equation (133) into Equation (64) and solve for P_3 :

$$P_3 = \frac{A (L_6 + L_6^*) \left[P_D + (L_3 - x) \frac{\rho g}{g_c} + \frac{\rho}{g_c} \left(\frac{dx}{dt} \right)^2 \right] + A_6 (L_3 - x) \left[P_5 + \frac{(1 + K_3) \rho V_6^2}{2 g_c} + \frac{H_3 \rho g}{g_c} \right]}{[A_6 (L_3 - x) + A (L_6 + L_6^*)]} \quad (135)$$

Transient from $t = T_2$ to $t = T_3$ ($t = T_3$ when $x = L_3$).

Initial conditions: at $t = T_2$

$$x = L_2, z = 0, \frac{dx}{dt} = V_{32}$$

$$\frac{dy}{dt} = V_{42}, \frac{dz}{dt} = V_{52}, V_6 = V_{62}$$

Continue d^2y/dt^2 from Equation (109).

Procedure:

- 1) Solve Equation (135) for P_3 .
- 2) From Equation (133) get d^2x/dt^2 and:

$$\frac{dx}{dt} = V_{32} + \int_{T_2}^t \frac{d^2x}{dt^2} dt; x = L_2 + (t - T_2) V_{32} + \int_{T_2}^t \frac{dx}{dt} dt$$

3) From Equation (134) get d^2z/dt^2 and:

$$\frac{dz}{dt} = V_{s2} + \int_{T_2}^t \frac{d^2z}{dt^2} dt ; z = (t - T_2) V_{s2} + \int_{T_2}^t \frac{dz}{dt} dt$$

4) From Equation (83) get $\frac{dV_6}{dt}$; $V_6 = V_{62} + \int_{T_2}^t \frac{dV_6}{dt} dt$

At any time during the transient, if $y = L_4$ then continue all equations with P_D , H_2 , and H_3 equal to P_D' , H_2' and H_3' , respectively. If $z = L_5$, then switch all

P_D' to P_D'' (P_D'' is calculated with \dot{m} equal to the flow through two vents, $y = L_4, z = L_5$). $P_D'' < P_D'$.

H_3' to H_3'' (more dynamic pressure with two vents injecting air into the suppression pool with one vent.)

$$H_3'' = H_3' + P_{Dyn.-2}$$

$P_{Dyn.-2}$ is the dynamic pressure resulting from air being injected into the suppression pool through two vents ($z = L_5$).

PART 5, after $x = L_3$. The situation is as shown in Figure 4-5. Continue d^2z/dt^2 from Equation (134). From similarity, we write:

$$\frac{d^2w}{dt^2} = \frac{g_c}{\rho} \frac{(P_D' - P_5) - H_3 g}{L_6 - w + L_6^*}$$

(136)

Calculate transient:

Initial conditions; $t = T_3, x = L_3$

$$W = 0, \frac{dw}{dt} = V_{63}$$

Calculate d^2w/dt^2 from (136) and:

$$\frac{dw}{dt} = V_{63} + \int_{T_3}^t \frac{d^2w}{dt^2} dt ; w = (t - T_3) V_{63} + \int_{T_3}^t \frac{dw}{dt} dt$$

When $z = L_5$, continue with $P_D' = P_D$ and $H_3' = H_3''$.

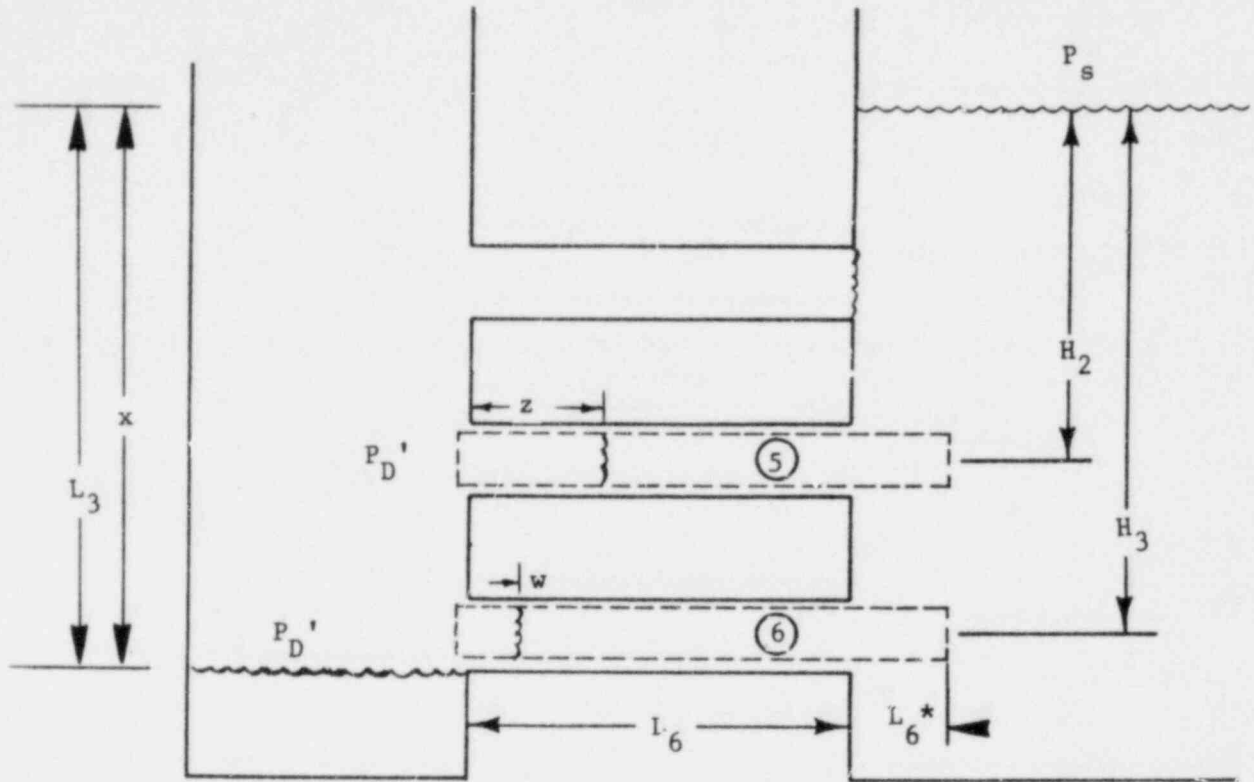
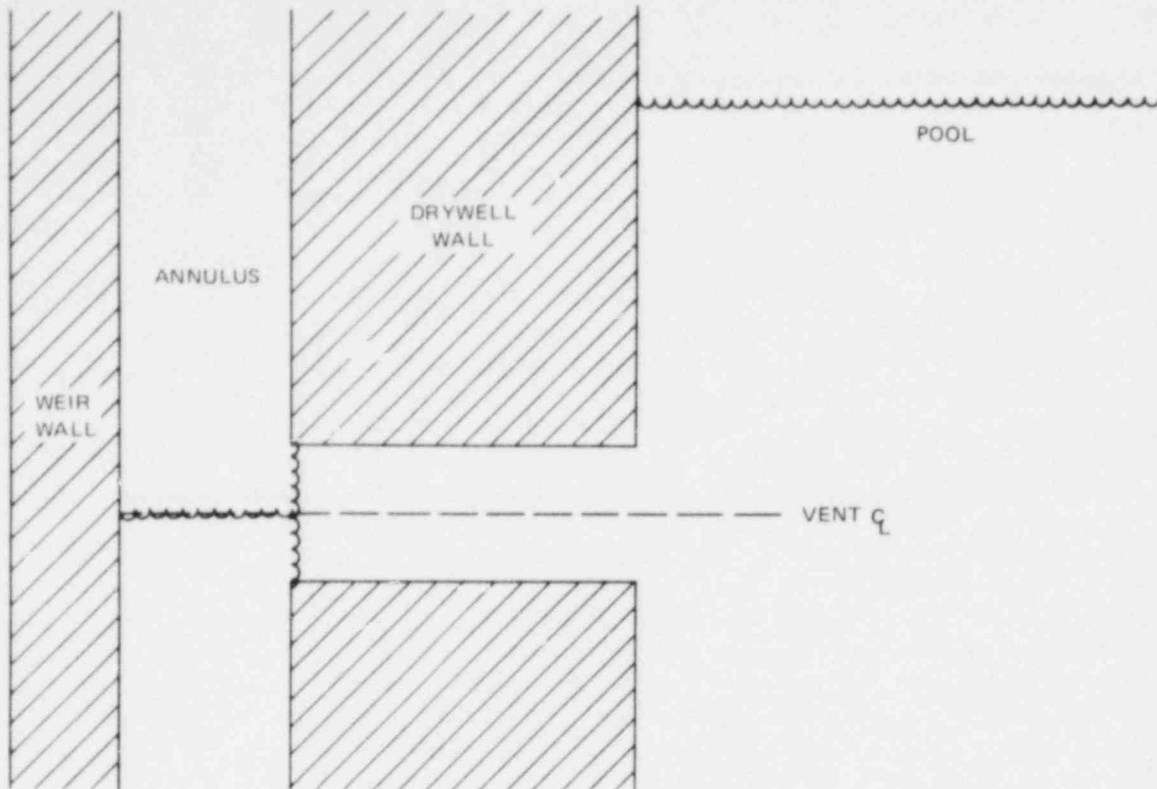


Figure 4-5. Third Vent Uncovered

4.2 ASSUMPTIONS

The key assumptions in the derivation of the vent clearing model are presented in Subsection 4.1. The key assumptions in the use of the model are:

1. For containment response analysis, it is assumed that the horizontal vent air-water interface starts to move when the air-water interface level in the annulus section is at the center line of the vent as shown in the following sketch.
2. Prior to vent clearing the pressure at each vent outlet is the containment air-space pressure plus the hydrostatic pressure head corresponding to that vent. At the instant a row of vents clears, the drywell air being injected into the pool produces a bubble. This bubble will attempt to expand and depressurize to the local hydrostatic pressure; during this expansion process the bubble will exert back pressure on the lower uncleared rows of vents. Since this will tend to delay clearing of these vents it represents a phenomenon which must be included in any conservative modeling of the vent clearing transient. The bubble pressure model is discussed in Section 6.
3. During the vent clearing transient, it is necessary to account for the apparent mass effect caused by the water in front of the submerged vent. This water has to be accelerated to make way for the water entering the pool from the vent system. This effect is accounted for in the vent clearing model by adding an equivalent length to each horizontal vent. The equivalent length for the horizontal vent clearing model is based on the equivalent lengths calculated for past pressure suppression systems; see Reference 2 for the procedure. For the standard Mark III containment system response, an equivalent-length-to-vent-diameter ratio of $L^*/D = 1.25$ is used.



T35-21

4. The suppression pool is assumed to be at high water level; this maximizes the amount of water in the vent system and therefore maximizes the calculated drywell pressure.
5. Toward the end of blowdown where the blowdown flow rates are diminishing, the horizontal vents are assumed to sequentially recover as the drywell-containment pressure differential reduces to the corresponding hydrostatic pressure of each row of vents. The recovery of the vents sequentially reduces the vent flow area between the drywell and containment; this sequential reduction in the vent area is considered when using the vent flow model (discussed in Section 5) to calculate vent flow rates.

4.3 EXPERIMENTAL VERIFICATION

All available PSTF one-, two-, and three-vent steam blowdown tests have been compared with the analytical vent clearing model and are presented in this section. During these tests both vent submergence and vessel blowdown area were parameterized. The vent center line submergence was varied between 2 and 12 feet. The vessel blowdown areas used were approximately 70, 100, and 200% of the DBA-scaled blowdown area of a typical BWR/6. All tests were performed on the large-scale PSTF; the one- and two-vent tests were performed tests involved blocking off the top and middle vents, and the top vent, respectively.

For the analytical comparisons the vent clearing model was isolated from the over-all pressure suppression containment system model and programmed with the necessary input which includes:

1. Experimentally measured drywell and containment pressure
2. Vent system and pool geometry
3. Initial submergence
4. Vent system loss coefficients, derived from data contained in Reference 7.

For these comparisons any vent back pressure effects other than containment pressure plus the associated hydrostatic head were neglected, unlike for the Mark III containment system analysis. This is a conservative procedure since the addition of any other vent back pressure would further delay the calculated vent clearing times.

Figure 4-6 is a plot of the analytically predicted versus experimentally measured vent clearing times for all available one-, two-, and three-vent steam blowdown tests. For the one-vent tests the bottom vent was used, for the two-vent tests the middle and bottom vent were used, and for the three-vent tests the top, middle, and bottom vents were used. The indicated experimentally determined vent clearing times represent the measurement obtained with a level probe located 6 inches from the end of the vent. The potential inaccuracy in defining vent clearing as the time at which the air-water interface passes a probe at this location is less than or equal to the scan accuracy of the data recording system. The vent clearing times plotted on Figure 4-6, with only one exception, are to the left (conservative side) of the diagonal. This indicates that the observed vent clearing transients are more rapid than those predicted by the model; this is an important factor since the drywell pressure profile is determined by the vent clearing times, and it is conservative for the vent clearing model to predict slow vent clearing. During a postulated steam line accident for a typical BWR/6-Mark III containment system, the three rows of vents sequentially uncover between 1 and 1.5 seconds after the break. At 1 and 1.5 seconds, the average conservatism of the vent clearing model, as demonstrated on Figure 4-6, is approximately 15 and 10%, respectively.

It should be emphasized that the comparison on Figure 4-6 was made by isolating the vent clearing model and providing it with the actual observed PSTF boundary conditions. Figure 4-6 indicates the conservatism of the vent clearing model itself; when evaluating the transient response of a Mark III containment system the conservatism of the vent clearing model is added to the other conservative models and assumptions discussed in this report. This conservatism gives confidence the vent clearing model will adequately simulate BWR/6-Mark III containment system vent clearing transients during a design basis accident.

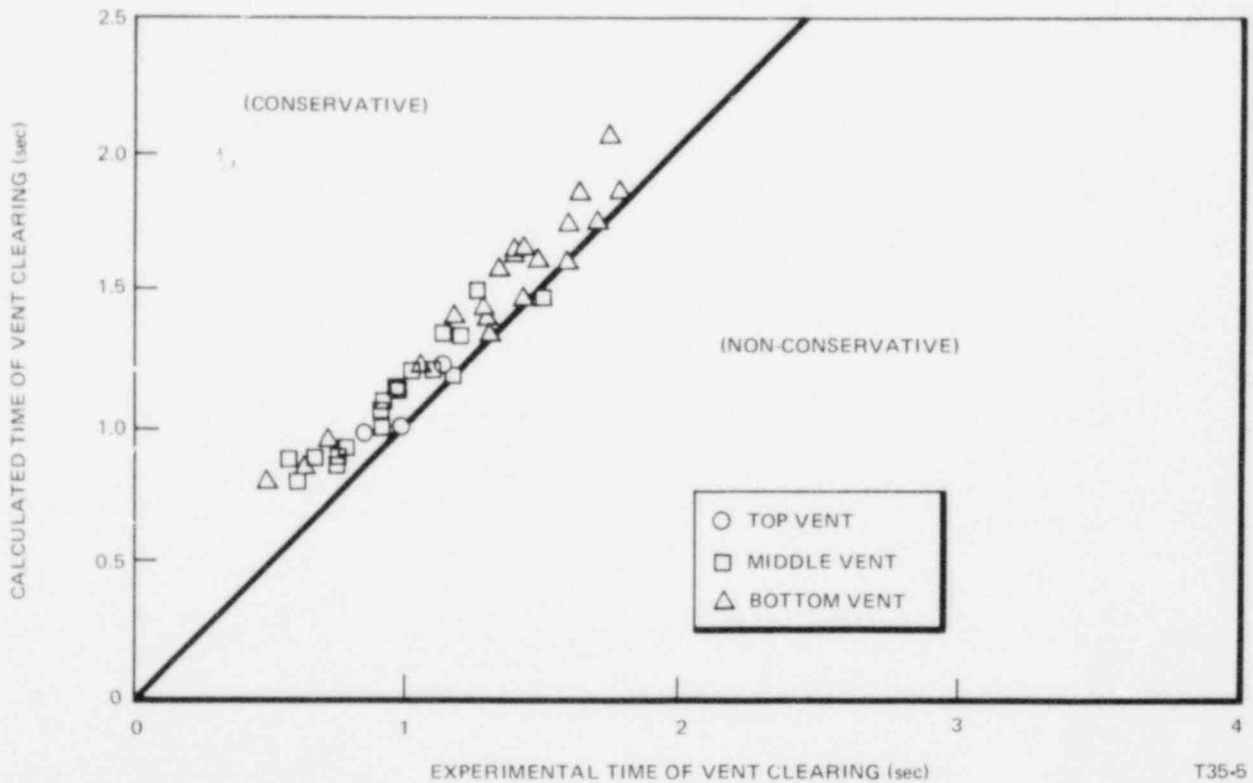


Figure 4-6. Large-Size Steam Blowdown Tests – 1, 2, and 3 Vents

5. VENT FLOW MODEL

5.1 INTRODUCTION

Following a loss-of-coolant accident inside the containment of a BWR, the pressure in the drywell will start to rise because of mass and energy entering from the primary system. This rising pressure will start to accelerate the water from the vent system into the suppression pool. The model used to simulate the dynamics of this process is the vent clearing analytical model presented in Section 4.

Once the increasing drywell pressure has accelerated enough water from the vent system to clear the first row of vents, the process of flow will begin; the problem now becomes one of calculating the rate at which the drywell constituents will flow through the open vents. Similarly, as the second and third rows of vents are cleared of water, the vent clearing model is sequentially replaced by the vent flow model; the following is a description of the vent flow model.

The equations used to simulate the flow in the vents are described in Subsection 5.3; the basic approach differs only slightly from the classical treatment of compressible adiabatic flow of a gas in a constant area duct with wall shear (e.g., Reference 6).

The over-all approach to the analytical simulation of the containment response is to continuously integrate the air, water vapor, and liquid in both the drywell and containment. Thus at any time during the transient, the pressures at both ends of the vent system are known; the following discussion presents a method of calculating the flow that will occur in the vents as a result of this pressure difference. This flow rate is then used to advance (over a very small time step) the integration of drywell and containment inventories.

5.2 ASSUMPTIONS

The following is a list of the major assumptions used in the derivation of the vent flow model.

- a. The flow at any point in time is steady state. The basis for this assumption is the relatively fast transit time in the vent (<100 msec) compared to the maximum drywell pressure rate of approximately 20 psi/sec.
- b. The flow is adiabatic in that no heat transfer occurs between the vent and the fluid flow. Again this assumption was made based on the rapid transit time in the vents.
- c. The quality in the vents does not vary with displacement.
- d. The steam phase can be approximated as an ideal gas.
- e. The sonic velocity of the mixture is the sonic velocity of the gaseous phase only. The basis for this is experimental data which show that for void fractions which are expected to occur in the Mark III containment system, the sonic velocity of the flow is not affected by the presence of liquid droplets.^{8,9,10,11} (During a liquid blowdown the reactor fluid will decompress to less than 40% steam by weight; the corresponding average void fraction will be in excess of 99%.) This void fraction of water in the vents, though small, was considered when the analytical model was being formulated.
- f. The effects of the liquid are considered in the momentum equation for calculating acceleration and local irreversible losses.
- g. Flow is one dimensional.
- h. Both phases have the same linear velocity (slip ratio = 1.0).
- i. Pressure changes within the vent due to gravity effects are negligible.

- j. The total vent flow area at any time corresponds to the number of horizontal vents that are uncovered. Constant flow area vents are used to simulate each of the uncovered vent rows.
- k. The vent exit pressure (i.e., back pressure) can be calculated with the pool dynamic model discussed in Section 6.

5.3 DERIVATION OF EQUATIONS

In this section, the equations used in the simulation of the vent flow following a loss-of-coolant accident will be derived. The over-all approach is to write the equations of Energy, State, Continuity and Momentum for an incremental length of the vent and to then solve them and integrate them along the length of the duct in such a way as to yield a means of evaluating the vent inlet and exit Mach numbers as a function of the pressure ratio across the vent. Since other portions of the overall containment response model are calculating the transient drywell and containment pressures, the pressure ratio across the vents is continuously known, thus the mass flow at any time can be evaluated from a knowledge of the current inlet Mach number and the fluid properties in the drywell.

In formulating the basic equations, the presence of liquid droplets in the flow requires a treatment of the energy equation that deviates from the ideal gas energy equation. The energy equation is described in the following Subsection 5.3.1. The momentum equation is central to the vent flow model and is derived in Subsection 5.3.2. The remaining basic equations and the derivation of the final solution are presented in Subsection 5.3.3. Nomenclature is given in Subsection 5.5.

5.3.1 Energy Equation

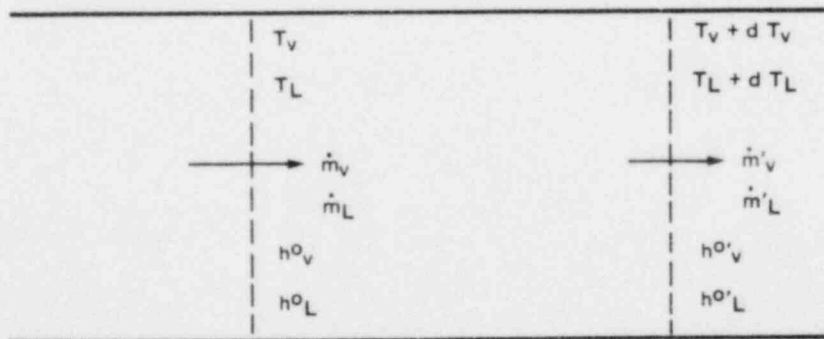
The energy equation for a perfect gas would be written

$$C_p dT + \frac{du^2}{2} = 0$$

i.e., total energy remains constant.

In the vent flow model, where both gas and liquid droplets are flowing, the assumption is made that the total energy is constant so that any decrease, say, in the stagnation enthalpy of the vapor phase is equal to the work done (increase in velocity) on the liquid phase.

Consider the vent flow across the control surfaces shown below:



where the subscripts L v refer to the liquid and vapor phase, respectively, and h^o is defined as the stagnation enthalpy; and where the prime indicates conditions at the exit section.

The stagnation enthalpy of any of the fluids is defined as:

$$h^{\circ} = h + \frac{u^2}{2}$$

or

$$h^{\circ} = C_p T + \frac{u^2}{2}$$

Hence:

$$h^{\circ}_L = h_L + \frac{u^2}{2}$$

$$h^{\circ}_v = h_v + \frac{u^2}{2}$$

$$h^{\circ\prime}_L = h'_L + \frac{(u + du)^2}{2}$$

$$h^{\circ\prime}_v = h'_v + \frac{(u + du)^2}{2}$$

and by definition (assumptions, a, b, c, h)

$$\dot{m}_L = \dot{m}'_L$$

$$\dot{m}_v = \dot{m}'_v$$

quasi steady-state

and the liquid and vapor velocities are equal. Thus the increase in vapor stagnation enthalpy flux is given by

$$\dot{m}'_v h^{\circ\prime}_v - \dot{m}_v h^{\circ}_v$$

i.e.,

$$\dot{m}'_v \left[h'_v + \frac{(u + du)^2}{2} \right] - \dot{m}_v \left[h_v + \frac{u^2}{2} \right]$$

which reduces to

$$\dot{m}_v [C_{p_v} dT_v + u du]$$

but

$$u du = \frac{1}{2} du^2$$

Thus the increase in vapor enthalpy flux reduces to

$$\dot{m}_v \left[C_{p_v} dT_v + \frac{1}{2} du^2 \right]$$

By similar reasoning, the increase in liquid droplet stagnation enthalpy flux is

$$\dot{m}_L \left[C_{p_L} dT_L + \frac{1}{2} du^2 \right]$$

but $dT_2 = 0$ by definition (there is no heat transfer from either the vapor or the duct to the liquid, assumption b) thus the increase in liquid enthalpy reduces to

$$\dot{m}_L \left[\frac{1}{2} du^2 \right] \quad \text{liquid does not thermally react}$$

Because energy is conserved

$$\dot{m}_v \left[C_{p_v} dT_v + \frac{1}{2} du^2 \right] + \dot{m}_L \frac{1}{2} du^2 = 0$$

If

$$X = \frac{\dot{m}_v}{\dot{m}_L + \dot{m}_v}$$

then the above equation reduces to

$$C_{p_v} dT_v + \frac{1}{2X} du^2 = 0 \quad (5-1)$$

In the general derivation described in Subsection 5.3.3, T_v becomes T . If Equation (5-1) is divided by $C_p T$ it becomes

$$\frac{dT}{T} + \frac{\beta}{2 C_p T} du^2 = 0 \quad (5-2)$$

remembering that

$$M^2 = \frac{u^2}{kRT}$$

and (for an ideal gas) k is constant

$$C_p = \frac{kR}{k-1}$$

then Equation (5-2) reduces to

$$\frac{dT}{T} + \frac{k-1}{2} M^2 \beta \frac{du^2}{u^2} \quad \left\{ \begin{array}{l} \text{relationship between vapor temp.} \\ \text{and vapor velocity for} \\ \text{conservation of energy} \end{array} \right. \quad (5-3)$$

where

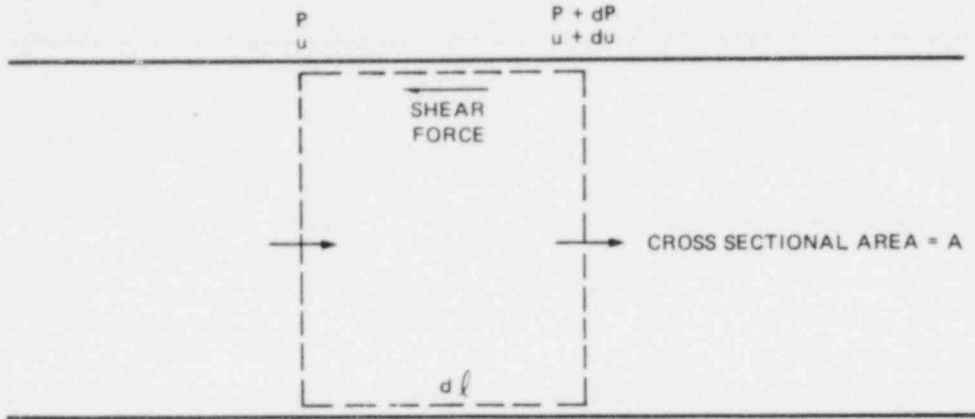
$$\beta = \frac{1}{X}$$

Equation (5-3) is the form of the energy equation which will be used in the general derivation presented in Subsection 5.3.3.

5.3.2 Momentum Equation

The momentum equation used in the analytical simulation of the vent flow is derived below. This is the classical derivation with the total density of the flow being used in both the acceleration and irreversible loss calculations.

Consider the flow across the control surfaces shown below



Pressure force on the control volume

$$= P A - (P + dP) A$$

$$= - dP A$$

Shear force due to wall friction

$$= - \frac{f \, dl}{D} \frac{u^2}{2g} \gamma A$$

$$f \approx \frac{\gamma_w}{\rho V^2 / 2}$$

where γ = Total density of flowing mixture.

The increase in momentum of the fluid as it flows through the control section is

$$(\gamma u A) \, du$$

Since net force is equal to the rate of creation of momentum, the following equation evolves

$$\gamma u \, du + dP + \gamma \frac{u^2}{2g} \cdot \frac{f \, dl}{D} = 0 \tag{5-4}$$

This is the form of the momentum equation that will be used in the general derivation presented in subsection 5.3.3.

5.3.3 General Solution

The preceding two sections derived the energy and momentum equations which are used in the vent flow model. These will now be combined with the other two governing equations, i.e., state and continuity; with the help of certain general thermodynamic identities, these equations will be solved to give a relationship between vent pressure ratio and inlet Mach number. Combination of this Mach number with the known drywell thermodynamic conditions will yield the mass flow rate into the vent system.

The momentum Equation (5-4) can be rewritten.

At any point, the total mass velocity, G , is given by

$$G = \gamma u$$

For steady-state flow, the conservation of mass (or continuity equation) becomes

$$dG = \gamma du + u d\gamma = 0$$

thus

$$\frac{du}{u} + \frac{d\gamma}{\gamma} = 0 \quad (5-5)$$

Also it can be seen that

$$\frac{du}{u} = \frac{2u}{2u} \frac{du}{u} = \frac{1}{2} \frac{du^2}{u^2} \quad (5-5a)$$

thus Equation (5-5) becomes

$$\frac{1}{2} \frac{du^2}{u^2} + \frac{d\gamma}{\gamma} = 0 \quad (5-6)$$

Equation (5-4) can be rewritten as

$$\gamma u du + dP + \gamma \frac{u^2}{2g} \frac{f d\ell}{D} = 0$$

Dividing by P and using $du/u = \frac{1}{2} du^2/u^2$ [from Equation (5-5a)] yields

$$\gamma \frac{u^2}{2P} \frac{du^2}{u^2} + \frac{dP}{P} + \frac{\gamma}{P} \frac{u^2}{2g} \frac{f d\ell}{D} = 0 \quad (5-7)$$

the definition of the sonic velocity can be written

$$C = \sqrt{k R T} = \sqrt{k P v}$$

Hence

$$M^2 = \frac{u^2}{C^2} = \frac{u^2}{k P v} = \frac{u^2 \rho}{k P}$$

where $\rho =$ gaseous phase density only (from assumption e)

Hence

$$\frac{\rho u^2}{P} = k M^2$$

Thus Equation (5-7) can be rewritten

$$\frac{\gamma}{\rho} \frac{kM^2}{2} \frac{du^2}{u^2} + \frac{dP}{P} + \frac{\gamma}{\rho} \frac{kM^2}{2g} \frac{f d\ell}{D} = 0 \quad (5-8)$$

From assumption d, the equation of state can be written, i.e.,

$$P V = m R T$$

or

$$P = \rho R T \quad (5-9)$$

by logarithmic differentiation, this can be rewritten

$$\frac{dP}{P} = \frac{d\rho}{\rho} + \frac{dT}{T} \quad (5-10)$$

This represents the last of the governing equations; hereafter, the derivation involves manipulating the above equations to arrive at an equation for inlet Mach number as a function of the pressure ratio across the vents. As will be seen, the algebra and integration produces two simultaneous equations in M_1 and M_2 (the inlet and outlet Mach numbers) which require an iterative solution. Readers who might wish to skip the algebra are referred to Equations (5-21) and (5-26) which are the two simultaneous equations in M_1 and M_2 . Examination of these equations shows that at all times, the other terms,

$$\rho, \gamma, k, \beta, \frac{f\ell}{D}, \frac{P_b}{P_d}$$

are known from either the current drywell/containment thermodynamic properties or system geometry. The equations can thus be solved.

Let us start on the algebra.

Eliminating $\frac{dT}{T}$ from Equations (5-10) and (5-3) gives

$$\frac{dP}{P} - \frac{d\rho}{\rho} + \frac{k-1}{2} M^2 \beta \frac{du^2}{u^2} = 0 \quad (5-11)$$

Because there is no slip, Equation (5-6) can also be applied to the vapor phase only, i.e.,

$$\frac{1}{2} \frac{du^2}{u^2} + \frac{d\rho}{\rho} = 0 \quad (5-12)$$

Thus combination of (5-12) and (5-11) yields

$$\frac{dP}{P} = -\frac{1}{2} [1 + (k-1)\beta M^2] \frac{du^2}{u^2} \quad (5-13)$$

or

$$\frac{du^2}{u^2} = \frac{-dP/P}{\frac{1}{2} [1 + (k-1)\beta M^2]} \quad (5-14)$$

Substituting (5-14) into (5-8) and reducing will yield

$$\frac{dP}{P} = - \frac{\frac{\gamma}{\rho} k M^2 [1 + (k-1) \beta M^2] \frac{f d\ell}{D}}{2g \left[1 + \left\{ (k-1) \beta - \frac{\gamma}{\rho} k \right\} M^2 \right]} \quad (5-15)$$

Now returning to the definition of Mach number, i.e.,

$$M^2 = \frac{u^2}{k R T}$$

This will yield, by logarithmic differentiation,

$$\frac{dM^2}{M^2} = \frac{du^2}{u^2} - \frac{dT}{T} \quad (5-16)$$

From (5-3)

$$-\frac{dT}{T} = - \frac{(k-1)}{2} \beta M^2 \frac{du^2}{u^2}$$

Combining the above two equations gives

$$\frac{dM^2}{M^2} = \frac{du^2}{u^2} \left[1 + \frac{(k-1)}{2} M^2 \beta \right] \quad (5-17)$$

Combining this and equation (5-13) gives

$$\frac{dP}{P} = - \left[\frac{1 + (k-1) M^2 \beta}{2 + (k-1) M^2 \beta} \right] \frac{dM^2}{M^2} \quad (5-18)$$

This is the first of two equations that will have to be integrated along the length of the vent. This integration is started with Equation (5-21a).

We will now proceed to derive the second equation that will require integration.

Equating Equations (5-18) and (5-15) gives

$$\frac{f d\ell}{D} = \frac{\left\{ 1 + \left[(k-1) \beta - \frac{\gamma}{\rho} k \right] M^2 \right\} \rho / \gamma dM^2}{k M^4 \left[1 + \frac{k-1}{2} M^2 \beta \right]} \quad (5-19)$$

This equation is now integrated from the duct inlet, 1, to the exit, 2.

$$\int_1^2 \frac{f d\ell}{D} = \int_1^2 \frac{\left\{ 1 + \left[(k-1) \beta - \frac{\gamma}{\rho} k \right] M^2 \right\} \rho / \gamma}{k M^4 \left[1 + \frac{k-1}{2} M^2 \beta \right]} dM^2 \quad (5-20)$$

(Note: This equation reduces to Equation (6-12) of Reference 8 when $\rho = \gamma$ and $\beta = 1$.)

The right hand integral is of the form $\int \frac{1 + ax}{x^2 (1 + bx)} dx$ and can be solved by rewriting it as

$$\int \frac{dx}{x^2 (1 + bx)} + \int \frac{a dx}{x (1 + bx)}$$

The results are

$$\begin{aligned} \frac{fL}{D} = & \frac{\rho}{\gamma k} \left[-\frac{1}{M^2} + \frac{(k-1)}{2} \beta \ln \left(\frac{1 + \frac{k-1}{2} \beta M^2}{M^2} \right) \right]_{M_1^2}^{M_2^2} \\ & - \frac{\rho \left\{ (k-1) \beta - \frac{\gamma}{\rho} k \right\}}{\gamma k} \left[\ln \frac{1 + \frac{k-1}{2} \beta M^2}{M^2} \right]_{M_1^2}^{M_2^2} \end{aligned}$$

Which yields

$$\boxed{\frac{fL}{D} = \frac{\rho}{\gamma k} \left[\frac{M_2^2 - M_1^2}{M_1^2 M_2^2} \right] + \left[1 - \frac{\rho \beta (k-1)}{\gamma 2k} \right] \ln \left[\frac{\left(1 + \frac{k-1}{2} \beta M_2^2 \right) M_1^2}{\left(1 + \frac{k-1}{2} \beta M_1^2 \right) M_2^2} \right]} \quad (5-21)$$

It can be seen that Equation (5-21) contains only two unknowns, M_1 and M_2 ; fL/D is determined from the vent geometry, ρ, γ, β are functions of the drywell thermodynamic properties at the time as well as the assumptions that are being imposed upon the model as to the proportions of the drywell constituents which are presumed to be entering the vent system.

Equation (5-18) will now be integrated to provide the second simultaneous equation in M_1 and M_2 .

$$P_1 \int_{P_1}^{P_2} \frac{dP}{P} = - \int_{M_1^2}^{M_2^2} \left[\frac{1 + (k-1)\beta M^2}{2 + (k-1)\beta M^2} \frac{dM^2}{M^2} \right] \quad (5-21a)$$

Integrating by the same procedure as before gives

$$\begin{aligned} \ln \frac{P_2}{P_1} = & \frac{1}{2} \ln \left(\frac{[2 + (k-1)\beta M_1^2] M_1^2}{2} \right) \\ & - \frac{1}{2} \ln \left(\frac{[2 + (k-1)\beta M_2^2] M_2^2}{2} \right) \end{aligned} \quad (5-21b)$$

which gives

$$\frac{P_2}{P_1} = \sqrt{\frac{[2 + (k-1)\beta M_1^2] M_1^2}{[2 + (k-1)\beta M_2^2] M_2^2}} \quad (5-22)$$

P_1 is the static pressure after the fluid in the drywell has been accelerated to the duct inlet velocity but before the fluid has entered the duct. P_1 is approximately related to the drywell stagnation pressure, P_D , by

$$P_1 = P_D - \gamma_1 \frac{u_1^2}{2g} \tag{5-23}$$

and by definition,

$$M_1^2 = \frac{u_1^2}{g k P_1 / \rho_1} \tag{5-24}$$

Where the subscript 1 refers to conditions at the same location as P_1 is occurring.

Hence from (5-23) and (5-24)

$$P_1 = P_D - \frac{\gamma_1}{\rho_1} \frac{k}{2} P_1 M_1^2$$

Hence

$$\frac{P_D}{P_1} = 1 + \frac{\gamma_1}{\rho_1} \frac{k}{2} M_1^2 \tag{5-25}$$

[γ_1 and ρ_1 and derived in Equation (5-28)]. P_2 is the pressure at the vent outlet and is equal to the bubble pressure (P_B) outside the vent. The bubble pressure is a function of the air flow rate through the individual rows of vents. The bubble pressure for the individual vents is calculated using an analytical vent back pressure model discussed in Section 6.

$$P_B = P_s + \gamma_w H$$

where P_s = suppression chamber pressure and $\gamma_w H$ = static water head due to vent submergence.

Combining (5-22) and (5-25) gives

$$\frac{P_B}{P_D} = \frac{M_1}{M_2 \left(1 + \frac{\gamma_1}{\rho_1} \frac{k}{2} M_1^2 \right)} \sqrt{\frac{2 + (k-1)\beta M_1^2}{2 + (k-1)\beta M_2^2}} \tag{5-26}$$

where

$$P_B = P_s + \gamma_w H$$

Equation (5-26) is the second simultaneous equation in M_1 and M_2 .

Since at any time during the transient both P_B and P_D are known, then Equations (5-26) and (5-21) will yield the current values of M_1 and M_2 . The solution is iterative.

When these equations are solved and M_1 and M_2 are known, it is a straightforward procedure to calculate the mass flow rate entering the vent system. The remaining equations present a method of calculating this flow rate in terms of the just calculated inlet Mach number and the current thermodynamic conditions in the drywell.

For the first, second, and third rows of vents, the vent inlet mass velocities are G_{11} , G_{21} , and G_{31} , respectively.

For the first row of vents the inlet mass velocity is given by

$$G_{11} = \gamma_1 u_1 \tag{5-27}$$

The inlet mixture density (γ_1), after being accelerated, is approximately equal to

$$\gamma_1 = \gamma_0 \left(\frac{P_1}{P_0} \right)^{\frac{1}{k}} \tag{5-28}$$

This equation represents an adiabatic expansion of the vapor/gas phase and is justified by the very high void fraction.

$P_0 = P_D$ and γ_0 is the mixture density before being accelerated and is given by

$$\gamma_0 = \frac{M_{fD} + M_{aD} + M_{gD}}{V_D} \tag{5-29}$$

Where

M_{fD} = Mass of liquid in the drywell

M_{aD} = Mass of air in the drywell

M_{gD} = Mass of vapor in the drywell

V_d = Drywell free volume

P_D = Drywell pressure

i.e., γ_0 = The homogeneous drywell fluid density.

Combination of Equations (5-27), (5-28) and (5-29) gives

$$G_{11} = \left[\frac{M_{fD} + M_{aD} + M_{gD}}{V_D} \right] \cdot \left(\frac{P_1}{P_0} \right)^{\frac{1}{k}} \cdot u_1 \tag{5-30}$$

From the definition of Mach number

$$u_1 = \sqrt{k g P_1 v_1} \cdot M_1$$

Since

$$P_1 v_1 \approx P_0 v_0 \left(\frac{P_1}{P_0} \right)^{\frac{k-1}{k}}$$

(for the same reasons that equation (5-28) is justified)

$$u_1 = \sqrt{k g \frac{P_0}{\rho_0} \left(\frac{P_1}{P_0} \right)^{\frac{k-1}{k}}} \cdot M_1 \tag{5-31}$$

where

$$\rho_0 = \frac{M_{aD} + M_{gD}}{V_D}$$

This definition is based upon assumption e, i.e., the sonic velocity of the mixture in the vents is the sonic velocity of the gaseous constituents of the flow.

Substituting (5-31) into (5-30) gives

$$G_{11} = \left[\frac{M_{fD} + M_{aD} + M_{gD}}{V_D} \right] \sqrt{\frac{k g P_0 V_D}{(M_{aD} + M_{gD})} \left(\frac{P_1}{P_0} \right)^{\frac{k+1}{k}}} \quad (5-32)$$

From equation (5-25)

$$\frac{P_D}{P_1} = 1 + \frac{\gamma_1}{\rho_1} \frac{k}{2} M_1^2$$

$$\therefore G_{11} = \frac{(M_{fD} + M_{aD} + M_{gD})}{V_D} \sqrt{\frac{k g P_D V_D}{(M_{aD} + M_{gD}) \left(1 + \frac{\gamma_1}{\rho_1} \frac{k}{2} M_1^2 \right)^{\frac{k+1}{k}}}}$$

Thus, the flow rate into the first row of vents can be calculated from the known conditions in the drywell and M_1 .

For the second and third rows of vents the same method is followed to calculate the flow rate in terms of the corresponding inlet Mach number and current thermodynamic conditions in the drywell.

Therefore, at any point in time the total vent system flow rate is expressed as the summation of the individual flow rates through each of the cleared vent rows. For the case of all vent rows cleared the total flow rate is expressed as:

$$G_{Total} = G_{11} + G_{21} + G_{31}$$

(Note: The second subscript on each term denotes inlet conditions.)

5.4 PREVIOUS COMPARISONS WITH EXPERIMENTAL DATA

The basic vent flow model described above is the same model used on past pressure suppression containment systems. The model has been checked against all available Bodega Bay and Humboldt Bay pressure suppression test data and found to give good agreement. The results are presented in Section 5.4 of Reference 2.

5.5 NOMENCLATURE

C_p	= Specific heat at constant pressure
D	= Diameter
f	= Darcy friction factor
A	= Mass velocity
h°	= Stagnation enthalpy
h	= Enthalpy
k	= Ratio of specific heats
ℓ	= Length
L	= Length
M	= Mach number, mass in drywell
\dot{m}	= Mass flow rate
P	= Pressure
R	= Gas constant
T	= Temperature
t	= Time
u	= Linear velocity
V	= Volume
v	= Specific volume
γ	= Density of mixture
ρ	= Density of gases

Subscripts

$D,$	= Drywell
$\ell,$	= Liquid
$s,$	= Containment
$v,$	= Vapor
$w,$	= Water

6. VENT BACK PRESSURE MODEL

6.1 INTRODUCTION

Following a loss-of-coolant accident in the drywell, the rapid increase in drywell pressure will accelerate the water initially standing in the weir annulus and horizontal vents. During this vent clearing process, the pressure at the exit of the vents will correspond to the containment pressure plus the appropriate hydrostatic pressure plus pool momentum pressure. The pool momentum pressure is a result of the pool being accelerated to accommodate the incoming water from the vent system. This is accounted for in the vent clearing model by adding an equivalent length to each horizontal vent. Immediately following the clearing of any vent, drywell air and steam will start to form a bubble at the vent exit and increase the acceleration of the pool mass. This bubble will attempt to expand and depressurize to the local hydrostatic pressure. The rate of expansion of the bubble is controlled by the inertia of the pool. During this expansion process, the bubble will exert a back pressure on the vent which will tend to delay vent flow. In addition the bubble pressure is propagated to the lower vents and tends to delay vent clearing.

Because both delayed vent flow and delayed vent clearing will result in increased peak calculated drywell pressures, the phenomenon of the vertical interaction between the vents associated with the initial bubble formation has been included in the Mark III containment analysis models.

The equations used to simulate the vent system back pressure effects are described below; the classical treatment of compressible adiabatic flow of a gas in a constant area duct (e.g., see Reference 6) and the equation of motion establish the basic approach of the analytical simulation. The method involves continuously integrating both the air flow rate through the vent system and the acceleration of the pool resulting from the drywell air injection. Thus at any time during the transient, the air pressure beneath the pool surface and the displacement of the pool can be calculated.

6.2 ASSUMPTIONS

The following is the sequence of the events which are assumed to occur when analytically simulating the vent back pressure effects during a loss-of-coolant accident.

Following a main steam line break loss-of-coolant accident, the pressure in the drywell will start to increase as a result of the incoming steam and energy from the primary system. This increasing drywell pressure establishes a pressure differential across the vent system which starts to accelerate the water out of the vent system and into the suppression pool. Prior to vent clearing, the pressure at the exit of the vents (the vent back pressure) is the containment air-pressure plus the suppression pool hydrostatic pressure plus pool momentum pressure.

Following vent uncover, drywell air will start flowing into the pool and an air bubble will be established. This bubble will attempt to expand and depressurize to the local hydrostatic pressure; during this expansion process the bubble will exert a back pressure on the vent system. This back pressure influences the flow through the top row of vents and, because the bubble pressure propagates through the pool, it affects the vent clearing of the lower two rows of vents. Following the clearing of the second row of vents, the second bubble is assumed to coalesce with the first bubble and establish one bubble charged by two rows of vents. This increasing charging rate causes the bubble pressure to rise. The pressure will continue to rise until the volumetric expansion rate of the bubble is greater than the volumetric vent charging rate. At this point the bubble pressure will decay to the hydrostatic pressure. This resulting back pressure affects the vent flow of the top two rows of vents and the vent clearing of the bottom row of vents. The clearing of the bottom row of vents produces the same effects as the top rows.

The following is a list of major assumptions used in the derivation of the vent back pressure model.

- a. The air initially within the drywell prior to vent clearing is adiabatically compressed by the incoming primary system; fluid and energy; heat transfer to the walls is conservatively neglected.
- b. Following vent clearing, the vent flow is assumed to be drywell air rather than some mixture of air and steam. This assumption (referred to as all-air carryover) maximizes the mass flow rate of non-condensibles underneath the pool surface and thus maximizes the vent back pressure.

- c. The all-air carryover flow rate is evaluated by applying the classical treatment of compressible flow of gas through a duct with friction.
- d. The temperature of the air beneath the water is conservatively assumed to be the maximum drywell temperature occurring any time during the transient. This assumption maximizes air volume, the pool acceleration, and therefore the bubble pressure.
- e. When the first vent is cleared, all the water above the first vent center line is assumed to be accelerated as a water slug of constant thickness. When the second vent clears, all the water above the second vent center line is assumed to be accelerated as a water slug of constant thickness. And for the third vent, all the water above the third vent center line is assumed to be accelerated. These assumptions maximize the amount of water to be accelerated when calculating the vent back pressure effects, and is therefore conservative.
- f. Friction losses between the moving water and confining walls are negligible; viscous forces are small compared to pressure and inertia forces.
- g. The containment air space is adiabatically compressed by the upward moving slug; heat transfer to the walls is conservatively neglected.
- h. The air in the system is assumed to be an ideal gas.

6.3 DERIVATION OF EQUATIONS

In this section, the equations used in the simulation of the vent back pressure following a loss-of-coolant accident will be derived. The modeling is based on the assumption that the conditions at the time of top vent clearing are known as well as the subsequent drywell pressure transient. These data are obtained from the over-all containment analytical model described in earlier sections of this report. Since the results of the over-all containment analytical model are somewhat dependent on vent back pressure, an iterative solution is sometimes required.

Using the known initial conditions and transient drywell pressure, the model simulates the transient by continuously integrating differential equations that define air bubble mass, water slug velocity, and water slug displacement.

It should be made clear that this model is not an integral part of the Mark III containment system analytical model; rather it is run independently and the results used as boundary conditions to the vent clearing and vent flow models. During the analytical simulation of the Mark III containment system to a LOCA, the detailed vent flow model discussed in Section 5 is used for all vent flow calculations.

6.3.1 Drywell Initial Conditions

From assumption h, the equation of state for air can be written, i.e.,

$$PV = mRT \tag{6-1}$$

and the initial mass of non-condensibles and density are solved for:

$$m = \left[\frac{(P - P_{sat}) V}{RT} \right]_{DW} \tag{6-2}$$

$$\rho = \left[\frac{(P - P_{sat})}{RT} \right]_{DW} \tag{6-3}$$

Where all parameters are at the drywell (DW) initial conditions,

- P = Drywell pressure
- P_{sat} = Drywell stagnation pressure
- ϕ = Drywell relative humidity
- T = Drywell temperature
- V = Drywell volume
- ρ = Drywell density
- R = Gas constant

6.3.2 Drywell Transient Conditions

From assumption a, i.e., the drywell air is adiabatically compressed, the identity $PV^k = \text{constant}$ is used to express the drywell transient temperature T as a function of known transient pressure P and the initial drywell pressure P_1 and Temperature T_1

$$T^{k/k-1}/P = \text{constant} \tag{6-4}$$

and thus for the transient temperature T in degrees F,

$$T = (T_1 + 460) (P/P_1)^{(k-1)/k} - 460 \tag{6-5}$$

The equation of state is used to express the transient drywell density in terms of known initial drywell pressure, temperature, density, and known transient drywell pressure and temperature.

$$\rho = \rho_1 \frac{P}{T} \frac{T_1}{P_1} \tag{6-6}$$

Throughout the following derivation, it will be assumed that the air velocity in the drywell is sufficiently small that stagnation and static conditions are equivalent, i.e.,

$$\left. \begin{aligned} P &= P_0 \\ T &= T_0 \\ \rho &= \rho_0 \end{aligned} \right\} \tag{6-7}$$

6.3.3 Vent System Transient Conditions

The vent flow model described in this subsection is essentially the same model used in the over-all containment analytical model (described in Section 5) though simplified for air-only flow.

Following the clearing of vents, the air mass flow rate into the vent system is expressed by the equation of continuity:

$$\dot{m} = \rho A V \tag{6-8}$$

Where the density, vent area, and vent velocity (ρ , A, and V) are evaluated at the vent inlet.

From assumption c, the air flow is treated as the classical flow of compressible gas through a duct, the following formulas are used to evaluate the vent inlet properties,⁶

$$\rho = \rho_0 \left\{ 1 + [(k-1)/2] M^2 \right\}^{1/k-1} \quad (6-9)$$

$$T = T_0 \left\{ 1 + [(k-1)/2] M^2 \right\} \quad (6-10)$$

Where ρ_0 and T_0 are stagnation density and temperature in the drywell and M is the vent inlet Mach number.

From the definition of Mach Number

$$M = \frac{V}{C} = \frac{V}{\sqrt{k g_c R T}} \quad (6-11)$$

Solving for the vent inlet velocity:

$$V = M \sqrt{k g_c R T} \quad (6-12)$$

Substituting Equation (6-10) into Equation (6-12) yields an expression for vent inlet velocity in terms of drywell stagnation temperature and vent inlet Mach number.

$$V = M \sqrt{k g_c R T_0} \sqrt{1 + [(k-1)/2] M^2} \quad (6-13)$$

Equations (6-9) and (6-13) are now substituted into the continuity Equation (6-8) to yield an expression of the vent inlet air mass flow rate in terms of known quantities and M , the inlet Mach number.

$$\dot{m} = \frac{\rho}{\left\{ 1 + [(k-1)/2] M^2 \right\}^{1/k-1}} \cdot A \cdot \frac{M \sqrt{k g_c R T_0}}{\sqrt{1 + [(k-1)/2] M^2}} \quad (6-14)$$

The inlet Mach number M as defined in Reference (6) is a function of the pressure ratio P_B/P_0 across the duct and the frictional loss of the vent (fl/d); P_B is the vent back pressure and P_0 the stagnation pressure of the drywell.

6.3.4 Pool Bubble Transient Conditions

The air within the pool bubble at some pressure P_B is also treated as an ideal gas. From the equation of state,

$$P_B = \frac{m_B R T_B}{V_B} \quad (6-15)$$

Where the mass, temperature, and volume of the bubble are m_B , T_B , and V_B , respectively.

From assumption d, the air temperature beneath the surface is the maximum drywell temperature throughout the transient in degrees F. From Equation (6-5)

$$T_B = (T_1 + 460) (P/P_1)^{(k-1)/k} - 460 \quad (6-16)$$

Where T_1 and P_1 represent initial conditions and P represents the maximum drywell pressure occurring during the transient.

The air mass beneath the pool surface at any time during the transient is expressed as the integral of Equation (6-14).

$$m_B = \int \dot{m} dt \quad (6-17)$$

Equation (6-17) [and Equations (6-22) and (6-23)] are solved using the classical Runge Kutta numerical analysis integration technique. A time step of one-thousandth of a second was used in the solution.

From assumption e, the pool moves as a constant-thickness water slug, the following expression for the bubble volume is expressed in terms of pool area (A_p) and water slug displacement (X).

$$V_B = A_p \cdot X \quad (6-18)$$

Where X is the slug displacement which is calculated with the model in the following subsection.

6.3.5 Pool Slug Transient Conditions

From assumption e, the pool mass depends on the number of vents cleared. Corresponding to one vent being open the pool mass m_p accelerated by the bubble pressure P_B is expressed in terms of the pool area A_p and the vent submergence (H_1).

$$m_p = A_p \cdot H_1 \cdot \rho \quad (6-19)$$

This pool mass m_p is accelerated upward by the bubble pressure, P_B , against gravity, g , and the containment air space pressure, P_s . Writing the equation of motion of m_p , yields the following expression,

$$\ddot{X} m_p + P_s A_p + m_p g - P_B A_p = 0 \quad (6-20)$$

Rearranging and solving for the acceleration of m_p yields,

$$\ddot{X} = (P_B - P_s) A_p / m_p - g \quad (6-21)$$

From Equation (6-21) the velocity and thus displacement of m_p can be obtained by integration with respect to time

$$\dot{X} = \int \ddot{X} dt \quad (6-22)$$

$$X = \int \dot{X} dt \quad (6-23)$$

using updated values of bubble air mass.

The containment pressure, P_s , must be solved for in order to solve for the displacement X of m_p and thus the bubble pressure, P_B , and finally the mass flow rate into the vent system, \dot{m} .

6.3.6 Containment Air Space Transient Conditions

From assumption h, the air in the containment air space is treated as an ideal gas. As the water slug moves upward the containment air space is adiabatically compressed and $PV^k = \text{constant}$. Therefore the transient containment pressure, P , can be expressed in terms of the initial pressure, P_1 , and volume, V_1 , and the transient containment volume, V .

$$P = P_1 (V_1/V)^k \quad (6-24)$$

The transient containment volume V is in terms of the initial containment volume, V_1 , the pool area, A_p , and the pool displacement, X .

$$V = V_1 - A_p \cdot X \quad (6-25)$$

Substitution of Equation (6-25) into (6-24) yields the containment transient pressure in terms of pool displacement X and known quantities P_1 and V_1 .

With P_s solved for in terms of X , Equation (6-25) can be substituted into Equation (6-21) to yield the pool acceleration which in turn can be integrated to yield X , which is necessary for completing one transient time step.

Figure 6-1 is a representative vent back pressure response for a typical BWR/6-Mark III containment system. For this calculation initial air bubble pressure is assumed to be equal to drywell pressure at the time of vent clearing.

The next subsection demonstrates the conservatism of the vent back pressure model and therefore establishes justification for responses similar to Figure 6-1 to be used as boundary conditions for the vent clearing and vent flow models.

6.4 EXPERIMENTAL VERIFICATION

The ability of the analytical model described above to predict vent back pressure has been evaluated. PSTF vent back pressures were calculated by using measured PSTF drywell pressure transients as the driving pressure for the model. The PSTF vent back pressures are taken to be the vent exit static pressures. The calculations were performed for four 1-vent and four 2-vent runs. Figures 6-2 through 6-5 show the results of the four 1-vent comparisons and Figures 6-6 through 6-9 the results of the four 2-vent comparisons. For all comparisons presented the magnitudes of the vent back pressure are shown to be higher than the measured back pressure and therefore are conservative; in some of the cases the calculated back pressure differs from the measured back pressure with respect to time. This is because the measured vent clearing times used in the model do not always correspond to the exact time when the bubble reaches the pressure measuring device in the vent system.

This is not the case for Mark III containment system analytical simulation of a LOCA; the vent back pressure is applied to the vents the instant the vents clear. The comparisons presented given an over-all confidence that the vent back pressure model used for calculating the vent system back pressure will conservatively simulate the transient which would occur during a loss-of-coolant accident.

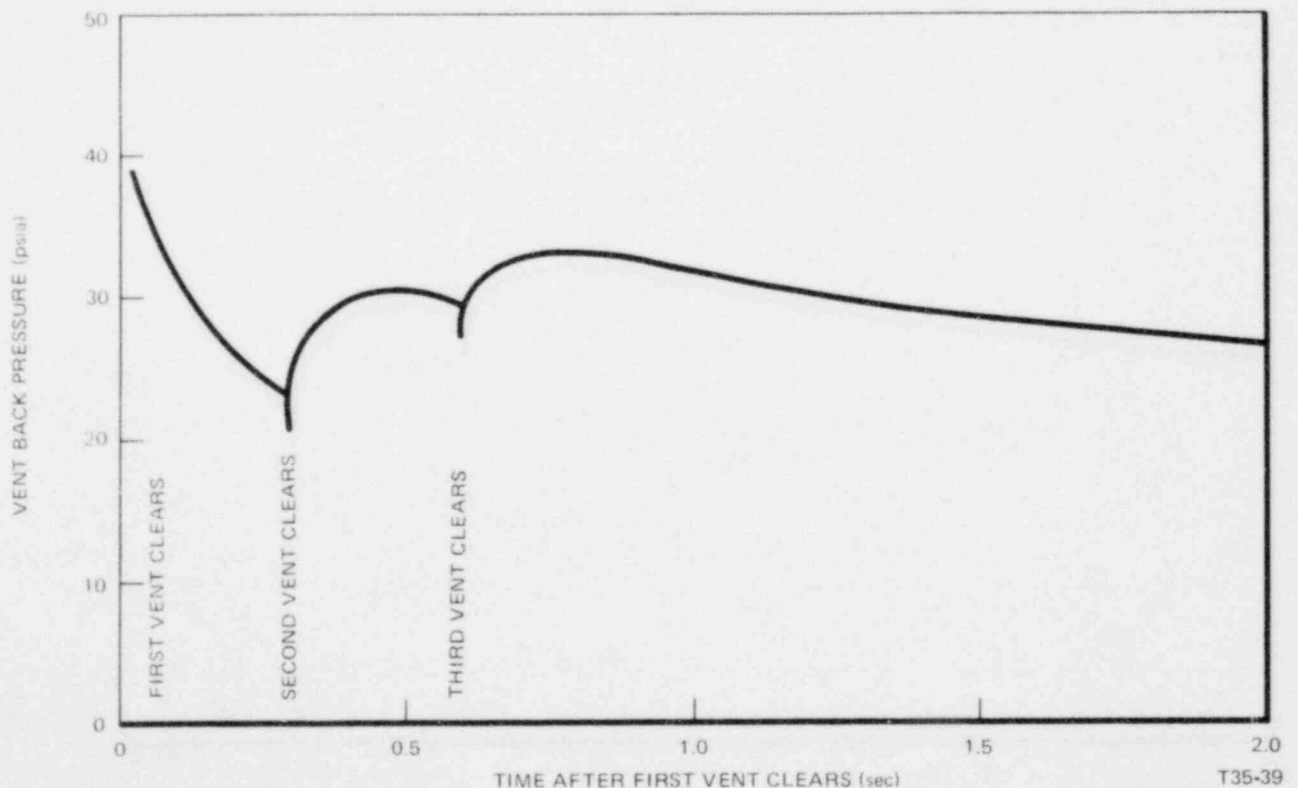


Figure 6-1. Typical Mark III Containment System Vent Back Pressure

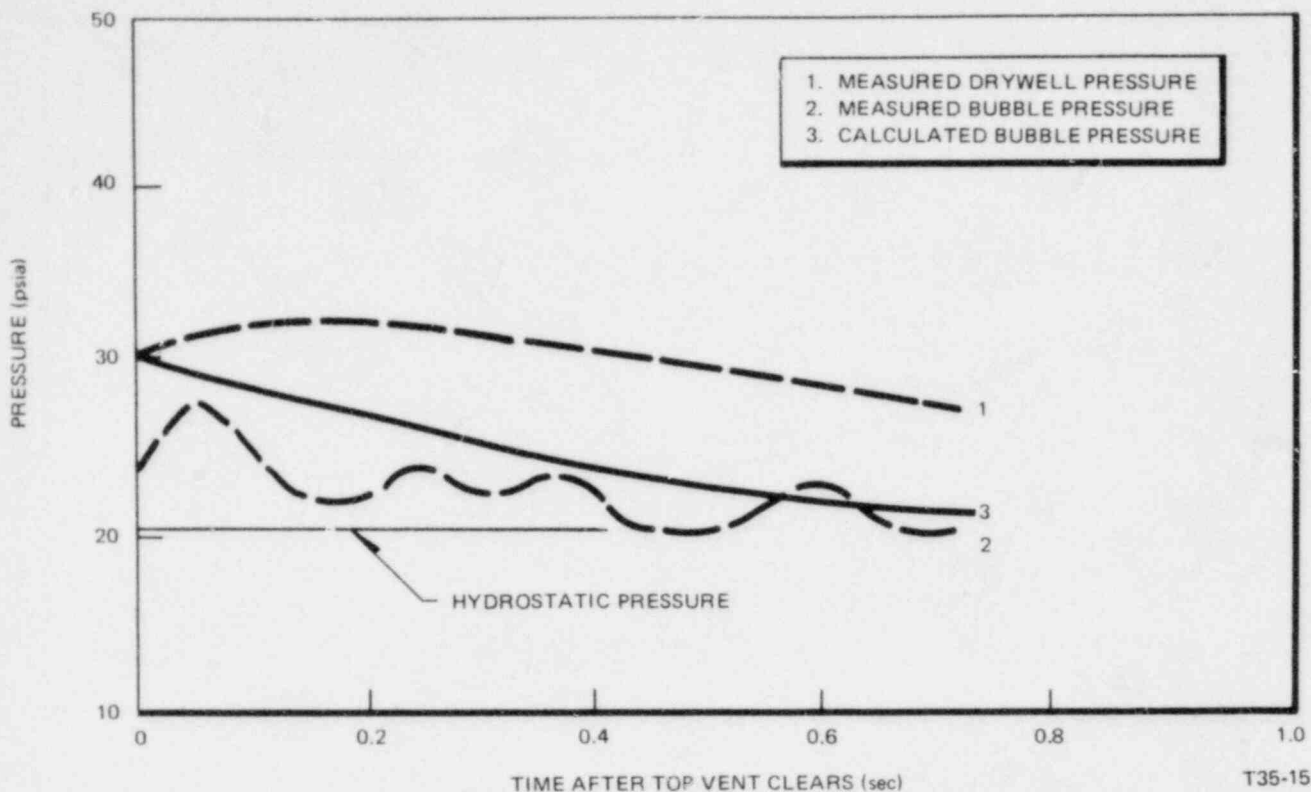


Figure 6-2. 70% BWR/6 Break Area/Vessel Volume; 1 Vent, 12-ft Submergence

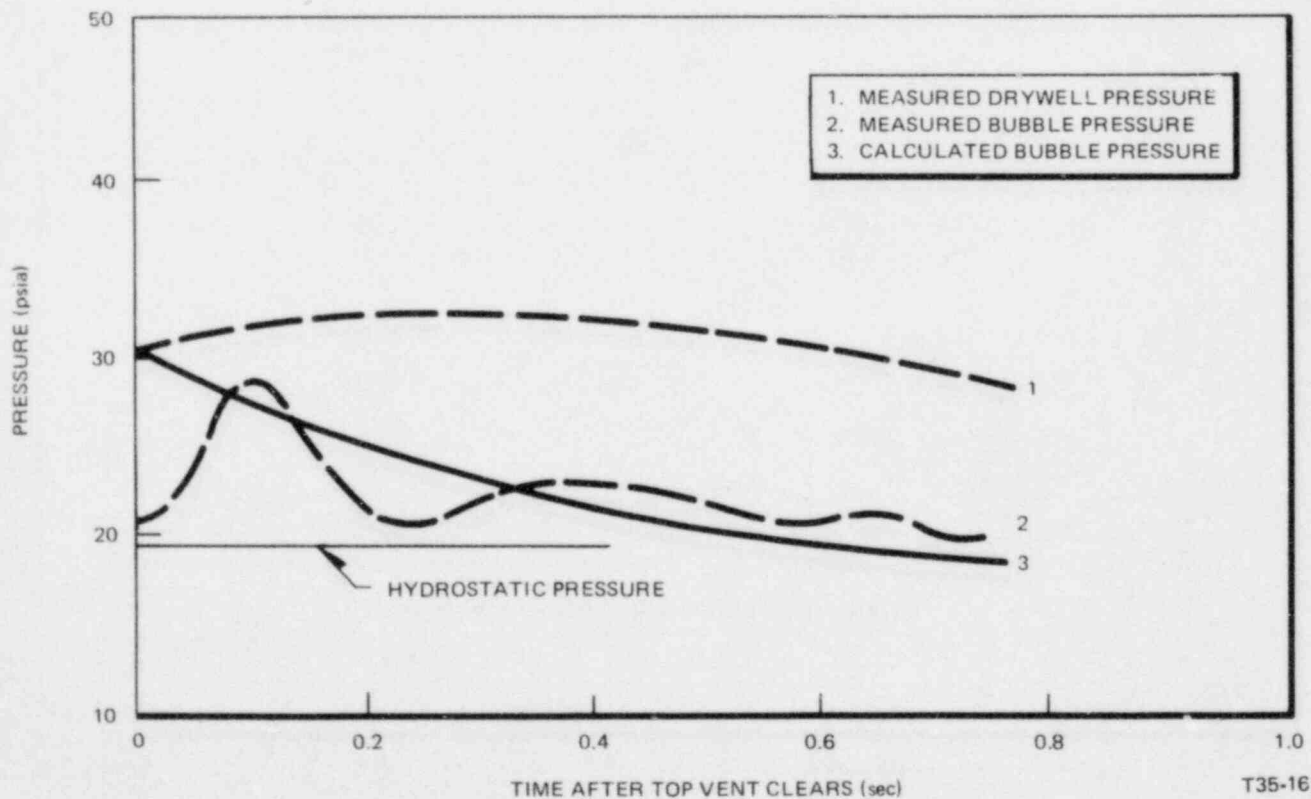


Figure 6-3. 100% BWR/6 Break Area/Vessel Volume; 1 Vent, 8-ft Submergence

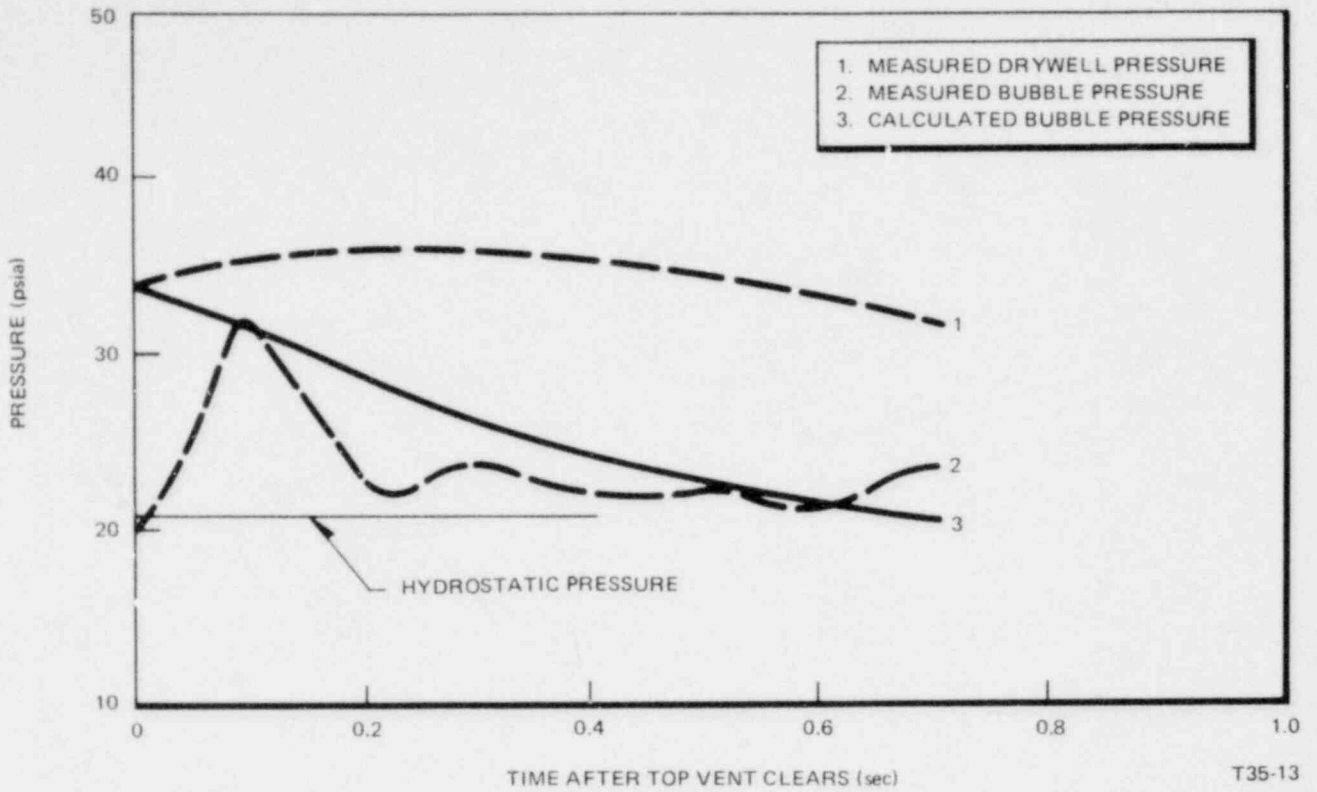


Figure 6-4. 100% BWR/6 Break Area/Vessel Volume; 1 Vent, 12-ft Submergence

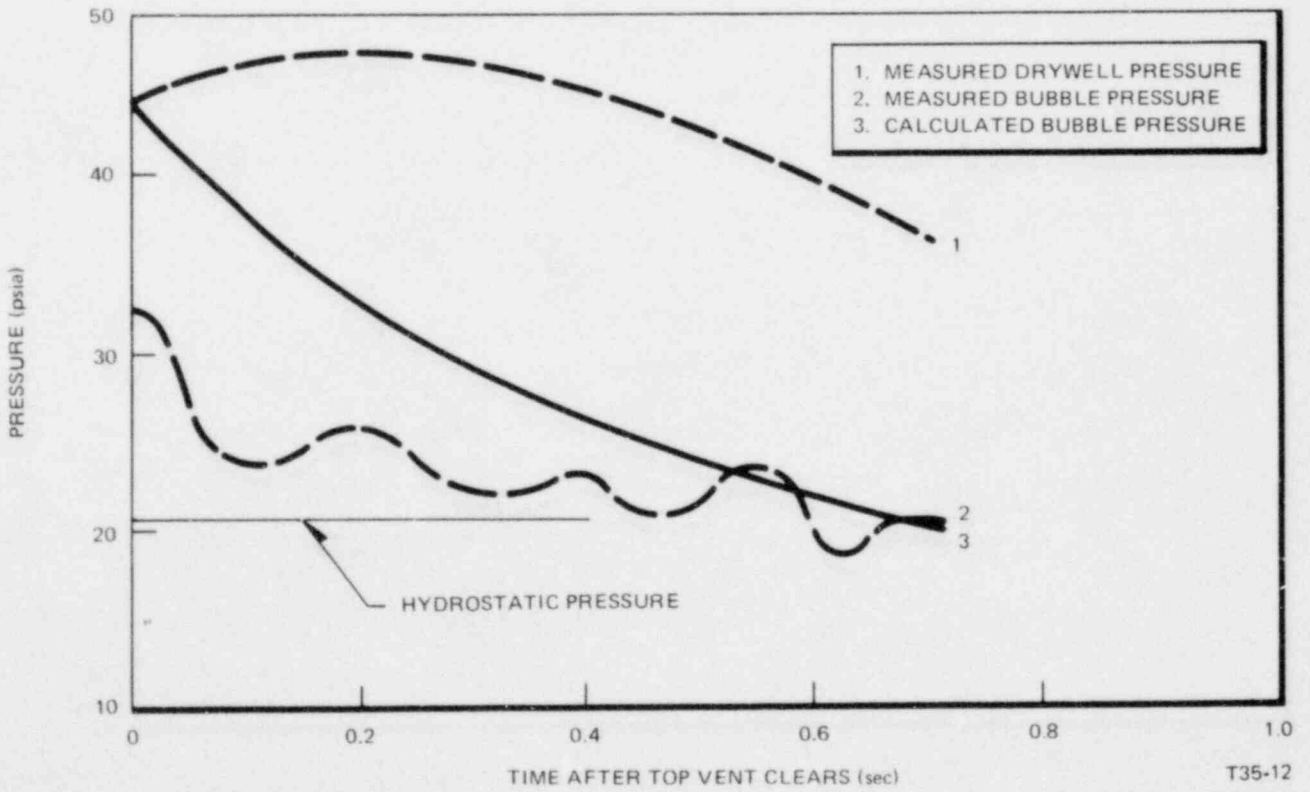


Figure 6-5. 200% BWR/6 Break Area/Vessel Volume; 1 Vent, 12-ft Submergence

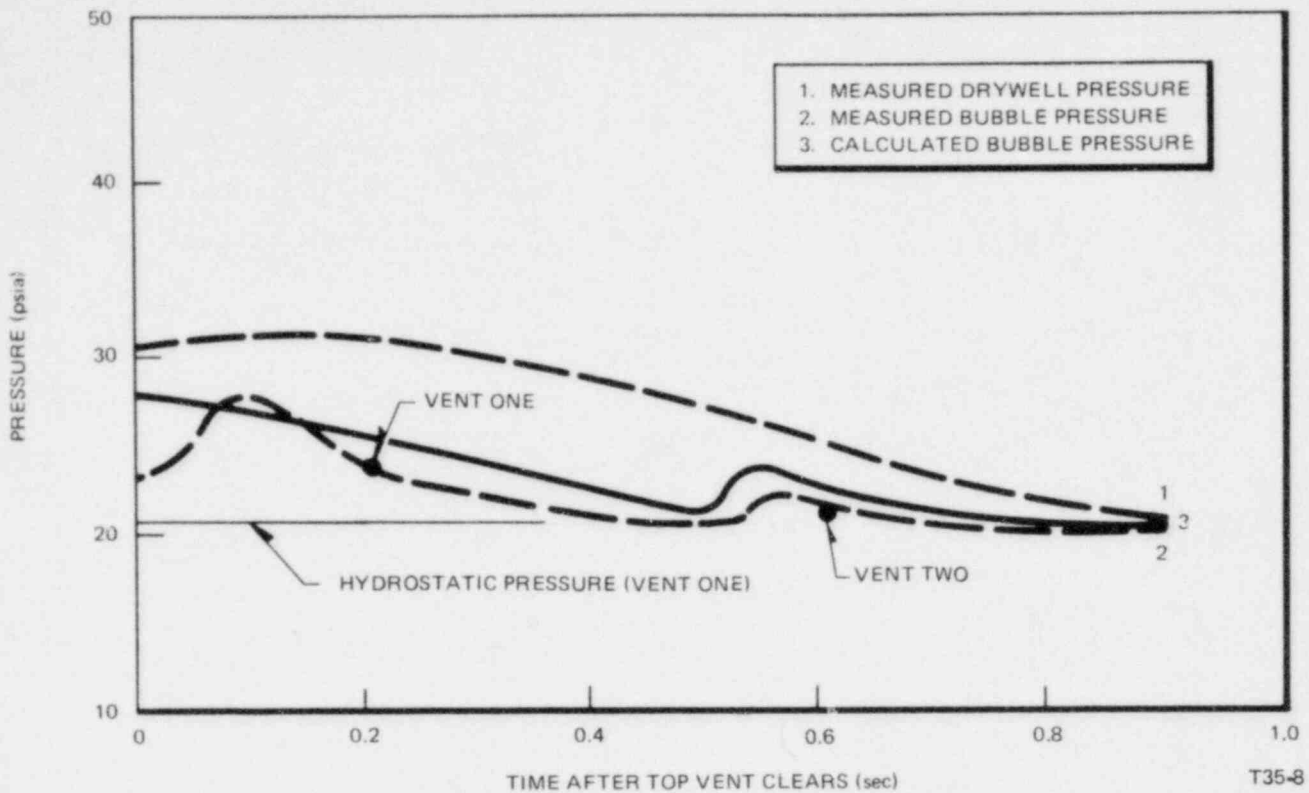


Figure 6-6. 70% BWR/6 Break Area/Vessel Volume; 2 Vents, 12-ft Submergence

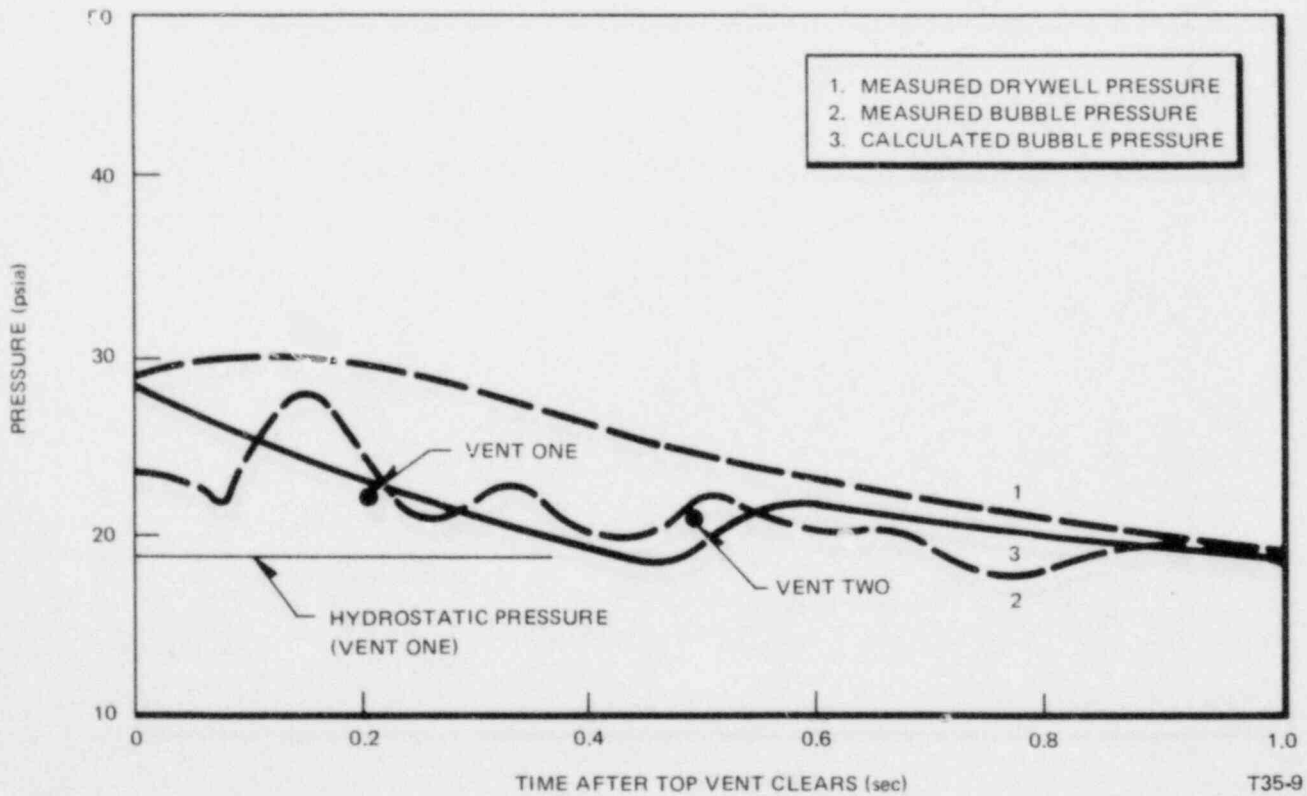


Figure 6-7. 100% BWR/6 Break Area/Vessel Volume; 2 Vents, 8-ft Submergence

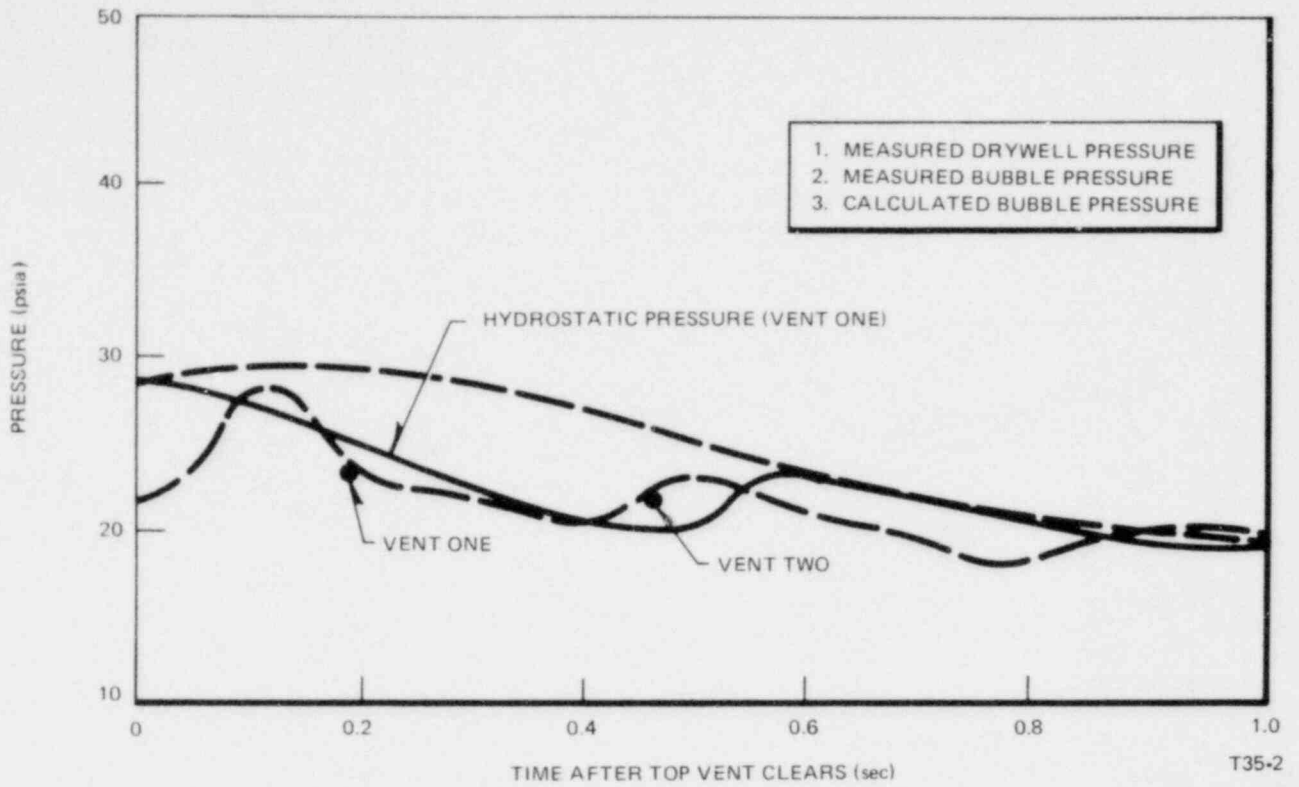


Figure 6-8. 100% BWR/6 Break Area/Vessel Volume; 2 Vents, 10-ft Submergence

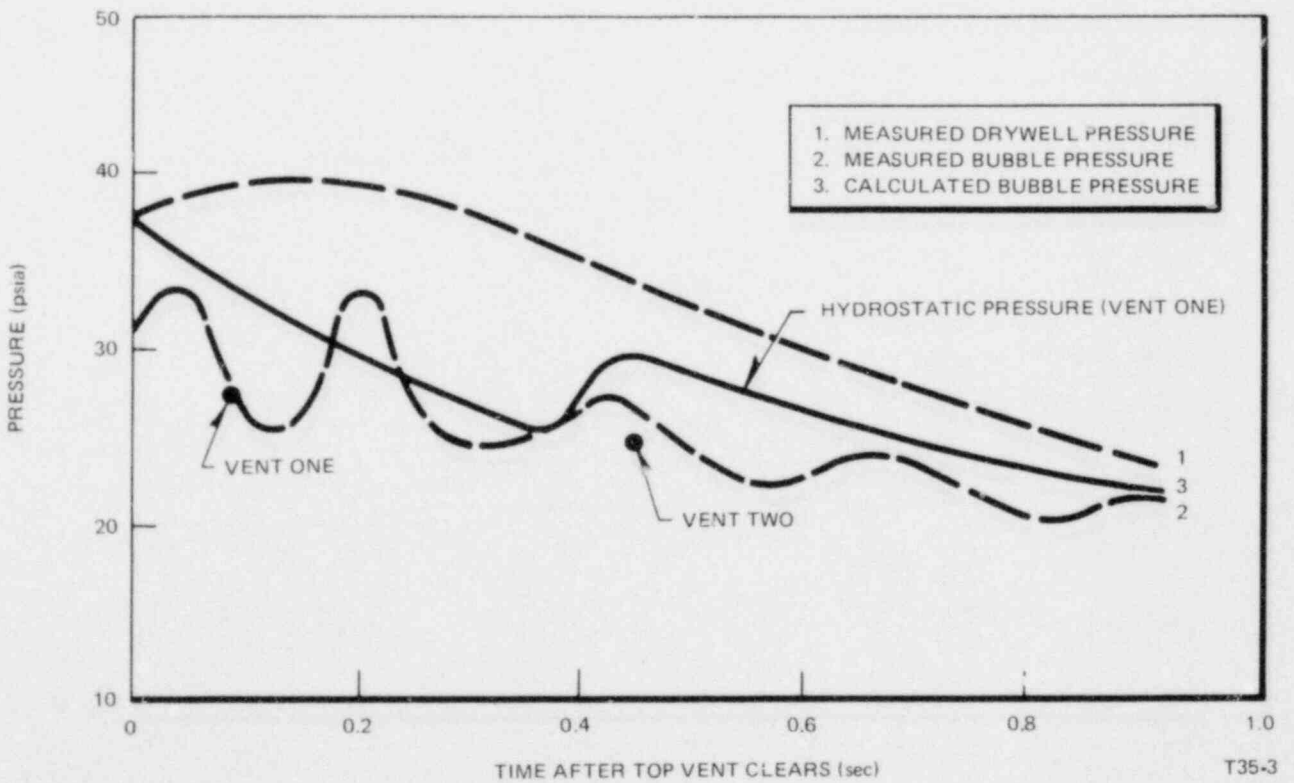


Figure 6-9. 200% BWR/6 Break Area/Vessel Volume; 2 Vents, 12-ft Submergence

7. SUPPRESSION POOL AND CONTAINMENT FREE SPACE ANALYTICAL MODEL

7.1 DERIVATION OF EQUATIONS

The suppression pool and containment free space model presupposes that the vent flow rate is known at any instant in time. With this assumption and making certain assumptions about the air temperature, the differential equations for pool temperature and pool mass can be derived. These equations are then solved using the finite difference techniques presented in Section 8.

Consider the pool mass. An energy balance assuming that all the steam and liquid entering from the drywell remains in the pool gives:

$$\begin{aligned}
 & h_{fD} \dot{m}_{fD} + h_{gD} \dot{m}_{gD} + \dot{m}_{aD} C_{pa} (T_D - T_a) \\
 & = \frac{\dot{M}_{ws}}{M_{ws}} h_{\ell} = h_{\ell} \dot{M}_{ws} + M_{ws} \dot{h}_{\ell}
 \end{aligned}
 \tag{7-1}$$

Where:

- h_{fD} = Enthalpy of liquid entering the suppression pool
- h_{gD} = Enthalpy of vapor entering the suppression pool
- \dot{m}_{fD} = Mass of liquid entering the pool
- \dot{m}_{gD} = Mass of vapor entering the pool
- \dot{m}_{aD} = Mass of air entering the containment
- T_D = Temperature of air entering the pool
- T_a = Temperature of air leaving the pool
- M_{ws} = Mass of water in the pool
- h_{ℓ} = Enthalpy of pool water

\dot{h}_{ℓ} , (ie $\frac{dh_{\ell}}{dt}$) can be rewritten

$$\dot{h}_{\ell} = \frac{\partial h_{\ell}}{\partial T_s} \frac{\partial T_s}{\partial t} + \frac{\partial h_{\ell}}{\partial P_s} \frac{\partial P_s}{\partial t}
 \tag{7-2}$$

Where:

- T_s = Pool temperature
- P_s = Pool pressure

and

$\frac{\partial h_{\ell}}{\partial T_s}$ = Partial derivative of liquid enthalpy with respect to temperature at constant pressure

$$\frac{\partial h_{\ell}}{\partial P_s} = \text{Partial derivative of liquid enthalpy with respect to pressure at constant temperature.}$$

For the conditions occurring in the containment of a BWR, $\frac{\partial h_{\ell}}{\partial P_s} = 0$.

[Equation (7-2) is true because if $x = f(y,z)$

then

$$dx = \frac{\partial x}{\partial y} dy + \frac{\partial x}{\partial z} dz$$

This equation (7-1) can be rewritten as

$$\dot{T}_s = \frac{h_{fD} \dot{m}_{fD} + h_{gD} \dot{m}_{gD} + \dot{m}_{aD} C_{pa} (T_D - T_{al}) - h_{\ell} \dot{M}_{ws}}{\dot{M}_{ws} \frac{\partial h_{\ell}}{\partial T_s}} \quad (7-3)$$

A mass balance on the pool, neglecting any mass transfer to the air region, gives

$$\dot{M}_{ws} = \dot{m}_{fD} + \dot{m}_{gD} \quad (7-4)$$

If it is assumed that the temperature of the air leaving the pool, T_a , is equal to the pool temperature, T_s , then equations (7-3) and (7-4) can be solved and the values of pool temperature and mass updated for the small time increment being considered.

The pressure in the containment is now evaluated by considering the contents of air region. It is assumed that at any time in the transient this space has a volume corresponding to the total containment space less the current volume of the water.

The partial pressure of the water vapor in the region, P_{sw} is assumed to be the saturation pressure corresponding to the pool temperature, i.e.,

$$P_{sw} = P_{sat_{T_s}}$$

The partial pressure of the noncondensable gases (air), P_{sa} , is given by

$$P_{sa} = \frac{M_{as} R (T_s + 460)}{144 V_{as}} \quad (7-5)$$

Where

$$\begin{aligned} M_{as} &= \text{Total mass of air in the containment} \\ R &= \text{Gas constant} \\ V_{as} &= \text{Volume of air region in the containment} \end{aligned}$$

and

$$V_{as} = V_s - v_\ell M_{ws}$$

where

$$\begin{aligned} V_s &= \text{Total containment volume} \\ v_\ell &= \text{Specific volume of liquid in the pool} \end{aligned}$$

The total pressure in the containment, P_s , is thus given by

$$P_s = P_{sa} + P_{sw}$$

7.2 ASSUMPTIONS

The analytical simulation of the containment transient following a loss-of-coolant accident is based upon and uses the following assumptions.

1. All liquid and vapor entering the pool from the vent system remains in the pool.
2. The temperature of the air in and entering the air space of the containment is at all times the same as the pool temperature. In practice, the long-term (4 to 6 hours) air temperature might be expected to lag the water temperature but since this would result in a reduction in the containment pressure it is not taken into account.
3. The air space is at all times saturated with water vapor. If the air is less than saturated, then the calculated containment pressure will be less.
4. There are no heat losses from the fluids contained in the containment. This assumption is also conservative in that any heat losses will reduce the pressure.
5. Minimum suppression pool water, to maximize peak calculated pool temperature and thus peak calculated containment pressure.

8. NUMERICAL METHODS

8.1 INTRODUCTION

The analytical models described in the preceding sections all involve the derivation of differential equations to mathematically model the transient response of the containment to a loss-of-coolant accident. Numerical values of the various transient parameters are calculated with the techniques described in this section.

8.2 INTEGRATION METHOD

If a function of time and its time derivatives are known at time t_1 , the value of the function at time $t_1 + \Delta t$ can be obtained by use of the well-known Taylor's series. The first three terms of the series are shown below

$$f(t_1 + \Delta t) = f(t_1) + \frac{\Delta t}{1!} f'(t_1) + \frac{(\Delta t)^2}{2!} f''(t_1) + \dots \quad (8-1)$$

Where

Δt = Size of the time step

$f'(t_1) = \frac{df}{dt}$ at $t = t_1$

$f''(t_1) = \frac{d^2f}{dt^2}$ at $t = t_1$

If the term involving the second derivative is assumed to be negligible, the Euler forward extrapolation formula is obtained, i.e.,

$$f(t_1 + \Delta t) = f(t_1) + \Delta t f'(t_1)$$

This equation allows the future value of the function to be found if the present value and its present derivative are known.

A corrected value of the function to be used in calculating the derivatives at $t_1 + \Delta t$ is obtained by defining a variable which equals function f at $t_1 + \Delta t$, but has a correction term added, i.e.,

$$F(t_1 + \Delta t) = f(t_1 + \Delta t) + \frac{1}{2} \Delta t f'(t_1)$$

This new variable F is used, rather than f , in calculating the derivatives at $t_1 + \Delta t$. The correction term extrapolates the function an extra one-half time step and provides essentially an average value of the function to be used in determining the new derivatives.

8.3 TIME STEP DETERMINATION

The digital computer code used to solve the differential equations describing the containment response uses a variable time step. The size of the time step at any point during the transient is determined by the error criterion described below.

The error made in any one extrapolation can be approximated by the third term of the Taylor series given in Equation (8-1), i.e.,

$$\text{Error} = e = \frac{\Delta t^2}{2!} f''(t_1)$$

An exact expression for the second time derivative is generally not known, but can be approximated by the rate of change of the first derivative, i.e.,

$$f''(t_1) \approx \frac{f'(t_1 + \Delta t) - f'(t_1)}{\Delta t} \quad (8-2)$$

Thus

$$e \approx \frac{\Delta t}{2} [f'(t_1 + \Delta t) - f'(t_1)]$$

The digital code conservatively estimates the error as being that given in Equation (8-2). During each time step, the error is calculated for each of the variables being integrated; if any error is larger than the "allowable" value then the time step is halved. This procedure is then repeated until the error criterion is satisfied.

Conversely, if the calculated error is less than one-tenth of the allowable, the time step is doubled.

The error criterion usually used for the containment analysis is that the unit error be less than 0.005, i.e.,

$$\frac{e}{f(t_1 + \Delta t)} \leq 0.005$$

or, remembering the code doubles the error calculated in Equation (8-2),

$$\frac{\Delta t}{f(t_1 + \Delta t)} [f'(t_1 + \Delta t) - f'(t_1)] \leq 0.005$$

REFERENCES

1. "Class I Version of G. E. Status Report NEDM-10848, Mark III Confirmatory Test Program Progress Report," Letter to V. A. Moore from J. A. Hinds, August 3, 1973.
2. *The General Electric Pressure Suppression Containment Analytical Model*, Licensing Topical Report NEDO-10320, April 1, 1970.
3. F. J. Moody, *Maximum Flow Rate of a Single Component, Two-Phase Mixture*, Transactions of the ASME, Volume 87, Series C, 1965.
4. AEC, ECCS Rule Making Hearings, Docket Number RM-50-1.
5. *Loss-of-Coolant Accident and Emergency Core Cooling Models for General Electric Boiling Water Reactors*," Licensing Topical Report NEDO-10329, April 1970.
6. *The Dynamics and Thermodynamics of Compressible Fluid Flow*, Ascher H. Shapiro, Volume 1.
7. I. E. Idel' chik, *Handbook of Hydraulic Resistance: Coefficients of Local Resistance and of Friction*, AEC-TR-6630, 1966.
8. R. E. Henry, M. A. Grolmes, and H. K. Fauske, "Propagation Velocity of Pressure Waves in Gas-Liquid Mixtures," Presented at the International Symposium on Research in Concurrent Gas-Liquid Flow, September 18-19, 1968, Waterloo, Ontario, Canada.
9. S. W. Gouse, Jr., and R. G. Evans, "Acoustic Velocity in Two-Phase Flow," Mechanical Engineering Department, Massachusetts Institute of Technology, Cambridge, Massachusetts.
10. F. J. Moody, "A Pressure Pulse Model for Two-Phase Critical Flow and Sonic Velocity," J.H.T. Trans. ASME, Series C, Vol. 91, No. 3, August 1969.
11. E. Quandt, "Analysis of Gas-Liquid Flow Patterns," A.I.Ch.E. Preprint No. 47, Presented at 6th National Heat Transfer Conference, Boston, Massachusetts, August 11-14, 1963.

ACKNOWLEDGMENTS

The pressure suppression containment analytical model presented in this document has evolved over many years and represents the combined efforts of many General Electric employees. However, significant contributors to this report are A. A. Goldspiel, A. J. James, T. R. McIntyre, F. J. Moody, W. A. Sangster, and J. M. Sorensen.

APPENDIX A**COMPARISON OF PREDICTED AND EXPERIMENTAL VALUES**

The original schedule for the General Electric Company's Pressure Suppression Test Facility (PSTF) called for running a matrix of tests divided equally between tests of 1, 2, and 3 rows of vents.

In practice, essentially all of the 1- and 2-vent tests were completed but a PSTF schedule and configuration change to investigate pool swell resulted in only three of the 3-vent tests being executed.

As part of the ongoing and close liaison between the General Electric Company and the AEC containment review staff, it was agreed that prior to running certain tests (selected by the Staff), GE would predict the PSTF performance using the same models as those used for full-scale Mark III analyses. The results were to be sent to the Staff prior to the tests being run.

Pre-test predictions were made for four of the tests in the 1- and 2-vent test series and for all three of the 3-vent tests; Figures A-1 through A-11 contain drywell and containment pressure comparisons of these 11 predictions to measured test results.

It can be seen that in all cases the model overpredicted the observed drywell pressure by a substantial margin. Table A-1 summarizes the extent of this overprediction.

It should be noted that with the exception of the vent back pressure model (Section 6), the pre-test predictions used the same model that is used for Mark III analyses. The vent back pressure model was not used because at the time the analyses were done, the performance of the vent clearing model was the major concern. Since the interaction between the vent clearing model and the suppression pool bubble model is very weak (it is non-existent for the 1-vent tests) and because including it in the simulations would have only resulted in an increase in the conservatism of the vent clearing model, the phenomenon of the suppression pool bubble was not included in the eleven pre-test predictions shown in Figures A-1 through A-11. Under these circumstances the model assumes that the vent back pressure is simply the containment pressure plus the hydrostatic pressure at that vent elevation.

As part of the ongoing analytical and experimental work, some test case analyses have been performed with the vent back pressure model included. Specifically, the four 1-vent pre-test predictions have been repeated with the vent back pressure model described in Section 6. The results are shown in Figures A-12 through A-15. As expected for these 1-vent tests, the phenomenon does not change the peak drywell pressure because this occurs at the time vent clearing occurs and therefore before any back pressure is created. However, it can be seen that the phenomenon substantially affects the performance of the model during the period of vent air flow that follows vent clearing. This is to be expected since a high bubble pressure will inhibit air vent flow and thus slow down the drywell depressurization that occurs after vent clearing. It can also be seen that including this phenomenon improves the correlation between the predicted performance and observed data.

Comparisons of analytical results and the test data are, and will continue to be, an ongoing process. The results of the various studies will be reported at the appropriate time.

Table A-1
COMPARISON OF PREDICTED AND EXPERIMENTAL VALUES

Horizontal Vents	Percent BWR/6 Break Area/Vessel Volume	Submergence to Top Vent Centerline (ft)	Peak Drywell Pressure (psig)		Over Prediction (%)
			Calculated	Observed	
1	70	12	21.6	16.8	28.6
1	100	8	20.7	17.0	21.8
1	100	12	26.4	20.5	28.8
1	200	12	41.8	30.2	38.4
2	70	12	16.9	14.3	18.2
2	100	8	17.8	15.3	16.3
2	100	10	20.8	14.8	40.5
2	200	12	32.9	23.3	41.2
3	100	7	16.3	13.3	22.6
3	100	11	20.6	14.3	44.1
3	200	11	29.6	21.8	35.8

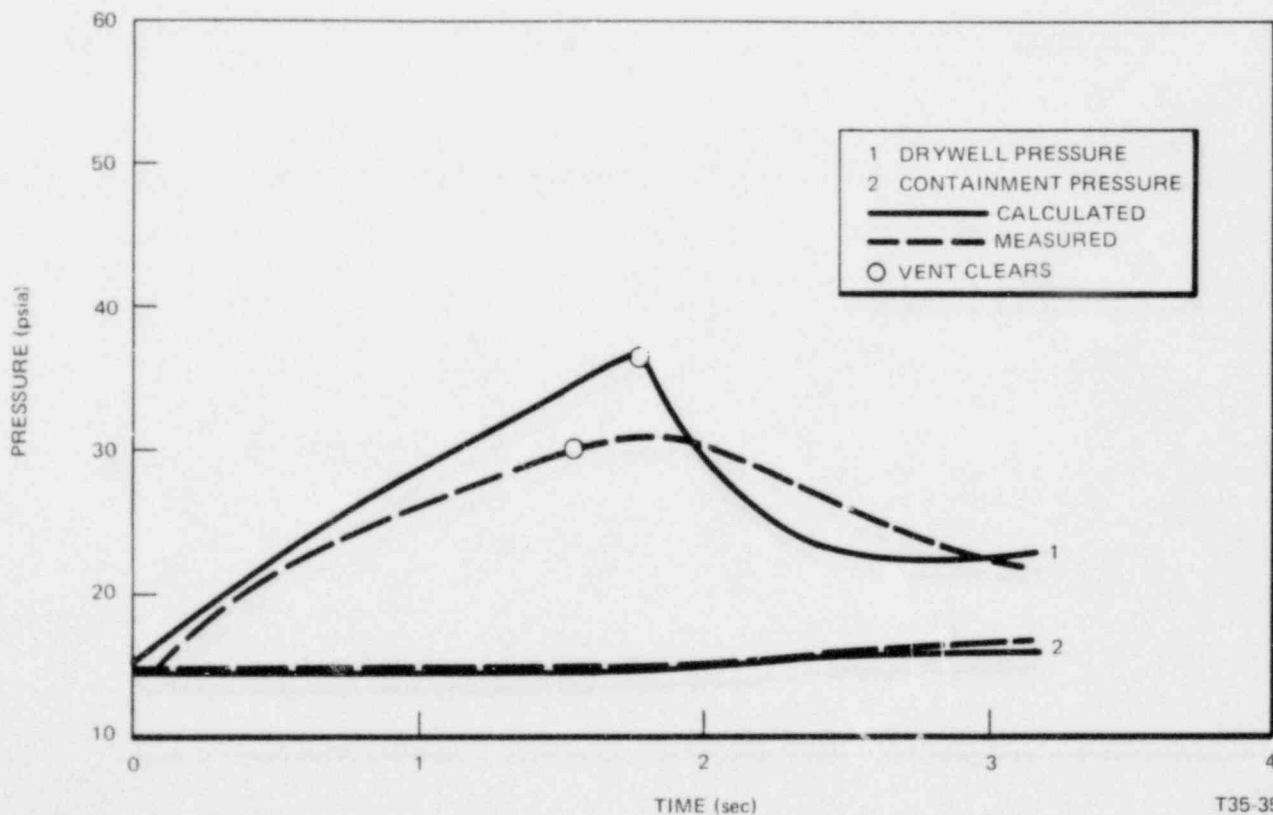


Figure A-1. Steam Blowdown, 70% BWR/6 Break Area/Vessel Volume; 1 Vent, 12-ft Submergence (Without Vent Back Pressure)

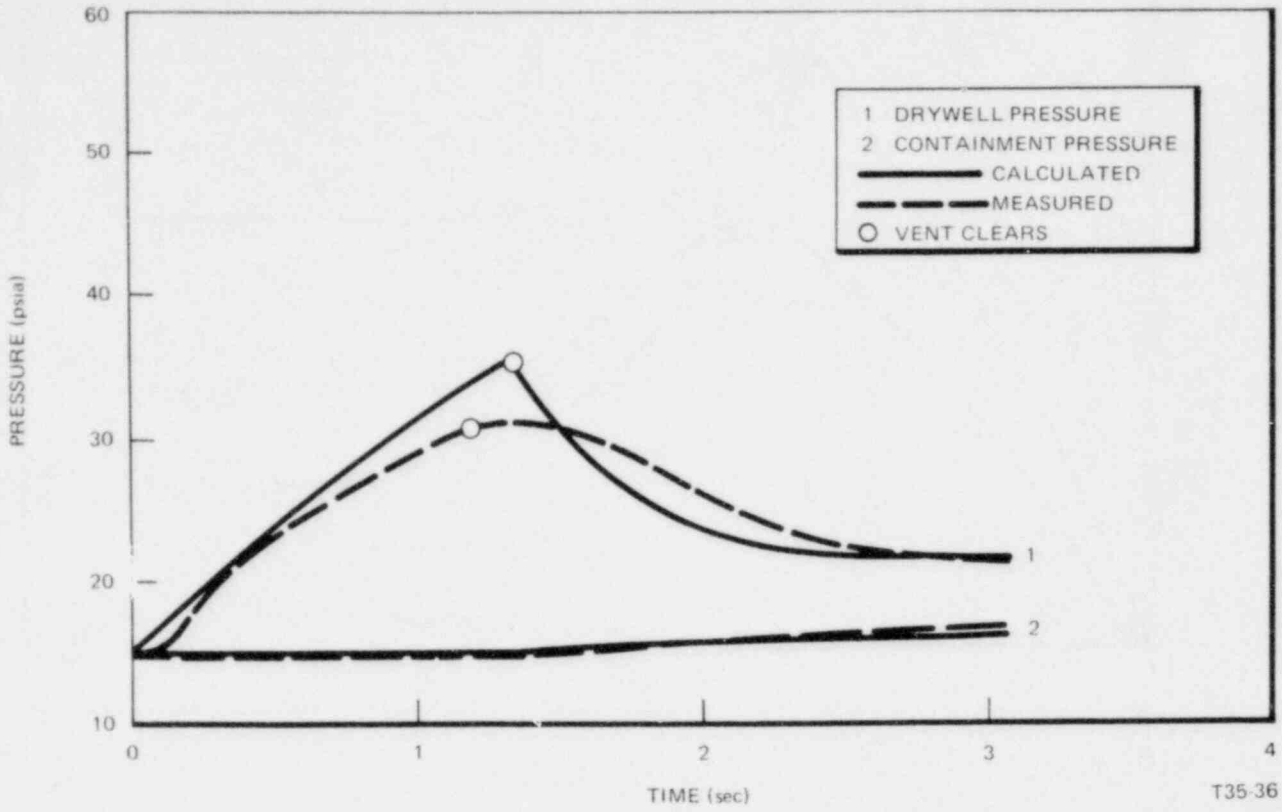


Figure A-2. Steam Blowdown, 100% BWR/6 Break Area/Vessel Volume; 1 Vent, 8-ft Submergence (Without Vent Back Pressure)

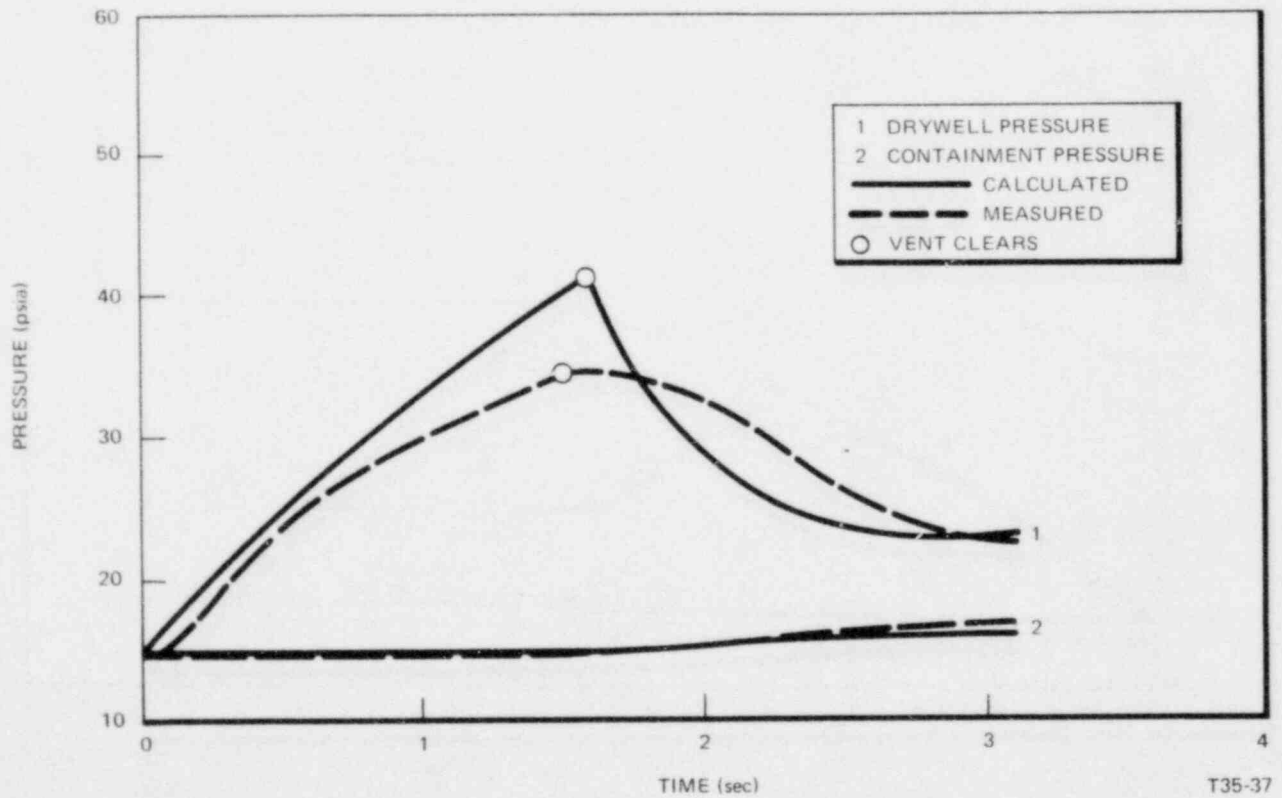
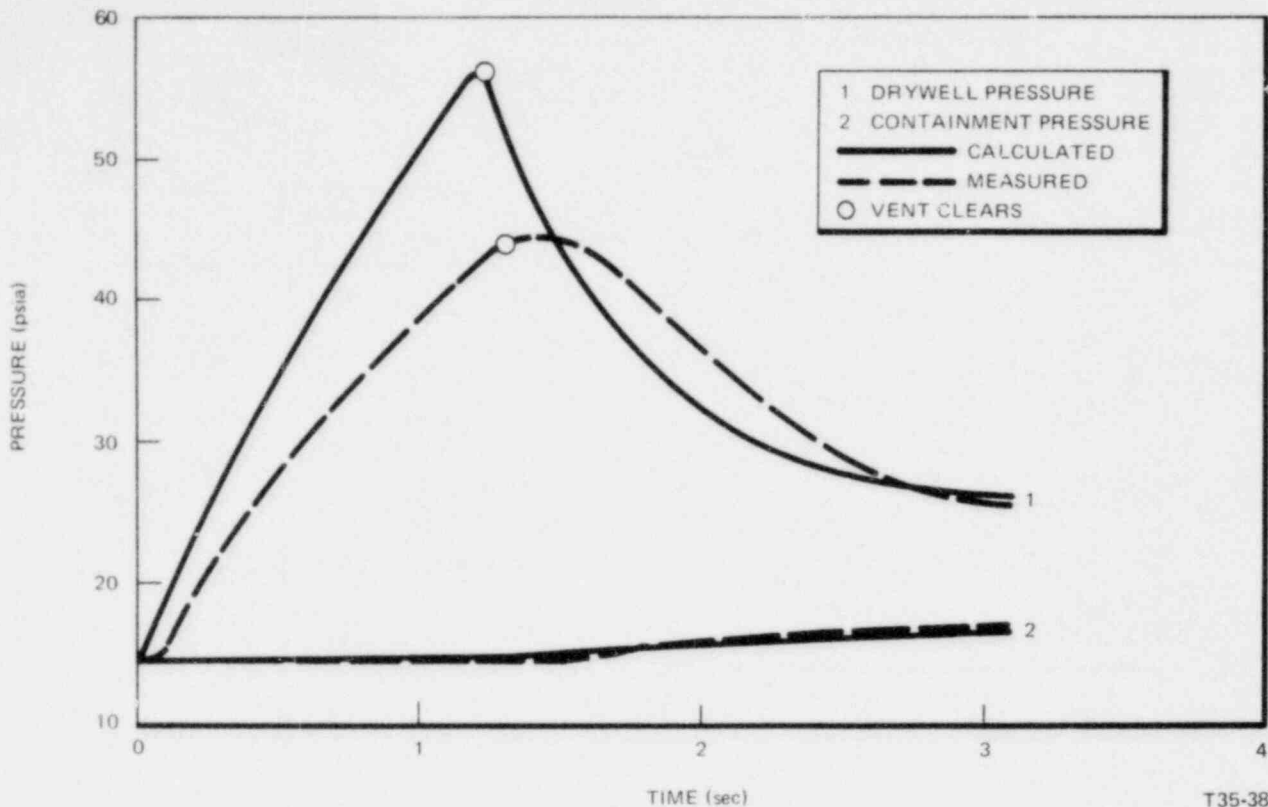
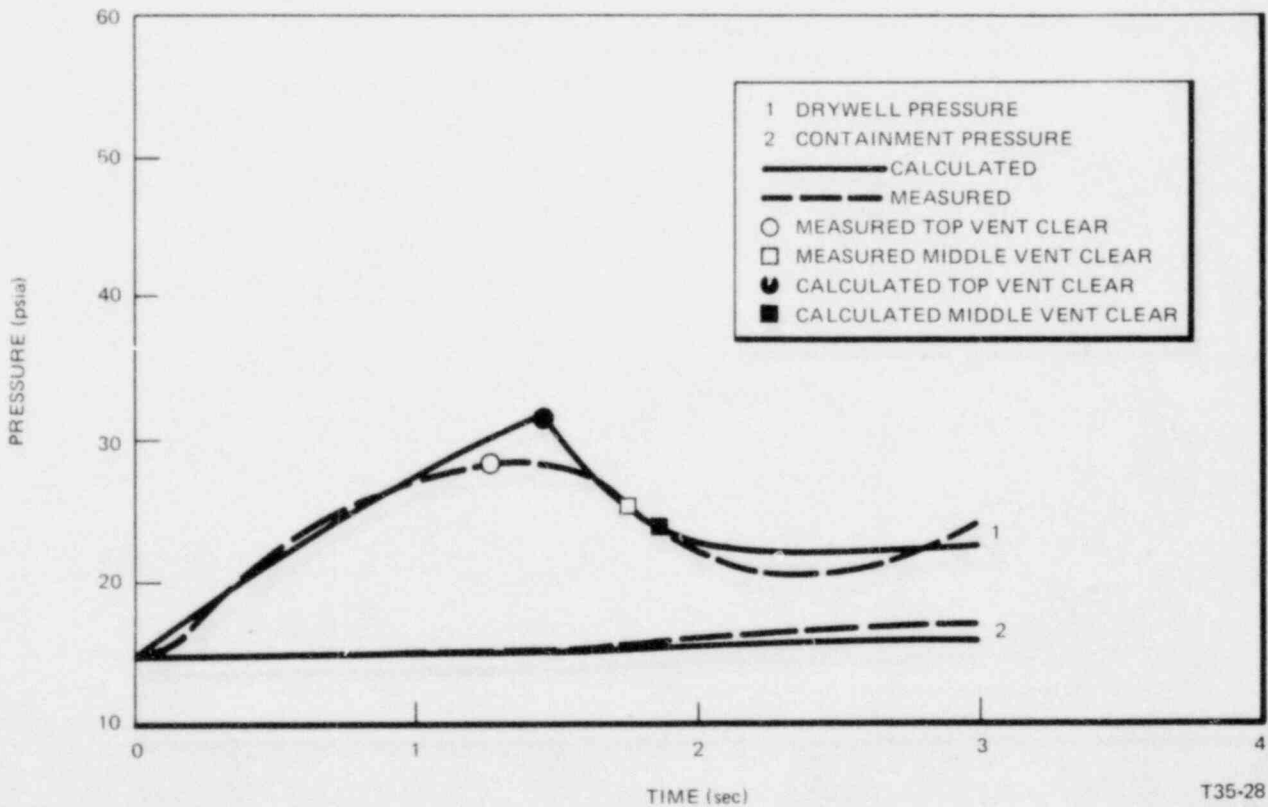


Figure A-3. Steam Blowdown, 100% BWR/6 Break Area/Vessel Volume; 1 Vent, 12-ft Submergence (Without Vent Back Pressure)



T35-38

Figure A-4. Steam Blowdown, 200% BWR/6 Break Area/Vessel Volume; 1 Vent, 12-ft Submergence (Without Vent Back Pressure)



T35-28

Figure A-5. Steam Blowdown, 70% BWR/6 Break Area/Vessel Volume; 2 Vents, 12-ft Submergence (Without Vent Back Pressure)

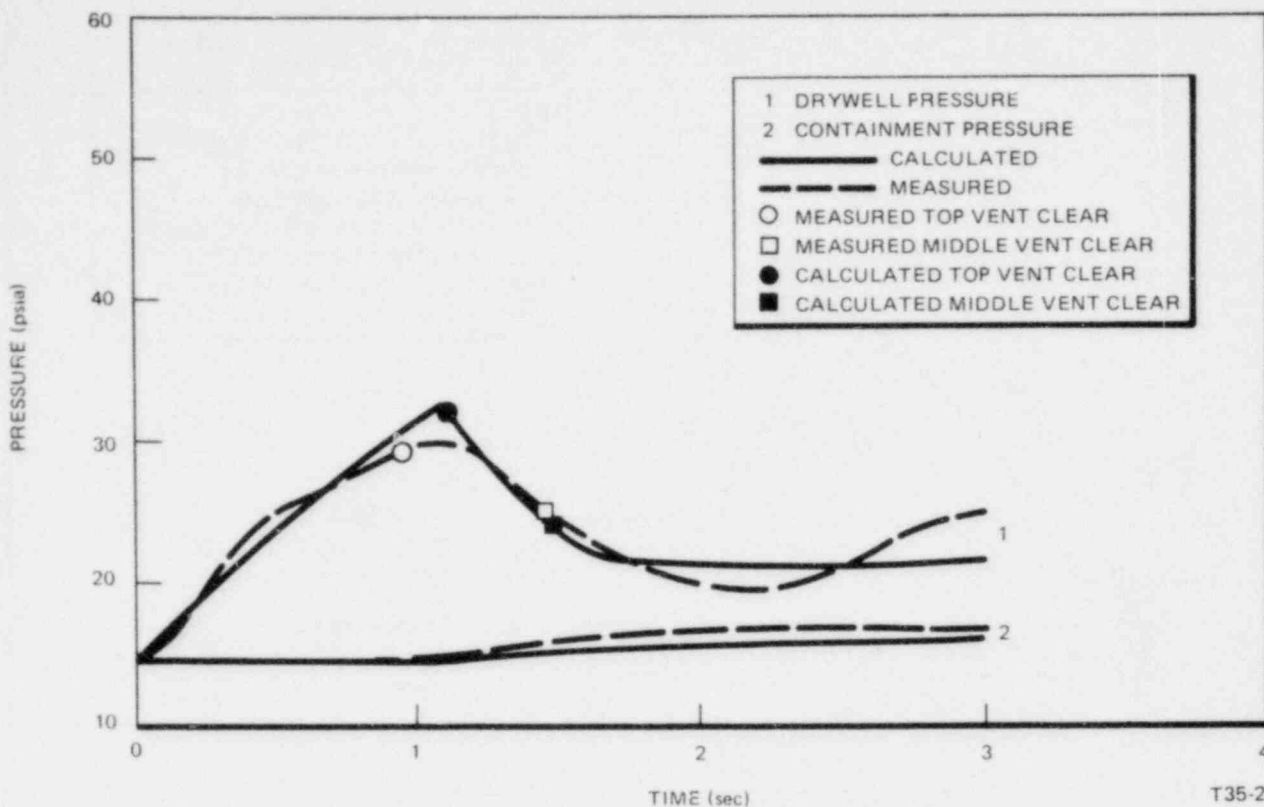


Figure A-6. Steam Blowdown, 100% BWR/6 Break Area/Vessel Volume; 2 Vents, 8-ft Submergence (Without Vent Back Pressure)

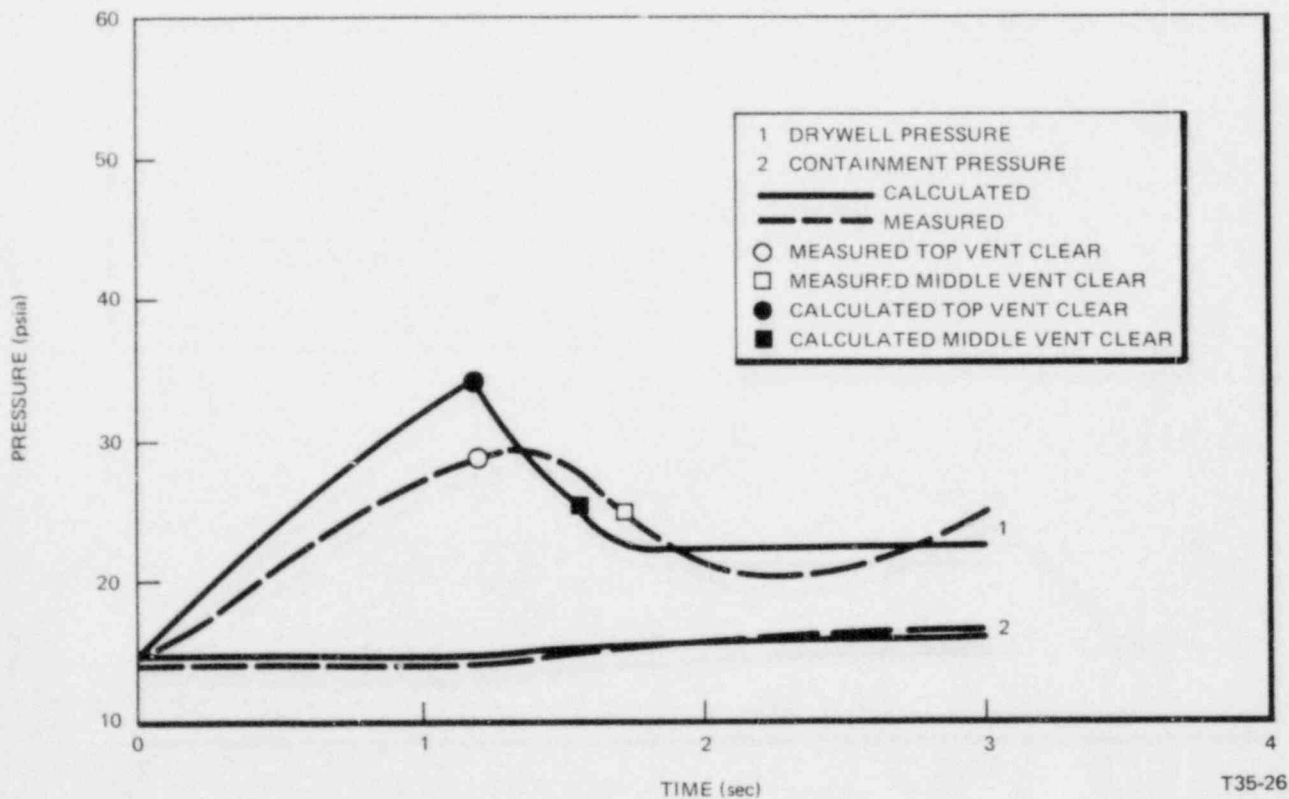


Figure A-7. Steam Blowdown, 100% BWR/6 Break Area/Vessel Volume; 2 Vents, 10-ft Submergence (Without Vent Back Pressure)

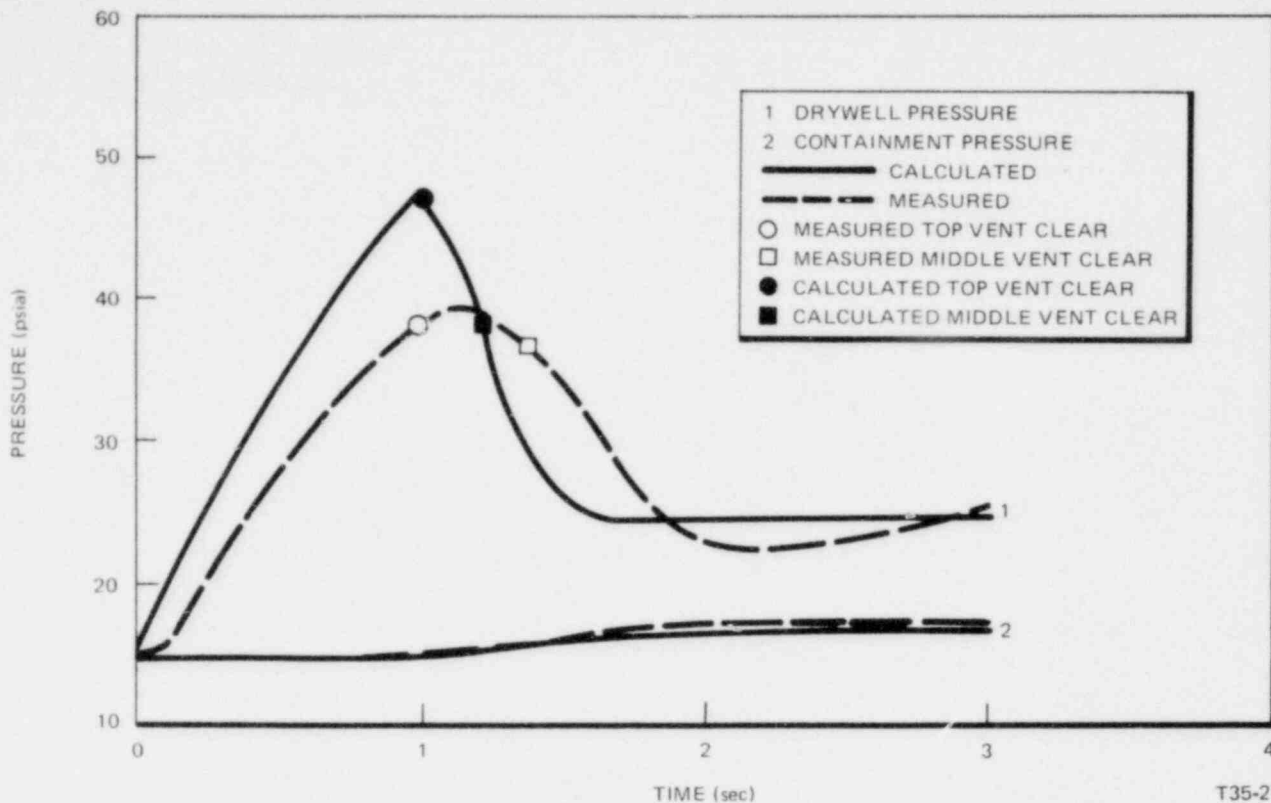


Figure A-8. Steam Blowdown, 200% BWR/6 Break Area/Vessel Volume; 2 Vents, 12-ft Submergence (Without Vent Back Pressure)

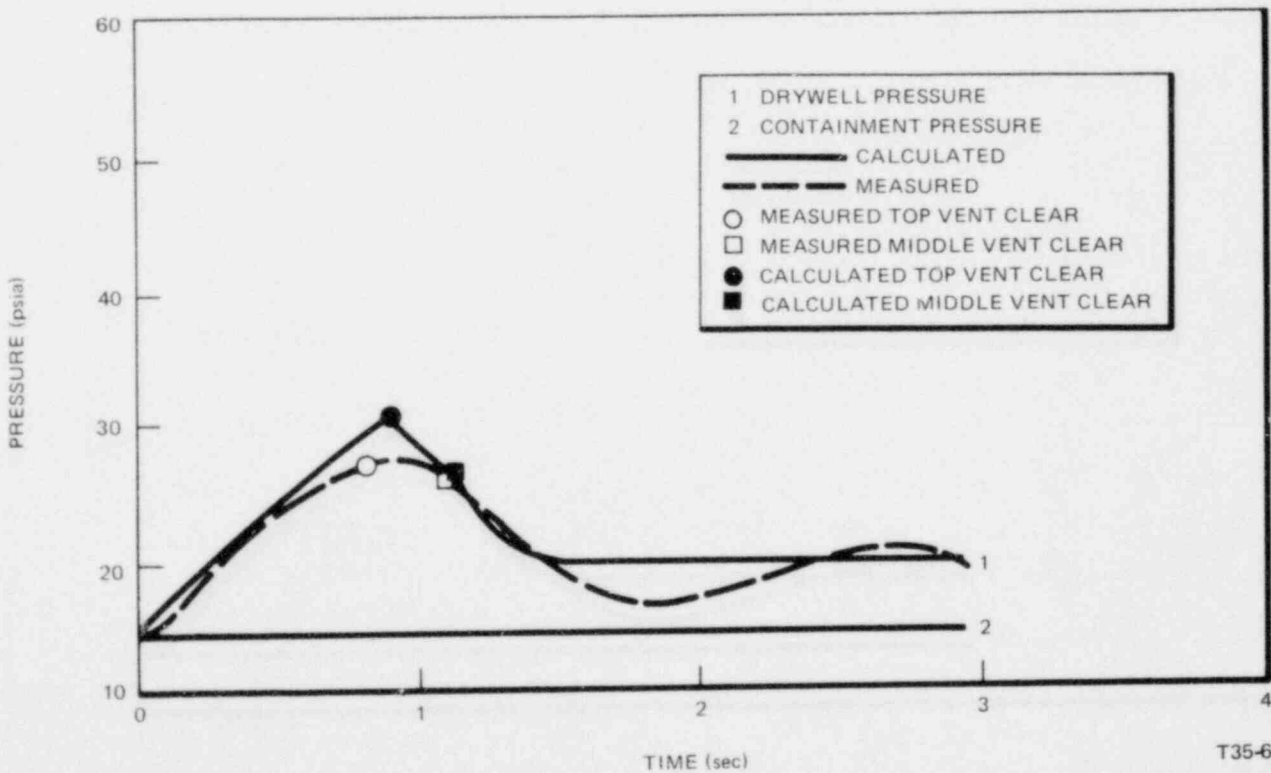


Figure A-9. Steam Blowdown, 100% BWR/6 Break Area/Vessel Volume; 3 Vents, 7-ft Submergence (Without Vent Back Pressure)

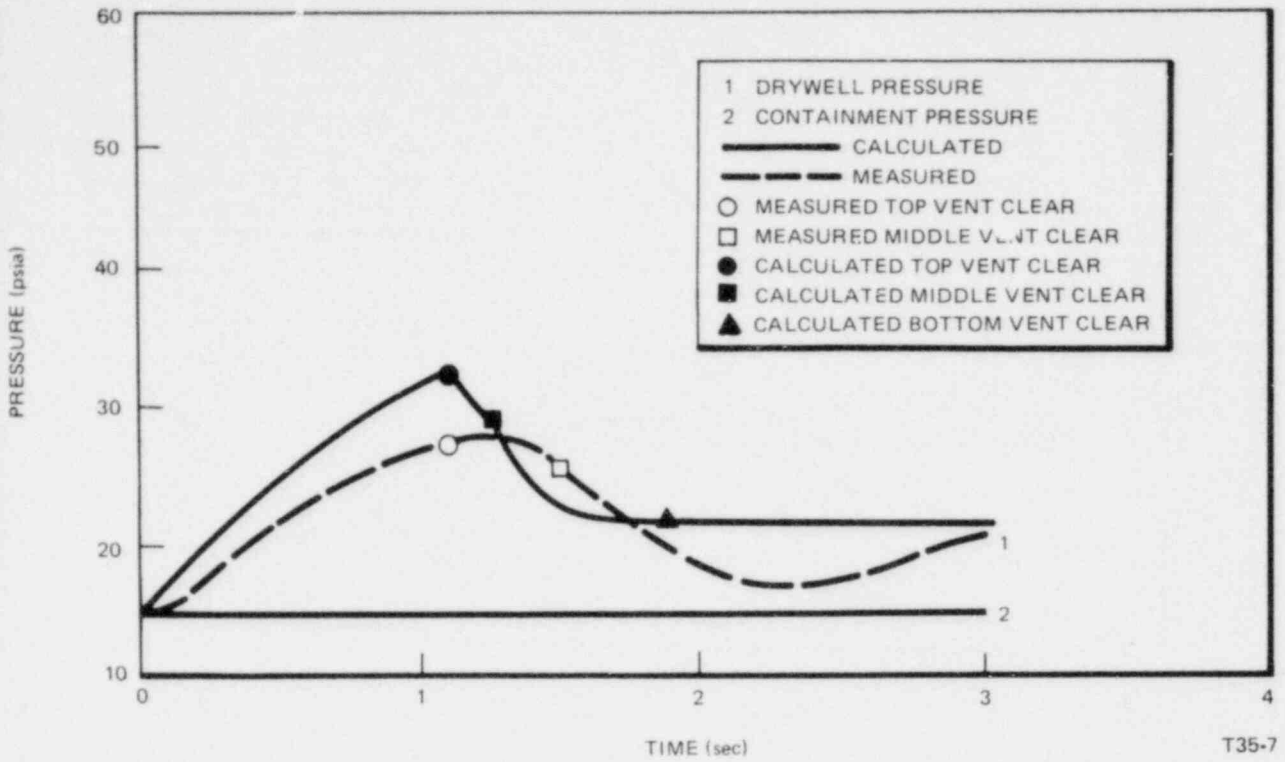


Figure A-10. Steam Blowdown, 100% BWR/6 Break Area/Vessel Volume; 3 Vents, 11-ft Submergence (Without Vent Back Pressure)

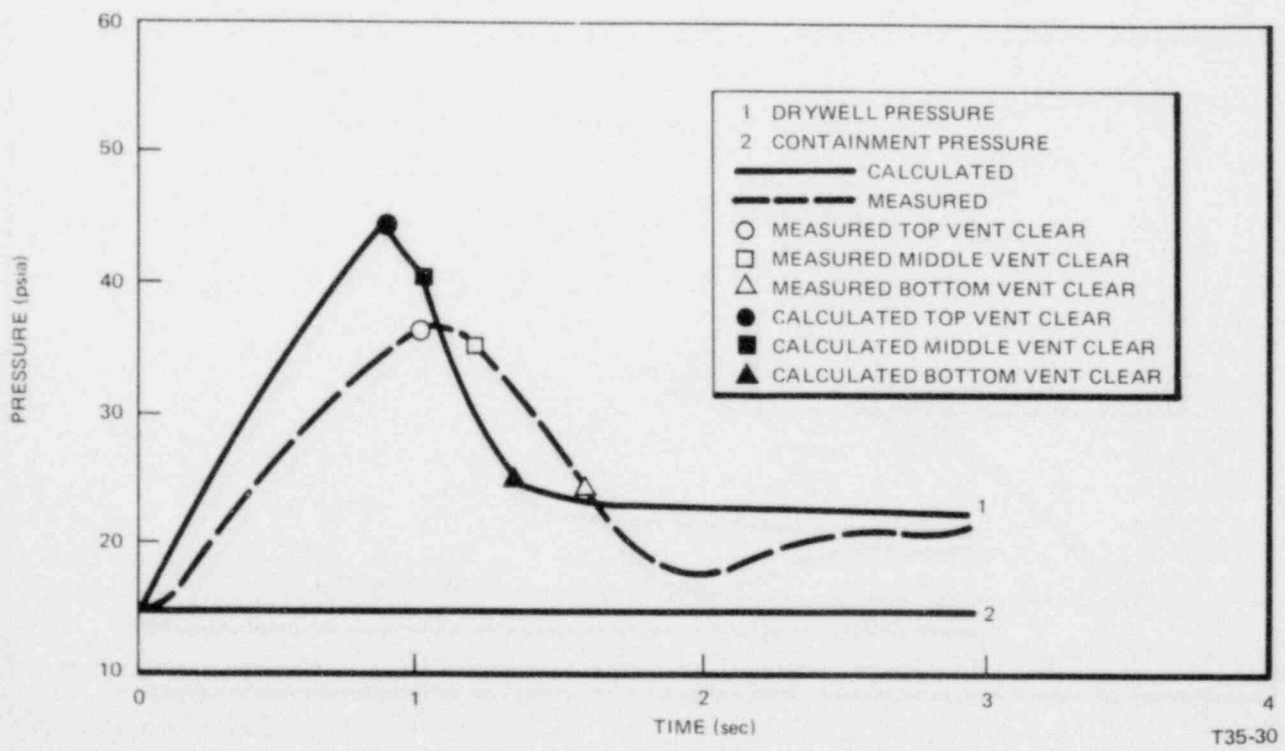


Figure A-11. Steam Blowdown, 200% BWR/6 Break Area/Vessel Volume; 3 Vents, 11-ft Submergence (Without Vent Back Pressure)

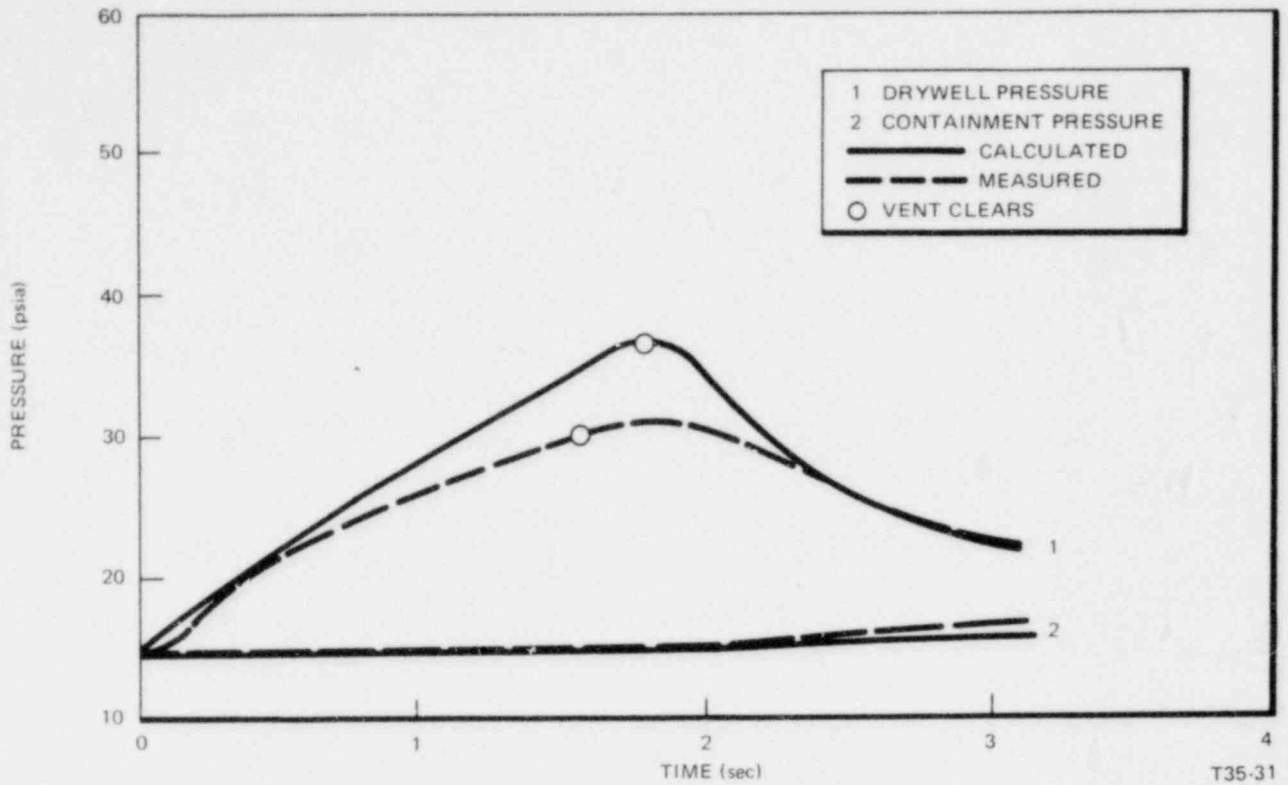


Figure A-12. Steam Blowdown, 70% BWR/6 Break Area/Vessel Volume; 1 Vent, 12-ft Submergence (With Vent Back Pressure)

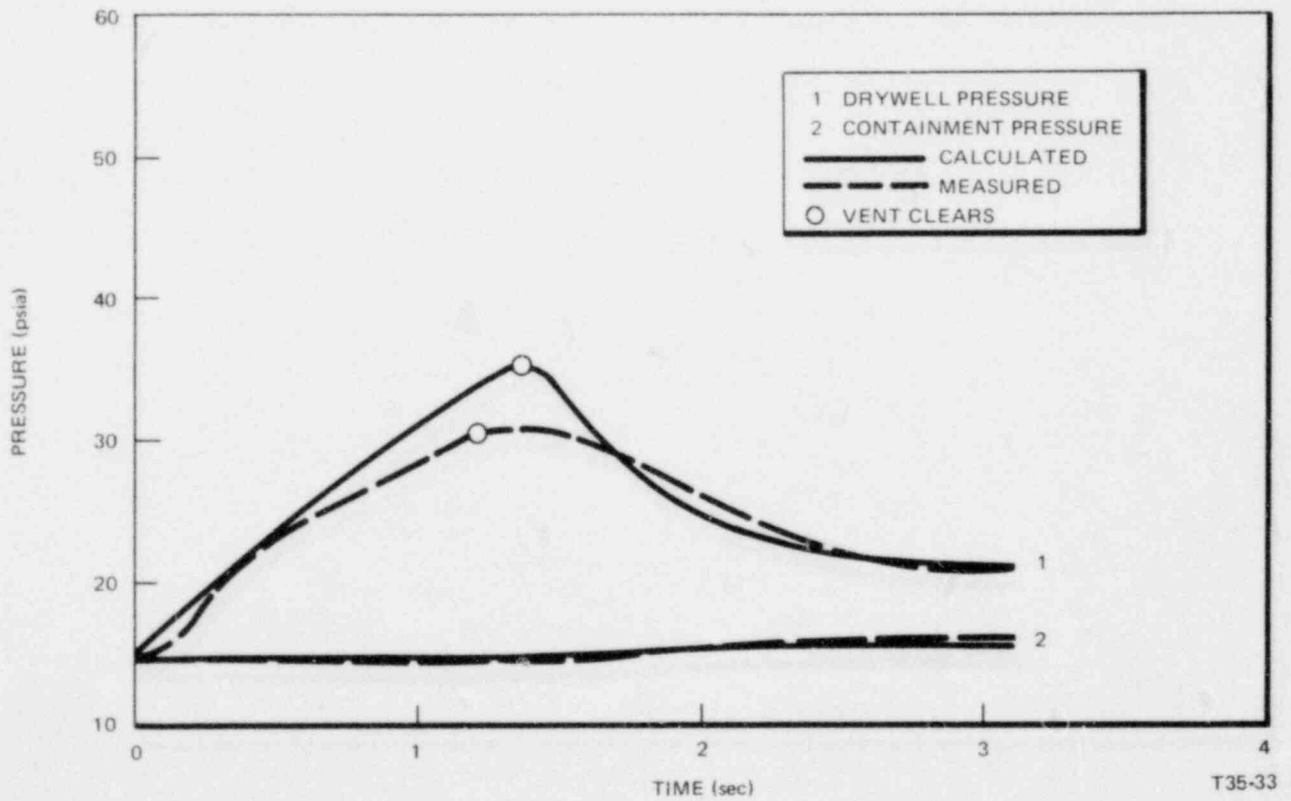


Figure A-13. Steam Blowdown, 100% BWR/6 Break Area/Vessel Volume; 1 Vent, 8-ft Submergence (With Vent Back Pressure)

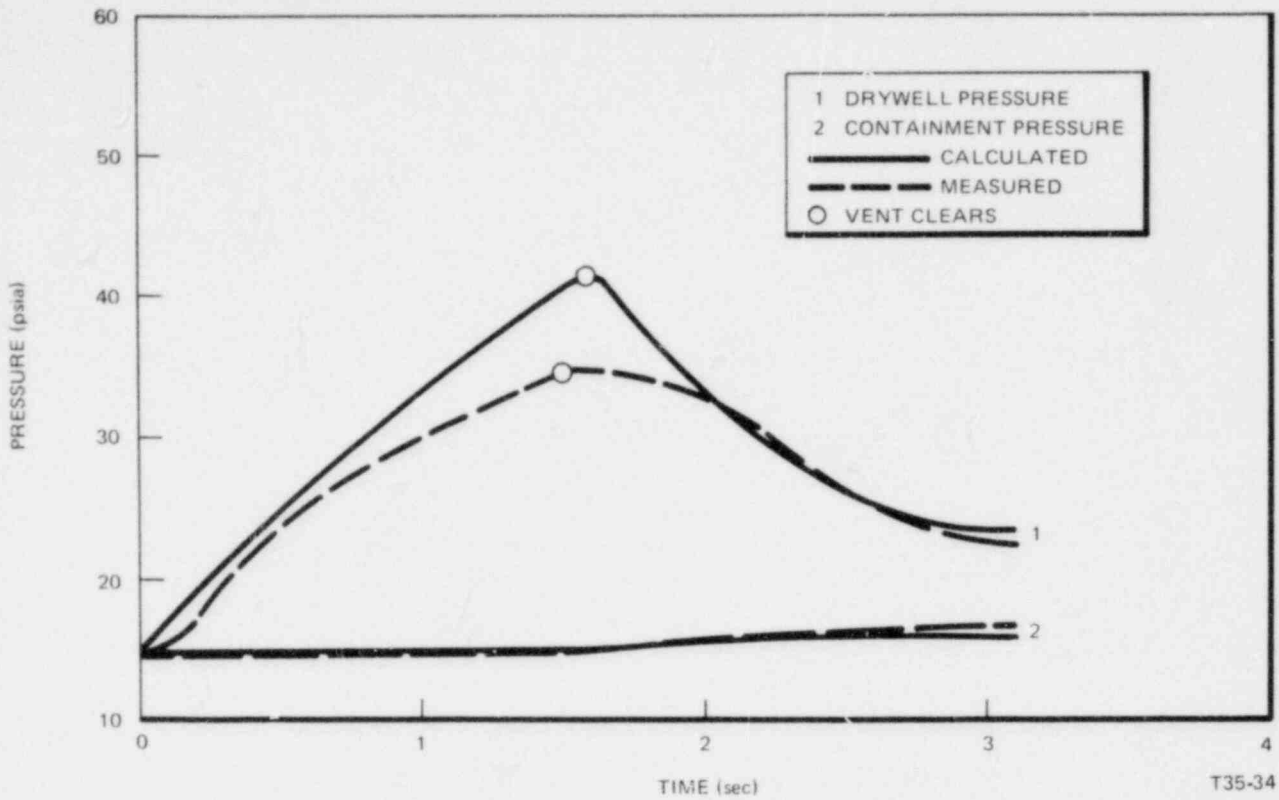


Figure A-14. Steam Blowdown, 100% BWR/6 Break Area/Vessel Volume; 1 Vent, 12-ft Submergence (With Vent Back Pressure)

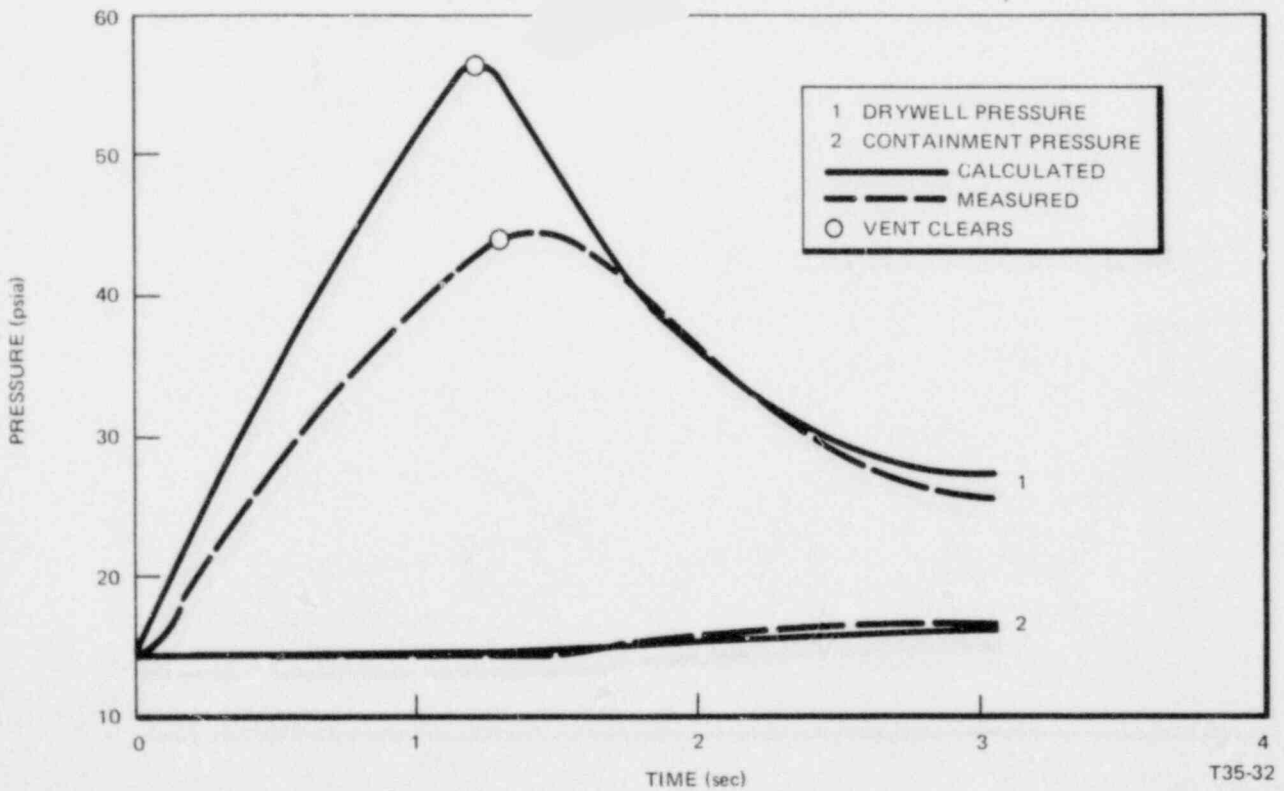


Figure A-15. Steam Blowdown, 200% BWR/6 Break Area/Vessel Volume; 1 Vent, 12-ft Submergence (With Vent Back Pressure)

APPENDIX B

PIPE INVENTORY BLOWDOWN

Immediately following a postulated instantaneous guillotine rupture of a primary system pipe at the reactor vessel nozzle, the blowdown flow rate into the dry well will consist of two components. At the RPV nozzle side of the break (the "short" side) the blowdown flow will correspond to choked flow over the entire area of the nozzle. Blowdown flow from the other side of the break (the "long" side) will be controlled initially by the rate at which the fluid inventory initially in the pipe decompresses and flows through the breaks, i.e., the so-called inventory effect. This flow will persist until the fluid inventory is depleted. At this time the flow from the long side will either cease or, if the other end of the pipe is also connected to the primary system, critical flow at the point of minimum flow area will be established. An example of the latter is the recirculation pipe rupture where choked reverse flow through the jet pump nozzles will follow the recirculation pipe inventory depletion.

This appendix summarizes important features of the methods used to compute early blowdown rates from the "long" side of both a recirculation pipe break and a steam line break.

The phenomena are described and the results of the inventory model are compared with available test data.

When evaluating the Mark III pressure response to a pipe rupture, the inventory effect is accounted for with an effective break area. The method of calculating this area is presented in the following sections.

B.1 THE EARLY BLOWDOWN PROCESS

If a small leak forms in a large pressurized vessel, mass and energy discharge rates cause vessel pressure to decrease over a period of time. The time required for full pressure reduction to the ambient value is roughly equal to the initial contained fluid mass divided by an average mass discharge rate. Usually decompression rates are slow relative to the time required to transmit pressure signals at acoustic speed throughout the vessel, and therefore, the vessel decompresses as a unit or single uniform system at quasi-equilibrium states.

A different situation occurs when the vessel is a long pipe and the break is assumed to be a circumferential failure. For this case, fluid in the pipe cannot decompress as a single system. Decompression occurs first at the break, but fluid inertia does not permit instantaneous expansion throughout the pipe. This behavior is much like series-connected alternate springs and masses, compressed in the confining walls of a pipe. A slow reduction of the compressive force at one end would permit the entire spring-mass system to respond as a unit or single uniform system. However, rapid reduction of the compressive restraining force at one end leaves the system in a state where the first mass to discharge from the pipe is accelerated by the spring joining it to the second mass. Movement of the first mass decreases compression of the adjoining spring or the second mass, and the second mass begins to accelerate, reducing the compressive force on the next spring and third mass, etc., until the decompression signal has propagated through the pipe.

Stiff springs, analogous to non-flashing water, transmit pressure signals faster than loose springs, which are analogous to saturated flashing water. Although it is convenient to consider rigid pipe walls, actual pipe elasticity has the effect of a slight reduction in propagation velocity.

The fluid mechanics equations discussed in the following sections contain the series spring-mass idea in a continuous sense such that they yield space- and time-dependent fluid properties throughout the pipe. Of particular interest are the properties at discharge, which determine the early blowdown rate before steady-state flow is reached. Fluid-state relationships are based on saturated, equilibrium steam and water properties.

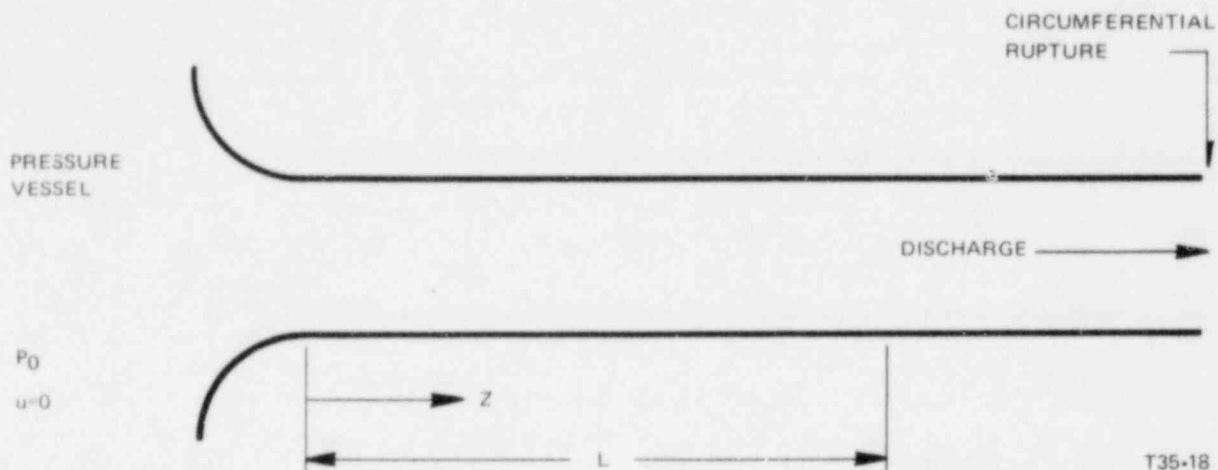
The method of characteristics was used to obtain numerical solution of the fluid flow equations, and is described in most text books dealing with advanced fluid mechanics. (For example, see Reference B-1.)

The following is the derivation of the pipe inventory model.

B.2 STARTING BLOWDOWN FROM A PIPE BREAK

B.2.1 Time and Space Dependent Flow Properties

Consider a uniform area pipe without flow restrictions, attached to a pressure vessel at one end. A sudden, circumferential rupture occurs at the other end.



For the idealized case described by uniform pipe flow area, adiabatic flow, and a frictionless pipe, the equations governing homogeneous time-dependent local flow properties are*

Mass conservation

$$\frac{\partial \rho}{\partial t} + \frac{\partial(\rho u)}{\partial Z} = 0 \tag{B-1}$$

Momentum conservation

$$\frac{\partial u}{\partial t} + u \frac{\partial u}{\partial Z} + \frac{g_c}{\rho} \frac{\partial P}{\partial Z} = 0 \tag{B-2}$$

Energy conservation

$$\frac{\partial h}{\partial t} + u \frac{\partial h}{\partial Z} - \frac{1}{\rho} \left(\frac{\partial P}{\partial t} + u \frac{\partial P}{\partial Z} \right) = 0 \tag{B-3}$$

The Gibbs equation

$$T ds = dh - \frac{dP}{\rho} \tag{B-4}$$

and Equation (B-3) can be combined to show that in the absence of shocks, fluid state changes in the pipe proceed at constant entropy.

*See Subsection B.3.

A solution to Equations (B-1) and (B-2) can be obtained by Riemann's method (Landau and Lifshitz, 1959).

The result is:

$$u(Z,t) = \pm g_c \int_{P_0}^P \frac{dP}{\rho(P)c(P)} + \text{constant} \quad (B-5)$$

$$Z = (u \pm c(u))t + f(u) \quad (B-6)$$

where the sonic speed $c(P)$ is given by

$$c = \sqrt{g_c \left(\frac{\partial P}{\partial \rho} \right)_s} = c(P) \quad (B-7)$$

and ρ is expressed as a function of P as

$$\rho = \rho(P). \quad (B-8)$$

The constant and $f(u)$ in Equations (B-5) and (B-6) are determined from initial and boundary conditions for the case being considered.

If fluid in the pipe is stationary when the break occurs, the constant in (B-5) is zero.

The + and - signs in (B-5) and (B-6) refer to right or left traveling waves or disturbances.

Note, therefore, that (B-5) relates local values of velocity and pressure, whereas (B-6) involves the time and space dependence of properties.

B.2.2 Initial Discharge Properties

When the pipe break occurs, it can be shown that for compressible fluids, the discharge velocity is sonic. It follows from (B-5) that for

$$u(L,t) = c(P) \quad (B-9)$$

there is a set of unique discharge pressure P and corresponding c and ρ which hold constant until the leftward decompression wave travels to the vessel and a rightward wave arrives back at the break. Then the discharge flow rate increases over a brief period of time until steady discharge is reached.

B.2.3 The Upstream Boundary

When a flow restriction is in the pipe upstream from the break, return signals toward the break will perhaps *reduce* discharge flow from its initial value.

If there is no flow restriction and effectively a loss-less attachment to the vessel, discharge rate will increase toward the steady state.

The main point here is that there is a unique *initial* discharge rate, dependent on the fluid properties, that continues until return signals arrive from upstream conditions.

B.2.4 Ideal Gas Discharge Rate

Figure B-1 shows discharge properties in the break end of a pipe which contains ideal steam. Note that the initial discharge mass flux is about 60% of the steady state for a pipe with no upstream restrictions.

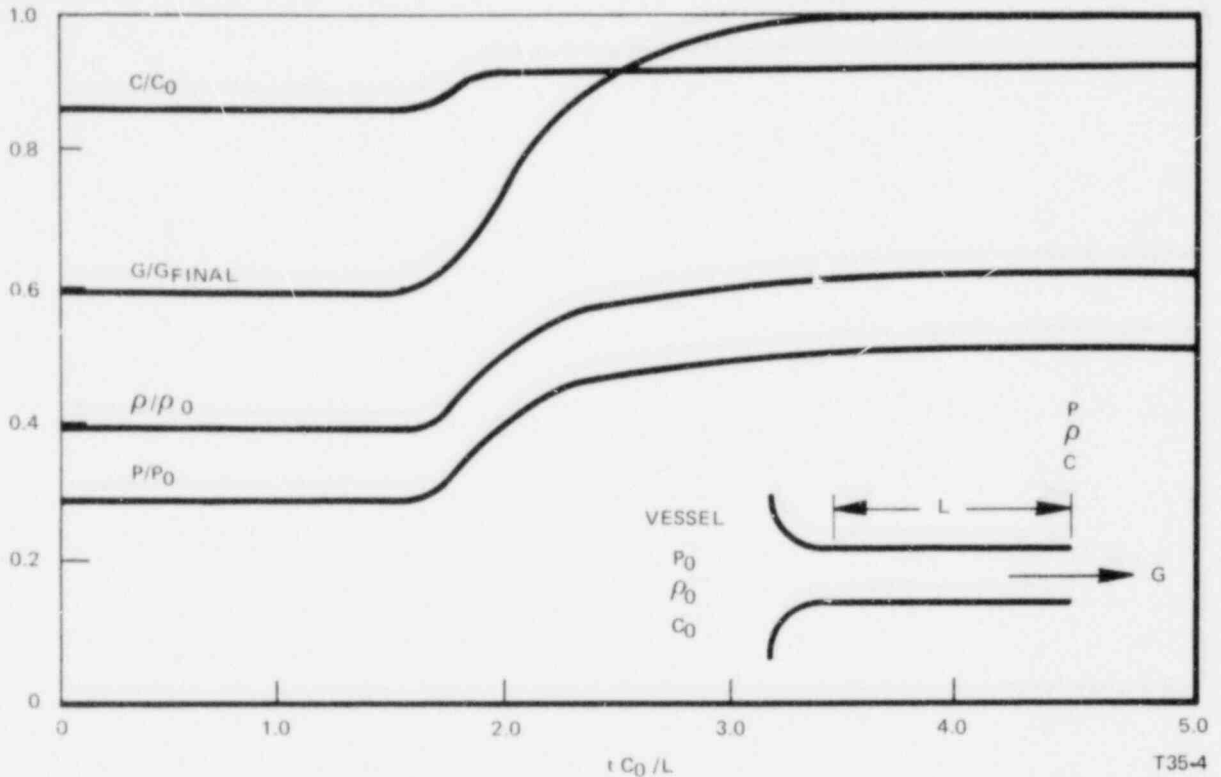
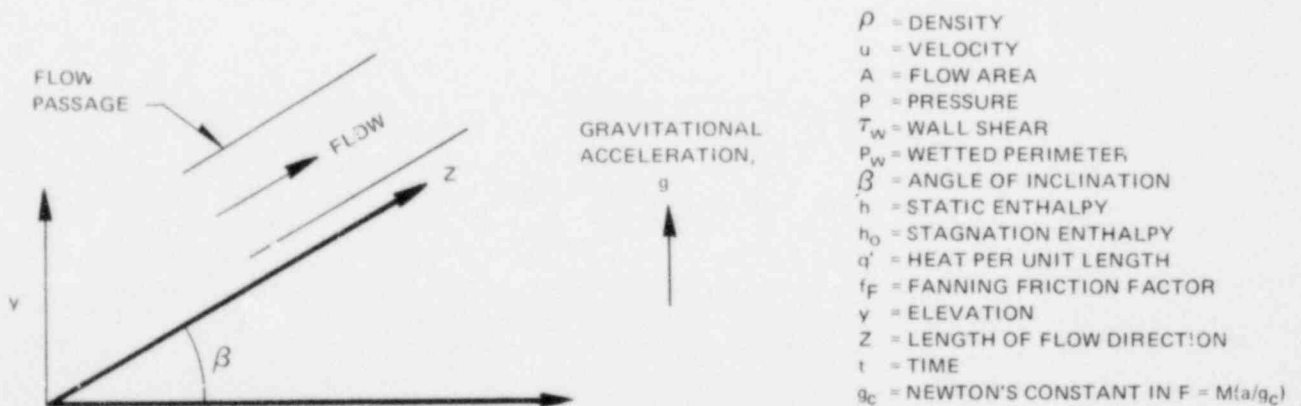


Figure B-1. Discharge Properties for Ideal Steam

B.2.5 Water Initial Discharge Rate

Saturated and subcooled water properties were used in equations (B-5) and (B-7) to determine initial discharge properties from a water pipe initially at 1000 psia and have temperature corresponding to various saturation pressures. Results of this computation are shown in Figure B-2.

Note that for saturated water at 1000 psia, the initial blowdown rate per unit area is less than 4000 lbm/sec-ft², whereas the final rate, based on the GE blowdown model is 8000 lbm/sec-ft². As subcooling increases and P_{SAT} decreases, the initial blowdown rate decreases and the final rate increases.



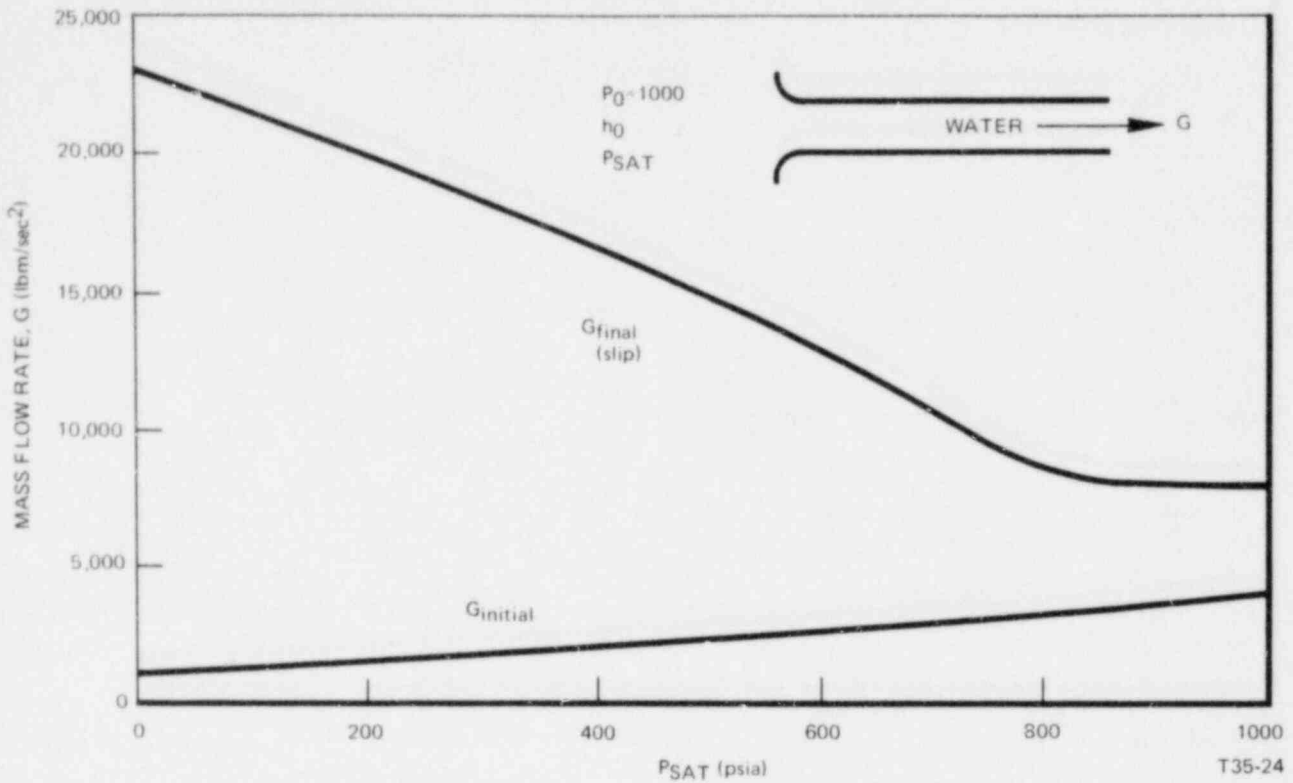


Figure B-2. Water Initial Discharge Rate

3.3.1 Conservation Equations

Mass

$$\frac{\partial \rho}{\partial t} + u \frac{\partial \rho}{\partial Z} + \rho \frac{\partial u}{\partial Z} + \frac{\rho u}{A} \frac{dA}{dZ} = 0 \tag{B-10}$$

Momentum

$$\frac{\partial u}{\partial t} + u \frac{\partial u}{\partial Z} + \frac{g_c}{\rho} \frac{\partial P}{\partial Z} = -g_c \left(\frac{\tau_w}{\rho} \frac{P_w}{A} + \frac{g}{g_c} \sin \beta \right) \tag{B-11}$$

Energy

$$\frac{\partial h_o}{\partial t} + u \frac{\partial h_o}{\partial Z} - \frac{1}{\rho} \frac{\partial P}{\partial t} - \frac{q'(Z,t)}{\rho A} = 0 \tag{B-12}$$

Shear stress is given by

$$\tau_w \triangleq f_F \frac{u|u|}{2g_c} \rho \tag{B-13}$$

Stagnation enthalpy is

$$h_o \triangleq h + \frac{u^2}{2g_c} + \frac{g}{g_c} y \tag{B-14}$$

Noting that

$$\frac{\partial v}{\partial t} = 0; \quad \frac{\partial y}{\partial Z} = \sin \beta$$

Equations (B-14), (B-11), (B-12) combine to give

$$\frac{\partial h}{\partial t} + u \frac{\partial h}{\partial Z} - \frac{1}{\rho} \left(\frac{\partial P}{\partial t} + u \frac{\partial P}{\partial Z} \right) = \frac{u \tau_w P_w}{\rho A} + \frac{q'(Z,t)}{\rho A} \tag{B-15}$$

For simple compressible fluids in the thermodynamic equilibrium, the state can be given by P and ρ such that

$$h = h(P, \rho) \tag{B-16}$$

Eliminate h with

$$\left. \begin{aligned} \frac{\partial h}{\partial t} &= \left(\frac{\partial h}{\partial P} \right)_\rho \frac{\partial P}{\partial t} + \left(\frac{\partial h}{\partial \rho} \right)_P \frac{\partial \rho}{\partial t} \\ \frac{\partial h}{\partial Z} &= \left(\frac{\partial h}{\partial P} \right)_\rho \frac{\partial P}{\partial Z} + \left(\frac{\partial h}{\partial \rho} \right)_P \frac{\partial \rho}{\partial Z} \end{aligned} \right\} \tag{B-17}$$

and the Gibbs equation

$$T ds = dh - \frac{1}{\rho} dP \tag{B-18}$$

which provides

$$\left. \begin{aligned} \left(\frac{\partial h}{\partial \rho} \right)_P &= T \left(\frac{\partial s}{\partial \rho} \right)_P \\ \left(\frac{\partial h}{\partial P} \right)_\rho - \frac{1}{\rho} &= T \left(\frac{\partial s}{\partial P} \right)_\rho \end{aligned} \right\} \tag{B-19}$$

Also express entropy as

$$s = s(P, \rho); \quad ds = \left(\frac{\partial s}{\partial P} \right)_\rho dP + \left(\frac{\partial s}{\partial \rho} \right)_P d\rho \tag{B-20}$$

Then it follows that

$$\left(\frac{\partial P}{\partial \rho}\right)_s = -\left(\frac{\partial s}{\partial \rho}\right)_P / \left(\frac{\partial s}{\partial P}\right)_\rho = \frac{C^2}{g_c} \quad (B-21)$$

where C is propagation speed, (B-15) now becomes

$$\frac{\partial P}{\partial t} + u \frac{\partial P}{\partial Z} - \frac{C^2}{g_c} \left(\frac{\partial \rho}{\partial t} + u \frac{\partial \rho}{\partial Z}\right) = \frac{\frac{u\tau_w P_w}{\rho A} + \frac{q'(Z,t)}{\rho A}}{\left[\left(\frac{\partial h}{\partial P}\right)_\rho - \frac{1}{\rho}\right]} \quad (B-22)$$

B.3.2 Creation of Entropy

Equations (B-15) and (B-18) show that

$$T \left(\frac{\partial s}{\partial t} + u \frac{\partial s}{\partial Z}\right) = \frac{u\tau_w P_w}{\rho A} + \frac{q'(Z,t)}{\rho A} \quad (B-23)$$

Note that for $\tau_w = q' = 0$, the flow (shocks absent) is isentropic.

B.3.3 Method of Characteristics

Rewriting the conservation equations, we have

$$\frac{\partial \rho}{\partial t} + u \frac{\partial \rho}{\partial Z} + \rho \frac{\partial u}{\partial Z} = F_1(Z,t) \quad (B-24)$$

$$\frac{\partial u}{\partial t} + u \frac{\partial u}{\partial Z} + \frac{g_c}{\rho} \frac{\partial P}{\partial Z} = F_2(Z,t) \quad (B-25)$$

$$\frac{\partial P}{\partial t} + u \frac{\partial P}{\partial Z} + F(Z,t) \left(\frac{\partial \rho}{\partial t} + u \frac{\partial \rho}{\partial Z}\right) = F_3(Z,t) \quad (B-26)$$

where

$$F_1(Z,t) = -\frac{\rho u}{A} \frac{dA}{dZ} \quad (B-27)$$

$$F_2(Z,t) = -g_c \left(\frac{\tau_w P_w}{\rho A} + \frac{g}{g_c} \sin \beta \right) \quad (B-28)$$

$$F_3(Z,t) = \frac{\frac{u\tau_w P_w}{\rho A} + \frac{q'(Z,t)}{\rho A}}{\left[\left(\frac{\partial h}{\partial P}\right)_\rho - \frac{1}{\rho}\right]} \quad (B-29)$$

$$F(Z,t) = \frac{\left(\frac{\partial h}{\partial \rho}\right)_P}{\left(\frac{\partial h}{\partial P}\right)_\rho - \frac{1}{\rho}} = -\frac{C^2}{g_c} \tag{B-30}$$

Multiply equations (B-24), (B-25), (B-26) by the undetermined constants $\lambda_1, \lambda_2, \lambda_3$ and add together:

$$\begin{aligned} &\lambda_3 \frac{\partial P}{\partial t} + (\lambda_1 + \lambda_3 F) \frac{\partial \rho}{\partial t} + \lambda_2 \frac{\partial u}{\partial t} + \left(\lambda_2 \frac{g_c}{\rho} + \lambda_3 u\right) \frac{\partial P}{\partial Z} \\ &+ \left(\lambda_1 u + \lambda_3 u F\right) \frac{\partial \rho}{\partial Z} + \left(\lambda_1 \rho + \lambda_2 u\right) \frac{\partial u}{\partial Z} = \lambda_1 F_1 + \lambda_2 F_2 + \lambda_3 F_3 \end{aligned} \tag{B-31}$$

Regarding

$$\left. \begin{aligned} P &= P(Z,t) \\ u &= u(Z,t) \\ \rho &= \rho(Z,t) \end{aligned} \right\} \tag{B-32}$$

We can write

$$\left. \begin{aligned} \frac{\partial P}{\partial Z} &= \frac{dP}{dZ} - \frac{\partial P}{\partial t} \frac{dt}{dZ} \\ \frac{\partial u}{\partial Z} &= \frac{du}{dZ} - \frac{\partial u}{\partial t} \frac{dt}{dZ} \\ \frac{\partial \rho}{\partial Z} &= \frac{d\rho}{dZ} - \frac{\partial \rho}{\partial t} \frac{dt}{dZ} \end{aligned} \right\} \tag{B-33}$$

And eliminate $\frac{\partial P}{\partial Z}, \frac{\partial u}{\partial Z}, \frac{\partial \rho}{\partial Z}$ from Equation (B-31). Then Equation (B-36) becomes

$$\begin{aligned} &\left[\lambda_3 - \left(\lambda_2 \frac{g_c}{\rho} + \lambda_3 u\right) \frac{dt}{dZ}\right] \frac{\partial P}{\partial t} + \left[\lambda_1 + \lambda_3 F - u\left(\lambda_1 + \lambda_3 F\right) \frac{dt}{dZ}\right] \frac{\partial \rho}{\partial t} \\ &+ \left[\lambda_2 - \left(\lambda_1 \rho + \lambda_2 u\right) \frac{dt}{dZ}\right] \frac{\partial u}{\partial t} + \left(\lambda_2 \frac{g_c}{\rho} + \lambda_3 u\right) \frac{dP}{dZ} + u\left(\lambda_1 + \lambda_3 F\right) \frac{d\rho}{dZ} \\ &+ \left(\lambda_1 \rho + \lambda_2 u\right) \frac{du}{dZ} = \lambda_1 F_1 + \lambda_2 F_2 + \lambda_3 F_3 \end{aligned} \tag{B-34}$$

The partial derivatives will vanish from (B-34) if $\lambda_1, \lambda_2, \lambda_3$ are chosen properly so that the coefficients of $\partial P/\partial t$, $\partial \rho/\partial t$, and $\partial u/\partial t$ are zero. Formally,

$$0\lambda_1 - \frac{g_c}{\rho} \frac{dt}{dZ} \lambda_2 + \left(1 - u \frac{dt}{dZ}\right) \lambda_3 = 0 \tag{B-35}$$

$$\left(1 - u \frac{dt}{dZ}\right) \lambda_1 + 0\lambda_2 + F \left(1 - u \frac{dt}{dZ}\right) \lambda_3 = 0 \tag{B-36}$$

$$-\rho \frac{dt}{dZ} \lambda_1 + \left(1 - u \frac{dt}{dZ}\right) \lambda_2 + 0\lambda_3 = 0 \tag{B-37}$$

The system (B-35), (B-36), (B-37) has a solution only if the coefficient determinant is zero, or,

$$\left(1 - u \frac{dt}{dZ}\right) \left[\left(g_c F + u^2\right) \left(\frac{dt}{dZ}\right)^2 - 2u \frac{dt}{dZ} + 1 \right] = 0 \tag{B-38}$$

Permissible solutions for dt/dZ give the characteristic lines,

$$\frac{dt}{dZ} = \left\{ \begin{array}{l} \frac{1}{u} \\ \frac{u + \sqrt{-g_c F}}{u^2 + g_c F} = \frac{1}{u - c} \\ \frac{u - \sqrt{-g_c F}}{u^2 + g_c F} = \frac{1}{u + c} \end{array} \right. \tag{B-39}$$

$$\frac{dt}{dZ} = \left\{ \begin{array}{l} \frac{u + \sqrt{-g_c F}}{u^2 + g_c F} = \frac{1}{u - c} \\ \frac{u - \sqrt{-g_c F}}{u^2 + g_c F} = \frac{1}{u + c} \end{array} \right. \tag{B-40}$$

$$\left\{ \begin{array}{l} \frac{u + \sqrt{-g_c F}}{u^2 + g_c F} = \frac{1}{u - c} \\ \frac{u - \sqrt{-g_c F}}{u^2 + g_c F} = \frac{1}{u + c} \end{array} \right. \tag{B-41}$$

If (B-39), (B-40), and (B-41) are substituted into (B-35), (B-36), and (B-37), it is found that

$$\frac{\lambda_2}{\lambda_3} = 0; \quad \frac{\lambda_1}{\lambda_3} = 0; \quad \text{for } \frac{dt}{dZ} = \frac{1}{u} \tag{B-42}$$

$$\frac{\lambda_2}{\lambda_3} = -\frac{\rho c}{g_c}; \quad \frac{\lambda_1}{\lambda_3} = \frac{c^2}{g_c}; \quad \text{for } \frac{dt}{dZ} = \frac{1}{u - c} \tag{B-43}$$

$$\frac{\lambda_2}{\lambda_3} = \frac{\rho c}{g_c}; \quad \frac{\lambda_1}{\lambda_3} = \frac{c^2}{g_c}; \quad \text{for } \frac{dt}{dZ} = \frac{1}{u + c} \tag{B-44}$$

Finally, if (B-42), (B-43), and (B-44) are substituted into (B-34), recalling that the partial derivative coefficients are zero, ordinary differential equations are obtained for $P, u,$ or

$$dP + \frac{\rho c}{g_c} du = \alpha dt \text{ on } \frac{dt}{dZ} = \frac{1}{u + c} \tag{B-45}$$

$$dP - \frac{\rho c}{g_c} du = \beta dt \text{ on } \frac{dt}{dZ} = \frac{1}{u-c} \tag{B-46}$$

$$d\rho - \frac{g_c}{c^2} dP = \gamma dt \text{ on } \frac{dt}{dZ} = \frac{1}{u} \tag{B-47}$$

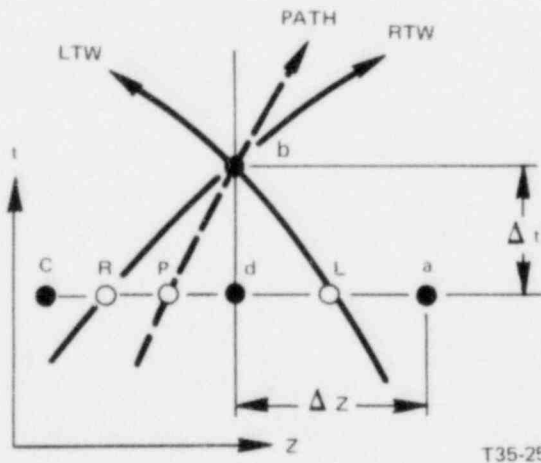
where

$$\alpha = \frac{c^2}{g_c} F_1 + \frac{\rho c}{g_c} F_2 + F_3 \tag{B-48}$$

$$\beta = \frac{c^2}{g_c} F_1 - \frac{\rho c}{g_c} F_2 + F_3 \tag{B-49}$$

$$\gamma = -\frac{g_c}{c^2} F_3 \tag{B-50}$$

B.3.4 Finite Difference Scheme



- RTW = Right traveling wave
- LTW = Left traveling wave
- PATH = Path line
- R, L, P = Points where RTW, LTW, PATH lines pass through b intersect the grid line t

T35-25

In the time increment Δt , Equations (B-45), (B-46), and (B-47) integrate as

$$P_b - P_R + \left(\frac{\rho c}{g_c}\right)_R (u_b - u_R) = \alpha_R \Delta t \tag{B-51}$$

$$P_b - P_L - \left(\frac{\rho c}{g_c}\right)_R (u_b - u_L) = \beta_L \Delta t \tag{B-52}$$

$$\rho_b - \rho_P - \left(\frac{g_c}{c^2}\right)_P (P_b - P_P) = \gamma_P \Delta t \tag{B-53}$$

All data are available at time t and every Z . Data at points R, L, and P can be interpolated between known data at points a, d, and c. Location of R, L, and P in Z can be readily found from (B-39), B-40), and (B-41), finding the characteristic line with slopes interpolated between a, d, c which pass through b.

B.4 IMPORTANT IDEALIZATIONS

At the instant of pipe break, a large decompression will propagate through non-flashing water at about 3500 ft/sec, discharging 3700 lbm/sec for perhaps a few milliseconds until flashing begins. References 2, 3, and 4 indicate that non-equilibrium states in water decompression persist (if at all) for about one millisecond. However, discharge rates based on saturated equilibrium are higher than non-flashing discharge rates. Therefore, it is conservatively assumed that the discharge instantly rises to the higher saturated equilibrium rate. This assumption slightly increases the total mass and energy discharged at this time during the early blowdown.

The long-side pipe is assumed to be straight and almost frictionless. Moreover, presence of the pump is ignored for simplification. Both of these idealizations cause the calculated discharge rates to be somewhat higher than expected, and are therefore conservative.

It is assumed that as the contained water decompresses, it undergoes homogeneous flashing, and consists of a homogeneous mixture of steam and water. This assumption closely matches the time-dependent blowdown experiments of Edwards.⁴

Furthermore, the steady blowdown data of Facke, Allemann, and Uchida for saturated water discharge through unrestricted pipes, summarized in Reference 5, are closely approached by the homogeneous mixture flow pattern assumption. Therefore, the assumption of homogeneous steam/water during the short term acceleration transient is well supported by experiments.

Edwards⁴ obtained pressure-time measurements at various stations during decompression of hot water in a pipe. The straight pipe was 13.44 feet long with an inside diameter of 2.88 inches. Water at about 467°F (500 psia saturation pressure) pressurized to 1000 psia was decompressed by the rupture of a glass diaphragm at one end. Figure B-3 shows a measured pressure-time history close to the discharge end.

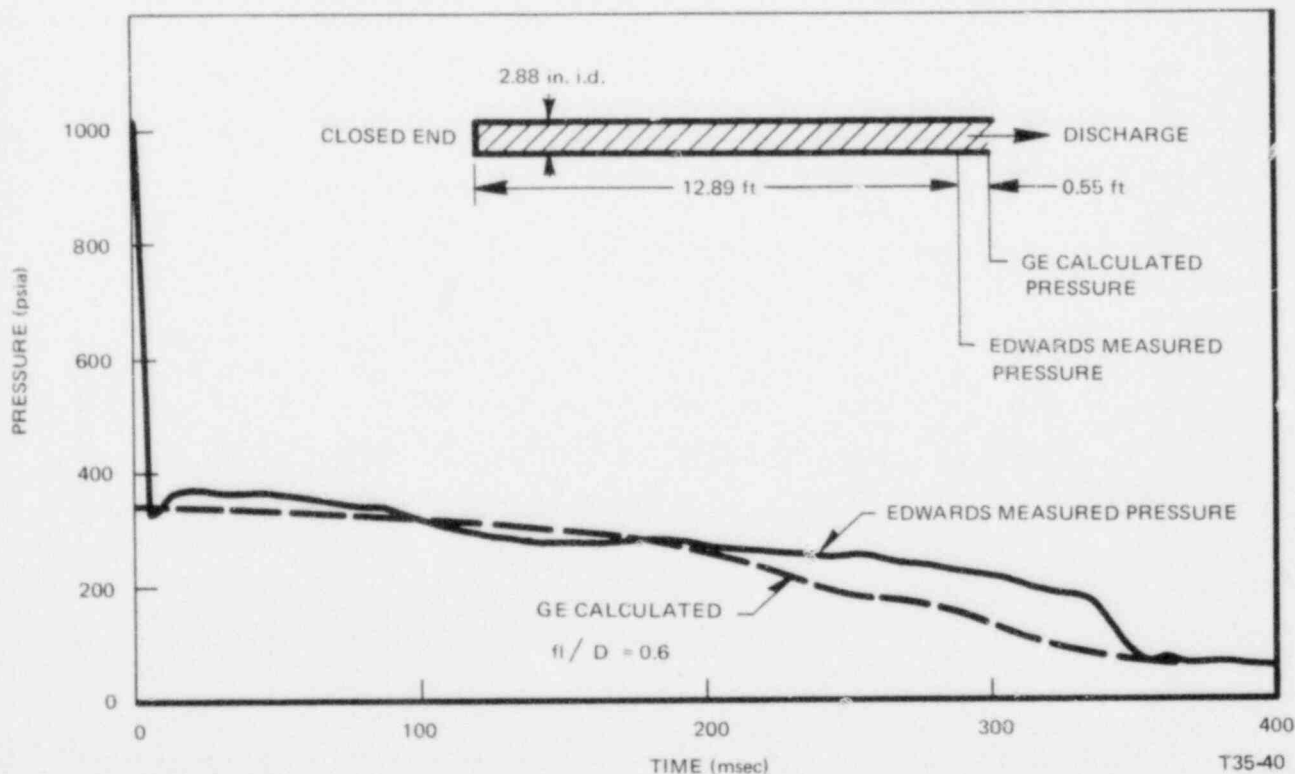


Figure B-3. Comparison with Edwards Experiment

It can be seen that the GE model with realistic friction closely predicts the experimental trace. Edwards pointed out that the discharge area was about 10 to 15% smaller than the pipe bore, and this probably accounts for the computed discharge pressure falling slightly below the measurement.

This comparison supports the idealization of homogeneous, equilibrium steam-water mixture states used in present inventory blowdown computations.

When simulating the response of the Mark III drywell to a postulated loss-of-coolant accident, the transient blowdown flow rate associated with decompression of the broken line is accounted for by using an artificial break area. From the above discussion of the rate at which blowdown flow accelerates, it has been concluded that the so-called "inventory effect" can be bounded by using the following assumptions.

1. For a recirculation line break, the blowdown flow rate from the "long" side of the break (see Figure B-3) will be calculated using an initial mass flux corresponding to approximately 50% of the mass flux predicted by the Moody flow model based on the initial fluid conditions in the pipe. This flow rate will be assumed to exist for as long as it takes to deplete the fluid originally in the pipe; following depletion the flow will be conservatively calculated using Moody flow at the upstream restriction (the jet pumps). For a typical BWR, the equivalent total break area used to simulate this sequence of events is shown in Figure B-4. The computer code used to numerically integrate the simultaneous differential equations that describe the transient conditions in the containment assumes that at any time, the total break flow is given by

$$\text{Flow} = A_{BR} \times G_M$$

Where

A_{BR} = The input value of break area, ft^2

G_M = Break mass flux, defined by the Moody model, $\text{lb}/\text{sec}\cdot\text{ft}^2$.

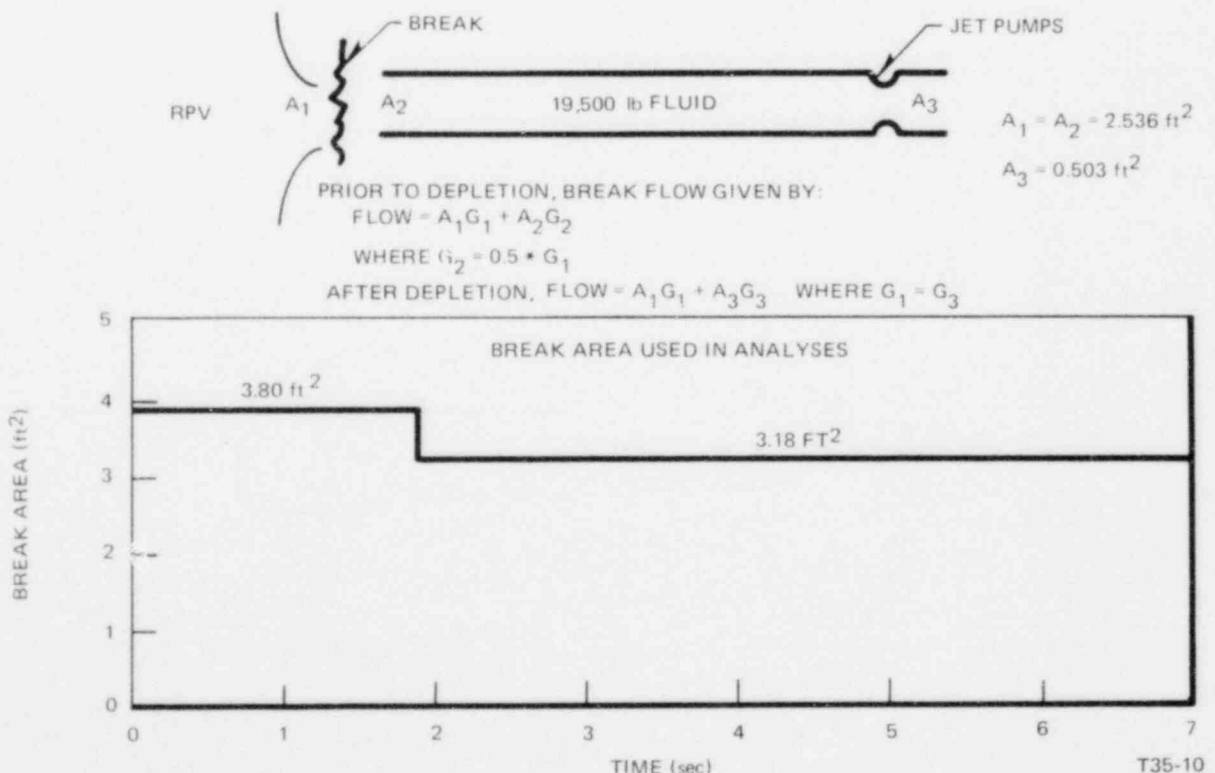


Figure B-4. Typical BWR Recirculation Line Break

To simulate the inventory effect, a total break flow equivalent to Moody blowdown flow through A₁, plus 50% Moody flow from the "long" side of the break. For a typical BWR, this process yields a total break area of 3.60 ft². Depletion time, t_D, is calculated by

$$t_D = \frac{M}{0.5 \times G_M \times A_2} \text{ sec}$$

Where

M = Initial fluid mass in the recirculation pipe, lb.

A depletion time of 1.9 sec is typical if a G_M of 8100 lb/sec-ft² is used. Following depletion, the total break area is reduced to 3.18 ft² which represents the sum of the line area and the jet pump nozzle area.

- A very similar procedure is used to calculate the effective break area for the steam line break except that during inventory depletion the mass flux is approximately 75% of rated Moody flow and depletion times are much shorter due to low inventory values. Figure B-5 shows the steam line effective break area.

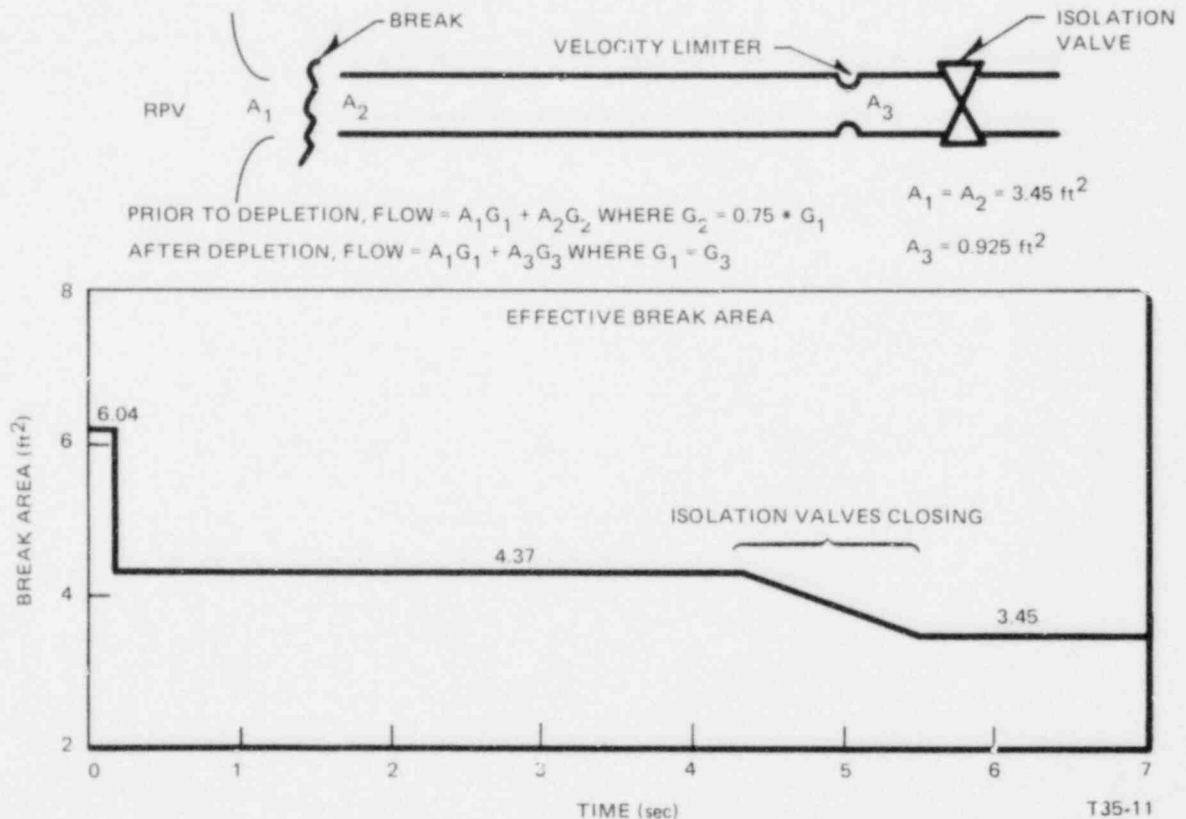


Figure B-5. Typical BWR Steam Line Break

Prior to depletion,

$$A_{BR} = A_1 + 0.75 \times A_2 \text{ ft}^2$$

which yields 6.04 ft². Depletion time is given by

$$t_D = \frac{M}{0.75 \times G_M \times A_2} \text{ sec}$$

which yields 0.19 second if a G_M of 2050 lb/sec-ft² is used.

Following depletion, the break area drops to 4.37 ft² which is the sum of the line area and the limiter area.

All of the numbers in the above discussion are for a particular reactor size (in this case a 251-inch-diameter pressure vessel BWR); they are typical for other size reactors.

REFERENCES

1. Ascher H. Shapiro, "The Dynamics and Thermodynamics of Compressible Fluid Flow," Volume II.
2. E. V. Gallagher, *Water Decompression Experiments and Analysis for Blowdown of Nuclear Reactor*, July 1970 (IITRI-578-P-21-39).
3. T. A. Zaker and A. H. Wiedermann, *Water Depressurization Studies*, June 1966 (IITRI-578-P-21-26).
4. A. R. Edwards and T. P. O'Brien, "Studies of Phenomena Connected With the Depressurization of Water Reactors," *Journal of the British Nuclear Energy Society*, **9**, pp 125-135 (April 1970). (Available as attachment to Interim Report I-212-74-5.1, Aerojet Nuclear Company, October 1973).
5. Docket No. RM-50-1, "In the Matter of Acceptance Criteria for Emergency Core Cooling System for Light-Water-Cooled Nuclear Power Reactors," Redirect-Rebuttal Testimony on Behalf of the General Electric Company, October 26, 1972.